A ROLE OF PRL-3 IN AUTOPHAGY AND ITS REGULATION IN HUMAN CANCERS

HUANG YUHAN

B. Sc. (Hons.), Sun Yat-sen University

A THESIS SUBMITTED

FOR THE DEGREE OF DOCTOR OF PHILOSOPHY

NUS GRADUATE SCHOOL FOR INTEGRATIVE

SCIENCE AND ENGINEERING

NATIONAL UNIVERSITY OF SINGAPORE

2015

DECLARATION

Declaration

I hereby declare that this thesis is my original work and it has been written by me in its entirety. I have duly acknowledged all the sources of information which have been used in the thesis.

This thesis has also not been submitted for any degree in any university previously.

Huang Yuhan

Huang Yuhan
21 January 2015

ACKNOWLEDGEMENTS

First of all, I would like to show my greatest gratitude to the most important person during my PhD candidature, my supervisor A/Prof. Zeng Qi. She is such a knowledgeable, wise, and kind supervisor. She can always dig out the most essential existing problem of the research projects during our discussions, and gives good suggestions. I also want to thank all past and present members from our lab. All of you are so kind and welcoming, which makes the lab like another home to me. I would like to show my especially grateful to Dr. Yuen Hiu-Fung (Eric), who was also my mentor when I first joined the lab. He taught me many basic research skills and techniques. The most touching thing is that he was still willing to give me suggestions on projects and help on data analysis even after leaving the lab. Dr. Abdul Qader Omer Al-aidaroos also gave me lots of guidance throughout these four years. He is very smart and always gives me great suggestions. I am also very grateful for his corrections of my thesis. Extraordinary mentions must be made to our lab office Li Jie. With her patience and good memory, the lab is always in good order, which makes us to work conveniently. Personally, she is also willing to help me outside the lab. I would like to thank Dr. Sitaram Harihar for his time to discuss with me and also help me correct my thesis. I also appreciate Mr. Ye Zu's help in the lab, and our happy lunch times. Dr. Min Thura and Mr. Abishek Gumpta's technical help is also well-appreciated. Ms. Tang Jing Ping, Dr. Guo Ke and Dr. June Park, our past lab members, I am very grateful to their coaching and their technical help.

Special mention also goes to Dr. Zhang Shu-dong and Dr. James Murray (Queen's University, Belfast, UK) for GEO data mining and contribution to the ULK1 data in the autophagy chapter.

I would also like to show my deepest acknowledgment to Prof. Jean-Paul Thiery for being my main supervisor, and A/Prof. Shen Han-Ming, A/Prof Vinay Tergaonkar for being my PhD Thesis Advisory Committee members. I deeply thank them for their

valuable input to my research project. Also, I would like to thank Agency of Science, Technology, and Research (A*STAR), Singapore, for supporting our lab with research funds, and National University of Singapore Graduate School for Integrative Sciences and Engineering (NUS-NGS) for supporting myself with scholarship. I would like to thank Professor T. Sasazuki, and Professor S. Shirasawa for providing the KRas mutant and wild type cell pairs.

Special thanks go to my families. My beloved husband Wang Tiansu is always encouraging, supportive, considerable and patient to me during these four years, and I am thankful. Also, I would like to thank my mother and mother-in-law, for helping me take care of my son, so that I can focus more on my study. I am also deeply grateful for all of my friends here in Singapore and in China for being encouraging and company me especially when I was frustrating. Finally, none of these could have been achieved without my mother, who is always willing to give me everything she has. I am always thankful to her.

I dedicate this thesis to my mother.

-Huang Yuhan

TABLE OF CONTENTS

SUMMARY

Phosphatase of regenerating liver 3 (PRL-3) is a metastatic phosphatase localized on plasma and endosomal membranes. It functions to promote multiple oncogenetic processes such as cell proliferation, angiogenesis, invasion and metastasis. In this study, I report that PRL-3 could function to promote autophagy dependent on the activation of Unc-51-Like Kinase 1 (ULK1), a key initiator of the autophagic process. Specifically, overexpression of PRL-3 enhanced hVps34-Beclin-1-dependent canonical autophagosome formation; accelerated LC3-I to LC3-II conversion dependent on autophagy related gene 5 (ATG5) expression; and promoted the degradation of p62, a well-known autophagy substrate. Autophagy is a "self-eating" process, which has dual roles in promoting or suppressing tumor growth depending on cellular context. I found that PRL-3 required autophagy to promote the growth of ovarian cancer cell line A2780. Clinically, in the biggest publically available ovarian cancer cohort, the prognostic value of PRL-3 expression levels was also found to be dependent on the co-expression of high levels of autophagy related genes (including hVps34, Beclin-1, and ATG5).

Surprisingly, both endogenous and exogenous PRL-3 protein were degraded specifically upon starvation induced autophagy, and accumulated upon chemically or genetically-induced autophagic inhibition. Thus, the autophagy enhancer PRL-3 also acts as an autophagy substrate. PRL-3 and autophagy is likely to forms a negative feedback loop to fine-tune their activity. My results characterize that PRL-3 is a novel autophagic substrate, and it also sheds new insight into post-translational regulation of PRL-3 expression.

Finally, I showed that constitutively active mutations of KRas (specifically KRas-G12V or KRas-G13D), frequently seen in many human cancers, upregulated expression levels of PRL-3 protein, but not mRNA. KRas upregulation of PRL-3 could be abolished upon treatment with the MEK inhibitors U0126 or PD98059. Thus, constitutively activate

KRas mutation is a novel post-transcriptional regulator of PRL-3, and this regulation acts through the RAF- MEK-ERK kinase cascade. Ultimately, the new mechanisms of PRL-3 regulation unraveled here, as well as the signaling pathways affected by PRL-3, might facilitate development of better, more focused, and more specific therapy for tumors with high expression of PRL-3.

LIST OF TABLES

LIST OF FIGURES

LIST OF ABBREVIATIONS

AKT	protein kinase B
AMPK	AMP-activated protein kinase
ARD1	arrest-defective protein 1 homolog A
Arf1	ADP-ribosylation factor 1
ATG	autophagy related gene
Baf A1	bafilomycin A1
CDK	cyclin dependent kinase
CHO	Chinese hamster ovary
CQ	chloroquine
EGFP	enhanced green florescence protien
EGFR	epidermal growth factor receptor
EMT	epithelial to mesenchymal transition
ERK	extracellular signal-regulated kinase
FBS	fetal bovine serum
FKBP38	FK506-binding protein 38
GAP	GTPase activating proteins
GDP	guanosine diphosphate

GEF	guanine nucleotide exchange factors
GEO	Gene Expression Omnibus
GTP	guanosine triphosphate
HDAC	histone deacetylases
HBSS	Hank's Balanced Salt Solution
HUVEC	human umbilical vascular endothelial cells
LC3	microtubule-associated protein 1 light chain 3
MAKP	mitogen-activated protein kinase
MEF2C	myocyte enhancer factor 2C
MTOR	mammalian target of rapamycin
NSCLC	non-small cell lung cancer
PCBP1	PolyC-RNA-binding protein 1
PDGF	Platelet Derived Growth Factor
PAS	phagophore assembly site
PE	phosphatidylethanolamine
PI3K	phosphatidylinositol-3-kinase
PTP	protein tyrosine phosphatase
PRL	phosphatase of regenerating liver

PTEN	Phosphatase and Tensin Homologue Deleted on Chromosome 10
RAF	Rapidly Accelerated Fibrosarcoma
RAS	rat sarcoma
RTK	receptor tyrosine kinases
SAHA	Suberoylanilide hydroxamic acid
SDS-PAGE	sodium dodecyl sulphate-polyacrylamide gel electrophoresis
SNCG	synuclein-gamma
STAT	Signal transducer and activator of transcription
TEMED	tetramethylethylenediamine
ULK	Unc-51-Like Kinase
UTR	untranslated region
VEGF	vascular endothelial growth factor
VPS34	vacuolar protein sorting

CHAPTER 1: INTRODUCTION

1.1 General introduction of PRL family

Protein phosphorylation, is essential for almost all aspects of cell life, including metabolism, cell-cycle progression, differentiation, cytoskeleton arrangement as well as cell motility (Johnson, 2009). The phosphorylation machinery within the cell involves a coordinate action of different kinases and phosphatases whose expression and activities are tightly controlled. Any deregulation in these enzymes has been known to contribute to a plethora of diseases, including cancer. One such group of enzymes is the phosphatases belonging to the Phosphatase of Regenerative Liver (PRL) family. The PRL phosphatases are classified as Protein Tyrosine Phosphatases (PTPs) with dual specificity. Which means they can dephosphorylate phosphorylated tyrosine as well as serine/ threonine residues in a protein (Alonso et al., 2004). Dual-specificity phosphatases are modulators of several critical signaling pathways (Patterson et al., 2009), and therefore understanding their mechanisms of action is of great significance. There are three members in PRL family, PRL-1 (PTP4A1), PRL-2 (PTP4A2), and PRL-3 (PTP4A3), which share at least 70% homology and have many domains in common, including:

1) a PTP domain required for phosphatase activity comprising of a WPD-loop, and a PTP-loop (CX_5R) (Yang et al., 1998). The WPD-loop is important for substrate recognition and binding, whereas the PTP-loop functions to catalyze the hydrolysis of the phosphate group in the substrate (Doctoral Degree thesis of Zimmerman, 2013).

2) a polybasic domain followed by a prenylation motif (CAAX box) at the C-terminus. The 6 basic amino acids in the polybasic domain provide a positive charge in this region. This contributes to the membrane- localization of PRL proteins. PRL proteins are prenylated at the C-terminus, by covalent addition of lipid side chains (Zhang and Casey,

1996). Both domains contribute to the membrane association localization of PRL family members. The conserved domains in PRL family are summarized in Figure 1.

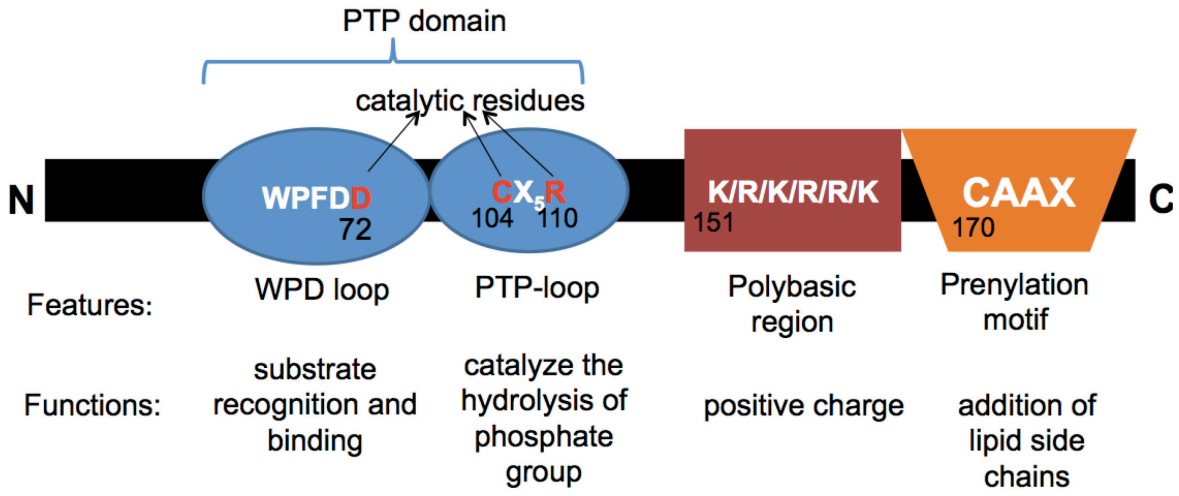

Figure 1. Protein domains of PRL family members. The domains shared by PRL family members are show in the figure. The PTP domain needed for their phosphatase activity is comprised of a WPD loop and a PTP loop. The polybasic domain and CAAX prenylation motif contribute to membrane-associated localization of these proteins.

During the last decade several reports have shown the involvement of all three PRL family members in multiple cancers of different tissue origins (Al-Aidaroos and Zeng, 2010). Being the first PRL family member shown to take an active part in cancer progression, PRL-3 has attracted the most attention among this family. How PRL-3 contributes to multiple aspects of cancer progression will be reviewed in this chapter.

1.2 The Roles of PRL-3 in Cancer

PRL-3 was first found positively correlated with colorectal cancer metastasis in 2001 (Saha et al., 2001). Since then, more and more research has been conducted to investigate the role of PRL-3 in cancer metastasis. PRL-3 was found to promote metastasis in tumors of different tissue origins (Al-Aidaroos and Zeng, 2010).

PRL-3 not only drives cancer metastasis, but also actively takes part in multiple aspects of other carcinogenesis processes. The traditional hallmarks of cancer comprise six biological capabilities: sustaining proliferative signaling, evading growth suppressors, resisting cell death, enabling replicative immortality, inducing angiogenesis and activating invasion and metastasis (Hanahan and Weinberg, 2000). PRL-3 has been found to affect four out of these six hallmarks of cancer, which are sustaining proliferative signaling, resisting cell death, inducing angiogenesis, and activating invasion and metastasis. These will be reviewed in detail in the following sections.

1.2.1 PRL-3 Sustains Proliferative Signals

Normal cells precisely regulate growth-promoting signals and cell cycle checkpoints to control their production, and thus maintain tissue architecture and function (Hanahan and Weinberg, 2011). However, cancerous cells have the ability to deregulate these proliferation-restricting pathways, which enable them to divide uncontrollably. Having sustained proliferative signals is one of the fundamental characteristic of cancer cells, and such proliferative signals are regulated by several key signaling cascades including the p53 pathway, phosphatidylinositol-3-kinase/ protein kinase B (PI3K/AKT) pathway, and mitogen-activated protein kinase (MAPK) pathway (Lawlor and Alessi, 2001; Vogelstein et al., 2000; Zhang and Liu, 2002). Strikingly, PRL-3 has been shown to modulate all

these pathways to drive cell proliferation (Basak et al., 2008; Fagerli et al., 2008b; Liu et al., 2008; Qian et al., 2007b). The related results will be discussed below.

p53, encoded by TP53 gene, is an important tumor suppressor. It functions as a cell cycle checkpoint causing cell cycle arrest for DNA repair (Vousden and Lu, 2002). PRL-3 overexpression was shown to downregulate p53 protein levels which depended on its phosphatase activity and prenylation motif (Min et al., 2010). Interestingly, PRL-3 was also shown to be a p53 inducible gene, whose overexpression induced G1 arrest downstream of p53 (Basak et al., 2008). Surprisingly, attenuation of PRL-3 expression also elicits an arrest response. This study highlights the key dose-dependent function of PRL-3 in cell cycle regulation in non-cancer conditions. However, in cancerous tissues, where myriad mutations arise, a high level of PRL-3 expression may fail to trigger cell-cycle arrest, thereby allowing other activities of PRL-3 to prevail (Basak et al., 2008).

PRL-3 has been shown to activate the PI3K/AKT pathway in several cancers. By producing PtdIns(3,4,5)P_3 (PIP3), PI3K promotes Akt translocation to the membrane for activation, which facilitates Akt to activate mammalian Target of Rapamycin (MTOR) to stimulate cell proliferation (Peltier et al., 2007; Rafalski and Brunet, 2011). Further, Akt phosphorylates cyclin-dependent kinase (CDK) inhibitor $p21^{CIP/WAF1}$ and $p27^{KIP1}$, which contributes to the degradation of these two proteins (Peltier et al., 2007; Shin et al., 2002). The expression of $p21^{CIP/WAF1}$ and $p27^{KIP1}$ leads to cell cycle arrest, so their degradation blocks cell cycle arrest. Simply put, the activation of PI3K/AKT pathway promotes cell proliferation and also blocks cell cycle arrest. PRL-3 has also been shown to downregulate Phosphatase and Tensin Homologue Deleted on Chromosome 10 (PTEN) in colorectal cancer, and PTEN is an important antagonist of PI3K. This could be abrogated by the PI3K inhibitor LY294002, implying that PRL-3 acted upstream of PI3K to enhance AKT activity, and thus led to increased cell proliferation (Wang et al., 2007).

RAF/MEK/ERK pathway is also modulated by PRL-3 to provide sustained proliferative signals in cancer tissues (Liang et al., 2007). RAF/MEK/ERK pathway is the best-studied MAPK pathway, and its deregulation has been found in approximately one-third of all human cancers (Dhillon et al., 2007; Hilger et al., 2002). On receiving extracellular stimuli such as mitogens, cytokines, and growth factors, MAPK pathway is activated, and follows a classic three tiered kinase cascade: MAPKKK (mitogen-activated protein kinase kinase kinase) → MAPKK (mitogen-activated protein kinase kinase) →MAPK (mitogen-activated protein kinase). Activated MAPKs leads to phosphorylation and activation of specific MAPK- activated protein kinases (MAPKAPKs). These activated MAPKAPKs regulate a broad range of biological processes such as growth, differentiation and development (Brunet et al., 1999). In RAF/MEK/ERK pathway, RAF functions as MAPKKK, MEK functions as MAPKK, and ERK functions as MAPK (Brunet et al., 1999). Activated ERK regulates growth factor-responsive targets in the cytosol and also translocates to the nucleus, where it phosphorylates a number of transcription factors to regulate gene expression (Wortzel and Seger, 2011). The activation of ERK is essential for G1 to S phase progression (Villanueva et al., 2007). The phenomenon that PRL-3 overexpression leads to increased ERK activity has been observed in multiple cell lines including: HEK293 human embryonic kidney cells (Liang et al., 2007), human leukemia cell line MOLM-14 (Zhou et al., 2011), and human epidermoid carcinoma cell line A431 (Al-aidaroos et al., 2013). Such activation of ERK/ MAPK pathway modulated by PRL-3 activates cell cycle progression, and sustains proliferative signaling.

Although several studies have reported that PRL-3 functions to promote cell proliferation, some studies showed that PRL-3 expression had no effect on cell proliferation. For example, in Multiple Myeloma (MM) cell line INA-6, the overexpression / knock down of PRL-3 did not affect cell proliferation rate (Fagerli et al., 2008b). Thus, the function of PRL-3 in promoting cell proliferation is dependent on genetic background, and possibly

some other co-factors. Determining these variables is of great significance. I will discuss findings related these co-factors in the thesis.

1.2.2 PRL-3 Induces Cell Death Resistance

In addition to having sustained proliferative signaling, cancer cells also have to circumvent the strategies the body employs to eliminate them (Hanahan and Weinberg, 2011). Apoptosis, a process of programmed cell death, is one of these strategies. Normal cells are able to sense genomic instability such as DNA damage, and initiate apoptosis. In this way, apoptosis serves to clear the cells with mutations and maintain genomic stability, forming a natural barrier to cancer development. By disrupting apoptosis, some oncogenic mutations can lead to tumor initiation and progression (Lowe and Lin, 2000).

There are many studies showing that PRL-3 contributes to cell death resistance in different systems. Activation of PI3K/AKT signaling by PRL-3 was shown to promote resistance to stress-induced apoptosis (Jiang et al., 2011). In another study, knock down of PRL-3 using siRNA caused a dramatic increase in apoptosis in H1299 cell line (Lian et al., 2012). Human gastric carcinoma cell line SFC-7901 treated with Emodin, a medicinal plant product, showed downregulation of PRL-3 and a corresponding increase in apoptosis (Sun and Bu, 2012). TF-1 is a cytokine dependent leukemia cell line, which undergoes apoptosis upon cytokine withdrawal (Lin et al., 2007). Overexpression of PRL-3 in this cell line was shown to inhibit apoptosis significantly upon cytokine withdrawal (Park et al., 2013). In addition, the overexpression of PRL-3 made it possible for non-cancer cell line Chinese Hamster Ovary (CHO) cells to survive *in vivo* in mouse by tail vein injection, indicating the overexpression of PRL-3 promotes cell survival in foreign conditions (Guo et al., 2004a). All these studies showed the overexpression of PRL-3 contributes to cell apoptosis resistance.

1.2.3 PRL-3 Promotes Tumor Angiogenesis

Sustained proliferative signals and the ability to escape apoptosis make it possible to initiate solid tumors. However, they are not able to grow beyond a certain size without adequate blood supply (Hanahan and Weinberg, 2011). Thus, the ability to form new blood vessels is of great significance for solid cancer progression. Angiogenesis is the physiological process through which new blood vessels form from pre-existing vessels (Birbrair et al., 2014; Hanahan and Folkman, 1996). Generally in normal tissues of an adult, angiogenesis is "off". However, during tumor progression, angiogenesis is always "on", stimulating the sprout of new vessels that provide nutrient and oxygen for sustaining rapid neoplastic growth (Hanahan and Weinberg, 2011). Different groups have shown the ability of PRL-3 to promote angiogenesis in tumor.

Guo *et al*. showed that PRL-3 protein expressed in developing blood vessels, but not in their mature counterparts, indicating that PRL-3 may be involved in the early development of the circulatory system. They also showed that PRL-3 overexpressing CHO or DLD-1 cells could redirect the migration of human umbilical vascular endothelial cells (HUVEC) to grow towards them, depending on the phosphatase activity of PRL-3. In addition, these cells could also enhance HUVEC vascular formation *in vivo.* PRL-3 drove this process by downregulating interleukin-4 (IL-4), which is an angiogenesis inhibitor (Guo et al., 2006). These results suggested that PRL-3 might direct angiogenesis in cancers.

PRL-3 overexpression was also shown to be associated with increased vascular endothelial growth factor (VEGF) expression in tumor samples from patients with non-small cell lung cancer (NSCLC). Moreover, blocking PRL-3 expression in lung cancer cell line A549 correspondingly reduced VEGF levels (Ming et al., 2009). The ligand

VEGF a signal protein produced by cells that have stimulated angiogenesis, and activates angiogenesis on binding to vascular endothelial growth factor receptor (VEGFR) (Neufeld et al., 1999). This suggests that PRL-3 induces microvascular vessel formation by facilitating VEGF expression in lung cancer tissues. Experiments done in transgenic mice also supported these *in vitro* results. Further, PRL-3 knockout mice exhibited reduced tumor angiogenesis, decreased VEGF-mediated endothelial cell motility and decreased vascular permeability (Zimmerman et al., 2014).

In summary, multiple studies have shown PRL-3 to promote angiogenesis *in vitro* (including multiple cell lines), *in vivo* (including mouse models), as well as in human patients' samples. Inhibiting angiogenesis is a promising strategy for cancer treatment, and PRL-3 appears to be an attractive molecular target for impeding angiogenesis in tumor progression.

1.2.4 PRL-3 Promotes Tumor Invasion and Metastasis

Tumor cells disseminate to various organs in the organism, searching for better environment with better supply of nutrients. This process of the spread of cells from primary neoplasm to distant organs is called metastasis (Hanahan and Weinberg, 2000).

Evolving genetic instability in tumor tissues has made metastatic cells greatly diversified from the primary tumor, and therefore difficult to be targeted by chemotherapy. What is more, due to the huge amount, metastases are difficult to be completely removed by surgery. All of these made metastatic tumors resistant to conventional therapy (Gupta and Massague, 2006; Khan and Mukhtar, 2010). As a result, it is metastasis that causes greater than 90% mortalities in solid cancers (Gupta and Massague, 2006).

To successfully metastasize, cancer cells have to acquire the ability to degrade basement membrane, and become motile. Such stepwise processes constitute the "metastasis cascade" (Thiery, 2002). One critical step of this cascade is the epithelial to mesenchymal transition (EMT). In this process the epithelial cells lose their cell polarity and cell-cell adhesion, and gain migratory and invasive properties to become mesenchymal. Normal epithelial cells have abundant amount of cell junctions, and are arranged in a tight and organized order, thus lacking mobility. Conversely, mesenchymal cells are loosely organized and surrounded by large extracellular matrix, thus having the ability to be mobile (Thiery, 2003). Here are some of the examples of "How PRL-3 contributes to this process".

PRL-3 was first proposed as an oncogene due to its role in promoting metastasis. In a study published in 2001, Saha *et al.* compared the global gene expression levels of metastatic colorectal cancers with their counterpart primary cancers, benign colorectal tumors, and normal colorectal epithelium, and found that PRL-3 was the only gene that was specifically expressed at high levels in cancer metastases, but in lower level in non-metastatic tumors and non-tumor tissues (Saha et al., 2001). This was a groundbreaking discovery, since the results came from an unbiased global gene expression profiling approach involving thousands of gene transcripts. The study suggests that PRL-3 plays a significant role in cancer metastasis. More recently, another study also analyzed the unbiased global gene expression profile between uveal melanoma patients who were diagnosed with liver metastasis and uveal melanoma patients without liver metastasis. Similarly, they pointed out that PRL-3 was upregulated specifically in the tumors from patients developed liver metastasis (Laurent et al., 2011). In addition, Zeng *et al*. found that stable overexpression of PRL-3 enhanced motility and invasive capability in CHO cells, and also induce metastatic tumor formation in mice dependent on its phosphatase activity (Zeng et al., 2003). PRL-3 has also been shown to promote cell motility and

metastasis in different systems including mouse melanoma cell line B16 (Peng et al., 2006; Qian et al., 2007a), human gastric carcinoma cell lines (Li et al., 2006), and human myeloma cell line (Fagerli et al., 2008a). Importantly, PRL-3 has also been shown to promote metastasis in cancer patients. Specifically, PRL-3 promotes lymph node metastasis in colon cancer patients (Ooki et al., 2010), and peritoneal metastasis in gastric cancer patients (Li et al., 2007).

Research to identify the signaling pathways regulated by PRL-3 in promoting invasion and metastasis showed that overexpression of PRL-3 resulted in upregulation of mesenchymal marker vimentin, and downregulation of epithelial marker E-cadherin *in vivo* (Liu et al., 2009). Similarly, in an *in vitro* system, PRL-3 overexpression was shown to upregulate mesenchymal markers fibronectin and Snail and downregulate epithelial markers E-cadherin and integrin β3, through PTEN-PI3K-AKT pathway (Wang et al., 2007).

Cell migration involves a great deal of remodeling of the actin cytoskeleton to ensure mobility (Ammer and Weed, 2008). Rho family GTPases are key regulators of this process (Maekawa et al., 1999). Interestingly, similar to PRL-3, Rho family GTPases expression also increased with tumor progression (Fritz et al., 1999). RhoA and RhoC are highly homologous members of the Rho family of GTPases. RhoA has been shown to contribute to cell motility by stimulating contractility and formation of actin stress fibers (Fritz et al., 1999). PRL-3 was shown to promote the activation of the Rho GTPases RhoA and RhoC, to increase invasion and cell motility in colorectal cancer cell line SW484 and DLD-1 (Fiordalisi et al., 2006; Wang et al., 2007). Further, PRL-3 also promoted invasion and metastasis through the regulation of integrin family. Integrins are a large family of cell surface receptors involved in adhesion, migration, and other crucial physical processes. CDH22, a member of the integrin family, is a known binding partner of PRL-3, however, the detailed function achieved by their binding needs further

investigation (Liu et al., 2009). Other than CDH22, PRL-3 has also been demonstrated to interact with or regulate other members of integrin family. Peng *et al*. showed that PRL-3 interacts with integrin α1, and also down-regulates the tyrosine-phosphorylation level of integrin β1 (Peng et al., 2004). These studies give some clues on how PRL-3 regulates metastasis. However, the detailed mechanisms involved should be investigated in future studies. PRL-3 also modulated recycling of integrins α5 through the interaction with ADP-ribosylation factor 1 (Arf1) and promoted cell migration (Krndija et al., 2012). Arf1 belongs to Arf family GTPase. Similar with Rho family GTPase, Arf family GTPases are also key players in actin cytoskeleton remodelling (D'Souza-Schorey and Chavrier, 2006). All these studies showed that integrins are important effectors of PRL-3 in promoting tumour metastasis.

Src is another PRL-3 effector in metastasis. Studies pointed out that PRL-3 promotes cell invasion by modulating Src activation. Src then activates its downstream targets such as ERK1/2 and Signal Transducer and Activator of Transcription 3 (STAT3). The activation of these genes promotes cancer invasion (Guarino, 2010). Similar results on PRL-3 promotion of metastasis through ERK phosphorylation and Rho-A/C activation was also reported in lung cancers (Ming et al., 2009).

PRL-3 also affects microRNA and calcium channels to regulate cancer metastasis. Zhang *et al.* showed in a miRNA array analysis, miR-21, miR-17 and miR-19a were upregulated by PRL-3. The group also pointed out that these miRNAs directly targeted PTEN to downregulate its expression, and promoted cell invasion as well as cell proliferation (Zhang et al., 2012a). By increasing expression of KCNN4 calcium channels, PRL-3 increased intracellular calcium levels, activated GSK-3β, increased Snail expression, and down-regulated E-cadherin, leading to EMT (Lai et al., 2013). All these studies showed that PRL-3 has multiple functions and has different effectors to promote metastasis.

Thus, as a strong oncogene, PRL-3 promotes multiple oncogenesis processes, including sustained proliferation, cell death resistance, induction of angiogenesis, and activating invasion and metastasis. Although most studies on PRL-3 focused on its role in promoting carcinogenesis processes, other roles of PRL-3 had also been shown in different studies.

1.3 The Roles of PRL-3 in Cancer Stem Cells

Other than promoting traditional carcinogenic processes, PRL-3 has also been found to promote self-renewal of cancer stem cells. It is believed that cancer stem cells are resistant to chemotherapy, and can give rise to distant metastases (Jordan et al., 2006). Cramer *et al.* found that expanded cells from colon tumor of PRL-3 knockout mice have reduced clonogenicity and inability to form secondary tumor. In contrast, cells expanded from colon tumor of a wild-type mouse exhibited enhanced clonogenicity even at higher passages, and were ubiquitously CD133+ (Cramer et al., 2014). CD133 is being used extensively as a marker for cancer stem cells (Wu and Wu, 2009). These results indicated reduced self-renewal ability in PRL-3 knockout cancer cells. Thus, PRL-3 may also contribute to cancer carcinogenesis by maintaining cancer stem cell population.

1.4 PRL-3 In Normal Physiological Functions

The functions of PRL-3 in non-cancer conditions have also been investigated by the generation of PRL-3 knockout mice. Generally, these mice are healthy, fertile and phenotypically similar to wild type counterparts. The only difference is that adult male homozygous knockout mice exhibited a slightly decreased body mass (Zimmerman et al., 2014). These results indicate PRL-3 may not be critical for normal physiological process. This may be due to compensation effects from PRL-1 and PRL-2. The three genes in PTP

family (PRL-1, PRL-2 and PRL-3) share at least 70% amino acid identity, and also have lots of consistent functional domains.

Most of the studies on PRL-3 were done in mammalian models. However, recently, PRL-3 was found to be required for *Xenopus laevis* cranial neural crest migration *in vivo* during embryonic development (Maacha et al., 2013). This study showed that PRL-3 also affected animal development other than cancer progression. Importantly, PRL-3 was shown to affect cell migration in non-mammalian animal model, suggesting a potential role for *Xenopus laevis* as a model to study the function of PRL-3.

1.5 The Regulation Of PRL-3

The excessive expression level of PRL-3 is a key element contributing to tumor metastasis, thus the investigation on how PRL-3 is regulated is of great significance to basic science as well as pharmaceutical research. PRL-3 expression level is regulated at multiple levels, including gene copy number amplification, RNA transcriptional, translational, and post-translational levels.

1.5.1 PRL-3 Is Regulated By Gene Copy Number Amplification

Gene amplification is a copy number increase of the restricted region in a chromosome arm. It may contribute to the overexpression of the amplified gene, and it is an important mechanism of oncogene activation (Albertson, 2006). PRL-3 gene amplification has been found both in primary colorectal cancers as well in liver metastasis of colorectal cancers (Buffart et al., 2005). Gene amplification of PRL-3 has also been found in several myeloma cell lines (Fagerli et al., 2008b). Thus, gene amplificaiton may contribute to the overexpression of PRL-3 in cancers.

1.5.2 PRL-3 Is Regulated At Transcriptional Level

Transcription regulation has been shown to affect PRL-3 levels significantly in different systems. Firstly, PRL-3 gene expression is regulated by extracellular stimuli transduced via growth factor signaling networks. Conditioned medium from carcinoma-associated fibroblasts (Molleví et al., 2009), or direct addition of mitogenic cytokines such as Phorbol ester phorbol 12- Myristate 13- Acetate (PMA), IL-6, TNF, and IL-21 (Fagerli et al., 2008a; Rouleau et al., 2006) regulates PRL-3 mRNA levels. Further, several transcription factor binding sites have been identified in the upstream regulatory site of PRL-3, including myocyte enhancer factor 2C (MEF2C) (Xu et al., 2011), Snail (Zheng et al., 2011), p53 (Basak et al., 2008), and STAT 3 (Zhou et al., 2011). These transcription factors have been shown to upregulate PRL-3 mRNA transcription. Interestingly, other than being transcriptionally upregulated by STAT 3, PRL-3 also contributes to the activation of STAT 3 (Zhou et al., 2011). Thus PRL-3 and STAT 3 form a positive autoregulatory loop to promote cancer progression.

Suppression of PRL-3 mRNA expression has also been identified. Specifically, TGFβ stimulation has been shown to suppress PRL-3 expression by inducing binding of Smad transcription factors to PRL-3 promoter (Jiang et al., 2011). TGFβ has been shown to suppress tumor initiation in a variety of cancers, and loss of TGFβ leads to malignancy (Wang et al., 1996; Wang et al., 1995; Ye et al., 1999).

1.5.3 PRL-3 Is Regulated At Translational Level

Transcriptional regulation of PRL-3 is important. However, PRL-3 overexpression is not directly associated with its transcript level in many cases, which indicates a post-transcriptional regulation of PRL-3 (Wang et al., 2010). Wang *et al*. found that PolyC-RNA-binding protein 1 (PCBP1) is able to bind to the triple six-base GC-rich *cis*-

elements in the 5' untranslated region (UTR) of PRL-3 mRNA, and suppress PRL-3 translation *in vitro*. More importantly, they confirmed their finding in human cancer samples, showing an inverse correlation between PRL-3 and PCBP1.

1.5.4 PRL-3 Is Regulated By Post-Translational Modifications

Protein post-translational modifications are important regulators of biological activity, molecular interactions, localization, and dynamic stability (Walsh et al., 2005). PRL-3 is also regulated by post-translational modifications. Firstly, the localization of PRL-3 is regulated by post-translational modification. Being prenylated at the C-terminus, PRL-3 localizes to the plasma membrane and early endosome. Prenylation is a lipid modification involving covalent addition isoprenoids to conserved cysteine residues at or near the C-terminus of the protein. With the addition of this hydrophobic lipid, prenylaiton not only enhances membrane interaction of the target protein, but also affects its interaction with other proteins (Zhang and Casey, 1996). This C-terminal prenylation-mediated localization of PRL-3 is very important for its function, since mutation in this domain altered its localization from the cytosolic membrane and to the nucleus (Zeng et al., 2000). Secondly, the dynamic stability of PRL-3 is also regulated by post-translational modifications. For example, the peptidyl prolyl cis/trans isomerase FK506-binding protein 38 (FKBP38) was identified as a PRL-3 interacting protein, which promotes the proteasome-mediated degradation of PRL-3 (Choi et al., 2011). Further, PRL-3 protein levels can be downregulated by Suberoylanilide hydroxamic acid (SAHA) treatment via a proteasome dependent pathway in AML cells with FLT3 mutations, thus inhibiting growth in these cells. SAHA is an anti-cancer drug for acute leukemia, functioning to inhibit histone deacetylases (HDAC), and this drug has already been approved by the Food and Drug Administration (FDA). This study also sheds light on the contribution of PRL-3 post-translational regulation on cancer therapy (Zhou et al., 2011). However, more

detailed mechanisms about the protein stability of PRL-3 are still lacking. There are two main pathways regulating protein stability: the proteasome degradation pathway and the autophagy degradation pathway. In this thesis, I will discuss more on the post-translational regulation of PRL-3 through autophagy.

The multi-level regulation of PRL-3 is summarized in Figure 2.

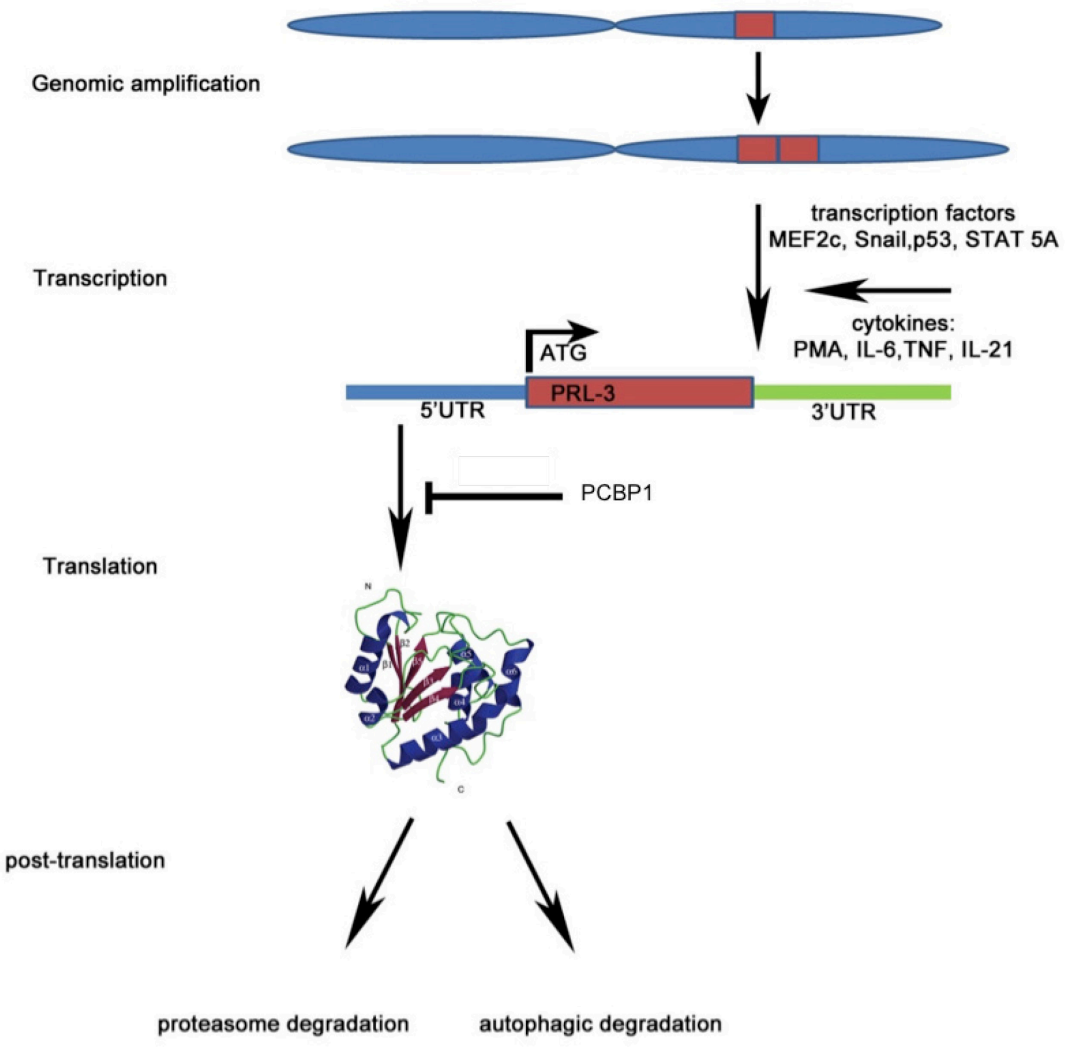

Figure 2. The regulation of PRL-3 in multiple levels. PRL-3 is regulated by genomic amplification, transcription, translation, as well as post-translational mechanisms.

1.6 Clinical Relevance Of PRL-3

PRL-3 is an important oncogene that promotes multiple carcinogenic processes and is regulated at multiple levels. It has already been shown as a prognostic biomarker in different cancer types. Further, higher expression levels of PRL-3 predict poorer survival in cancer patients. Thus, it is potentially a good target for cancer therapy.

1.6.1 Prognostic Significance Of PRL-3

Several studies have reported the importance of PRL-3 mRNA and protein levels for disease prognosis and metastasis prediction in patients with different types of cancers (Kato et al., 2004; Miskad et al., 2007; Mollevi et al., 2008; Sundar and Gnanasekar, 2013; Tamagawa et al., 2012; Xing et al., 2009), including gastric cancer (Bilici et al., 2012; Hu et al., 2013; Xing et al., 2013), nasopharyngeal carcinoma (Zhou et al., 2009), ovarian cancer (Huang et al., 2014; Ren et al., 2009), breast cancer (Hao et al., 2010; Radke et al., 2006; Ustaalioglu et al., 2012; Wang et al., 2006), uveal melanoma (Laurent et al., 2011), intrahepatic cholangiocarcinoma (Xu et al., 2010), esophageal squamous cell carcinoma (Liu et al., 2008; Ooki et al., 2010), oral squamous cell carcinoma (Hassan et al., 2011), endometrioid cancer (Guzinska-Ustymowicz et al., 2013), and acute myeloid leukemia (AML) with FLT3-ITD mutations (Park et al., 2013). Further, two studies showed high levels of PRL-3 in cancer metastases than primary tumor or non-metastatic tumor by unbiased global gene expression profile (Laurent et al., 2011; Saha et al., 2001), reinforcing PRL-3's significance in metastasis prediction.

Other than being an independent prognostic biomarker, PRL-3 has also been shown to have better prognostic value when combined with the expression levels of other genes. For example, combined analysis of synuclein-gamma (SNCG), a human homologue of

piwi (Hiwi), PRL-3, and arrest-defective protein 1 homolog A (ARD1) provides better prognosis value than PRL-3 alone in patients with colon cancer (Liu et al., 2012). In this thesis, I show that the combination of autophagy genes together with PRL-3 provides better prognostic value than using them separately (Huang et al., 2014). Being such an important predictor of cancer metastasis and general patient outcome, PRL-3 has good potential to be a therapeutic target.

1.6.2 PRL-3 Serves As A Therapeutic Target

Researchers have tried different ways to target PRL-3 for cancer therapy *in vitro* and *in vivo*. RNA interference based methods aimed at knocking down PRL-3 showed inhibition of cancer cell growth and metastasis. For example, the artificial miRNA based on murine miR-155 sequence, effectively silenced PRL-3 in SGF7901 gastric cancer cell line and significantly reduced cell growth, invasion and migration (Li et al., 2006). PRL-3 siRNA was also used as a molecular medicine to specifically reduce the expression of PRL-3 in B16-BL6 cells, a highly metastatic melanoma cell line. It showed both *in vitro* activities to inhibit cell migration and invasion, and *in vivo* activity to inhibit tumor progression in mouse models (Qian et al., 2007b).

Chemicals that function to block PRL-3 expression also proved their anti-cancer value *in vitro* and *in vivo*. Curcumin is a component of the spice turmeric, which selectively downregulates the expression of PRL-3, and the treatment of curcumin was able to inhibit mouse melanoma cancer cell B16BL6 growth (Wang et al., 2009). Another chemical 1-4-bromo-2-benzylidene rhodanine, as a PRL-3 inhibitor, was found to suppress metastatic properties of esophageal squamous cell carcinoma cell lines with PRL-3 overexpression (Ahn et al., 2006; Min et al., 2013). Rhodanine derivatives, such as CG-707 and BR-1,

inhibiting PRL-3 enzymatic activity strongly, also showed inhibition of the migration and invasion of PRL-3 overexpressing colon cancer cells (Min et al., 2013).

Exogenous antibodies against PRL-3 inhibited PRL-3 positive cancer cell growth in mouse models (Guo et al., 2011b). Antibody is more specific than chemical based PRL-3 inhibitors, causing less off-target and side effects in patients. Moreover, unlike RNA interference based methods, antibody therapy is a "DNA free" method, and therefore, safer to the patients. Being more specific and safer, antibody based methods to target PRL-3 is of great potential in clinical studies. Significantly, PRL-3 antigen induced host-produced antibody also provided an effective therapy in mouse harboring PRL-3 positive cancers (Guo et al., 2011b). Recently, we also found that targeting PRL-3 overexpressing ovarian cancer using autophagic inhibition shows effective inhibition on tumor cell proliferation (Huang et al., 2014).

Based on an immunohistochemistry screening assay, there are 22.3% PRL-3 positive cancers among 1000 cancer samples (Wang et al., 2010). Thus, PRL-3 is targetable in these large number of cancer patients. Finding more effective methods to target PRL-3 is of great value.

1.7 Rationale And Hypothesis

As a strong oncogene, PRL-3 promotes multiple carcinogenesis processes. More importantly, PRL-3 is specifically upregulated in cancers, making it a suitable target for cancer therapy. However, many studies showed that PRL-3 protein levels and RNA levels are not well correlated, indicating that post-transcriptional regulations of PRL-3 plays a significant role in determining its protein expression level. There is a study showing that

PRL-3 is regulated negatively by PCBP1 translationally, but the post-translational regulation of PRL-3 is still unclear.

In mammalian cells, there are mainly two protein degradation pathways, namely lysosomal proteolysis pathway (autophagy) and ubiquitin-proteasome pathway. The endosomal localization of PRL-3 indicates that it may be correlated with autophagy, since endosome fuses with autophagosome, the organelle for autophagy degradation (Cai et al., 2010; Hansen and Johansen, 2011; Razi et al., 2009). My initial hypothesis is:

PRL-3 protein is degraded by autophagy.

To investigate this hypothesis, I set the following aims:

1. To test the localization of PRL-3, and its correlation with autophagosome, which is the organelle for autophagic degradation.

2. To test the changes in the expression level of PRL-3 upon autophagic degradation inhibition / induction.

3. To study the possible mechanisms for the degradation of PRL-3 by autophagy.

Confirming the specific autophagosomal localization of PRL-3 by immunofluorescence imaging, I also found that with the overexpression of PRL-3, LC3 signals increased upon autophagic degradation inhibition. LC3 is an autophagosome marker. Thus the results suggest that the overexpression of PRL-3 contributes to increased autophagosome formation. This led to my second hypothesis:

PRL-3 enhances autophagy.

To investigate this hypothesis, I set the following aims:

1. To test the whether the overexpression of PRL-3 is able to speed up autophagy process including autophagosome formation and autophagy substrate degradation.

2. To test the signaling pathways affected by PRL-3 to in promoting autophagy.

3. To test the biological significance of PRL-3 in promoting autophagy. More specifically, to determine the role autophagy plays in PRL-3 mediated cancer cell proliferation.

4. To test the clinical relevance of my *in vitro* finding in ovarian cancer patients' cohort.

According a screen of PRL-3 expression level in different cancer cell lines, we found that HCT116 cell line expresses relatively high level of endogenous PRL-3 protein, while PRL-3 protein expression level is significantly lower in Hkh-2 cell line. HCT116 is a human colorectal cancer cell line that harbors a constitutively activated mutant KRas allele (KRas-G13D), and Hkh-2 is an isogeneic cell line of HCT116. The only difference between HCT116 and Hkh-2 is that the mutant KRas allele (KRas-G13D) was disrupted in Hkh-2 cell line. Thus, Hkh-2 is a KRas wild type counterpart cell line of HCT116. The results suggest that constitutive mutant KRas expression is positively correlated with PRL-3 protein level. This led to my third hypothesis:

PRL-3 expression level can be upregulated by constitutively activated KRas.

To investigate this hypothesis, I set the following aims:

1. To test whether PRL-3 protein level is affected by constitutively activated mutant KRas, by knocking down / overexpressing constitutive activated mutant KRas.

2. To determine such regulation is through transcriptional level or post-transcriptional level.

3. Find out the signaling pathways that regulate PRL-3 expression level by KRas mutation.

The results from my experiments investigating all three hypotheses above constitute the primary body of my thesis.

CHAPTER 2: MATERIALS AND METHODS

2.1 Reagents

2.1.1 Chemicals

Unless otherwise specified, chemicals were used at the following concentrations: Chloroquine diphosphate salt (CQ) (50 μM, Sigma-Aldrich, #C6628); Rapamycin (2 μM, Sigma-Aldrich, #R8781); E64D (10 μg/mL, Sigma-Aldrich, #E8640); Pepstatin A (10 μg/mL, Sigma-Aldrich, #P5318); bafilomycin A1 (100 nM, Sigma-Aldrich, #B1793), U0126 monoethanolate (U0126) (10 μM, Sigma-Aldrich, #U120); PD98059 (50 μM, Sigma-Aldrich, #P215).

2.2 Plasmids

2.2.1 EGFP-tagged wild-type and mutant PRL-3 constructs

EGFP-tagged wild-type and phosphatase dead (PDM) mutant PRL-3 constructs were generated previously (Al-Aidaroos, 2012). Simply put, cDNA of PRL-3 was cloned into pEGFP-C1 vector (Clontech USA), using forward and reverse primers containing EcoRI and BamHI restrictions sites. pEGFP-PRL-3-PDM was generated using iNtRON Site-Directed Mutagenesis Kit (iNtRON, #15071) according to the manufacturers' manual.

2.2.2 myc-tagged PRL-1 and PRL-3 constructs

Myc-tagged PRL-1 and PRL-3 constructs were generated previously (Zeng et al., 2003). Simply put, Myc epitope (10 amino acid residues) was introduced at the N terminus of PRL-1 or PRL-3 by a PCR-based approach. The restriction sites EcoRI and BamhI were used to insert into vector pStar (Zeng et al., 1998b).

2.2.3 Untagged PRL-3 Construct pBabe-PRL-3

RNA from human colorectal cancer cell line HCT116 was extracted using RNeasy Mini Kit (QIAGEN, 74104) according to the manufactures' manual. cDNA of these RNA was generated using RevertAid Reverse Transcriptase (Thermo Scientific, #EP0441). cDNA corresponding to human PRL-3 was cloned into the pBabe-puro vector (Clontech, USA) using forward and reverse primers containing restriction sites BamHI or EcoRI. Phusion High-Fidelity DNA Polymerase (Thermo Scientific, F-534S) was used according to the manufactures' manuals. The PCR cycling parameters were as follows: initial denaturation 98 °C, (30 sec); amplification – 25 cycles of 98°C (10 sec), 55°C (15 sec), 72°C (15 sec); final extension 72 °C (5 min). PCR products were purified by 1% agarose gel, and gel-extraction kit. Purified PCR product and pBabe-puro vector were digested with EcoRI (EcoRI-HF) and BamHI (BamHI-HF) restriction enzymes from New England Biolabs (NEB), followed by ligation using Quick Ligation Kit (New England BioLabs, M2200L) according to the manufacturers' manuals. After incubation in room temperature for 10 minutes, 2 µl of the ligation mixture was added to 50 µl competent cells in a 1.5ml microcentrifuge tube on ice. Incubate the competent cells on ice for 30 minutes, followed by 30 seconds heat shock at 42 °C. Add 950 µl LB to this microcentrifuge tube. Shake at 37°C for 60 minutes. Spread the mixture from this tube onto agar plates containing antibiotics. Up to 5 single colonies were picked, and plasmids were extracted for DNA sequencing. Sequencing data were collected in an ABI prism 377 DNA Sequencer (Applied Biosystems, SUA) by the DNA Sequencing Unit of Institute of Molecular and Cell Biology (IMCB), Singapore.

2.2.4 pLKO.1 shRNA Constructs

2.2.4.1 pLKO.1-shPRL-3, pLKO.1-shBeclin-1, pLKO.1-shhVps34, pLKO.1-shATG5

All these shRNA constructs were purchased from Sigma-Aldrich.

2.2.4.2 pLKO.1-shKRas-1, pLKO.1-shKRas-2 constructs

pLKO.1 - TRC Cloning Vector (Addgene, #10878) was used as backbone. The oligos contain shRNA specifically against KRas were cloned into this backbone according to the manuals from Addgene. Two target sequences of KRas were used. shKRas-1: 5′ GATACAGCTAATTCAGAATC 3′; and shKRas-2: 5′ AGGCTCAGGACTTAGCAAGA 3′.

2.3 Cell Lines And Derivatives

2.3.1 Cell Culture

CHO (Chinese Hamster Ovary) -K1 cells (ATCC), human ovarian carcinoma cell line A2780 (ATCC), were cultured in RPMI-1640 medium supplemented with 10% fetal bovine serum (hyClone, SV30160.03), 2 mM L-glutamine (Life Technologies, 25030-081), and 1% antibiotic/anti-mycotic (Life Technologies, 15140-122), which is defined in the text as “full media”. Human colorectal cancer cell line HCT116 (ATCC) was kept in Dulbecco’s Modified Eagle’s Medium (DMEM) - high glucose (4500mg/L) supplemented with 10% fetal bovine serum (hyClone, SV30160.03), 2 mM L-glutamine (Life Technologies, 25030-081), and 1% antibiotic/anti-mycotic (Life Technologies, 15140-122). Cells were starved in FBS depleted medium (serum-free medium) or HBSS as indicated. The viral packaging cell line Phoenix Ampho (a gift from the Nolan Laboratory, Stanford University) and HEK 293T cells (ATCC) were also maintained in DMEM high glucose full media.

HCT116 (active K-Ras mutant) and its wild-type isogenic counterpart Hkh-2 cancer cell lines were maintained in DMEM full media supplemented with sodium pyruvate. DLD-1(active K-Ras mutant) and its wild-type isogenic counterpart DKO3 cells cancer cell lines were maintained in RPMI full media (Shirasawa et al., 1993) (all these four cell

lines are from Professor T. Sasazuki, Department of Genetics, Medical Institute of Bioregulation, Kyushu University, Higashi, Japan, and Professor S. Shirasawa, Department of Pathology, International Medical Center of Japan, Tokyo, Japan). All cells were maintained in a 5% CO_2 atmosphere at 37 °C.

2.3.2 Generation of CHO-K1 Cells Stably Overexpress PRL-1 or PRL-3

CHO-PRL-1 and CHO-PRL-3 were generated previously (Zeng et al., 2003).

2.3.3 Generation of A2780 Cell Line Stably Expresses EGFP, EGFP-PRL-3 or EGFP-PRL-3-PDM

A2780-Vec, A2780-PRL-3 and A2780-PRL-3-PDM were generated previously (Al-Aidaroos, 2012).

2.3.4 Generation of cancer cell lines stably express untagged PRL-3 (retrovirus based method)

The day before transfection, Phoenix Ampho were seeded in a 6-well culture plate (5 x 10^5 cells/well). Transfection was achieved using JetPRIME according to the manufacturers' instructions (Polyplus-transfection, 114-75). Detailed procedures are as below: change fresh DMEM for the cells to be transfected (2mL for each 6-well). 10 minutes before transfecting cells, mixed pBabe-PRL-3 or pBabe-PRL-3-PDM plasmid DNA with 200 µL jetPRIME buffer. Mix by vortexing. After that, add 4 µL jetPRIME reagent, vortex for 10 seconds, and spin down briefly. Incubate at room temperature for 10 minutes. Add the transfection mix drop wise and slowly to the cells in each 6-well (2µg DNA is sufficient for the transfection of one 6-well), and distribute evenly. Gently rock the plate back and forth and from side to side. Replace transfection medium after 4 hours by fresh DMEM full-media. Cells were let grown for 48 hours. After 48 hours, supernatant containing retrovirus was collected, and filtered through a 0.45µm filter. Directly use it to infect target cells for making stable cell lines (see below).

24 hours before infection, around 3 X 10^5 of target cells were seeded in a well of a 6-well-plate. Polybrene was added to the retroviral supernatant got in the previous step, the final concentration of polybrene was 6μg/mL. Viral supernatant from one 6-well is sufficient to infect target cells in one 6-well. Incubate target cells in viral supernatant overnight. After that, remove viral supernatant and recover cells in fresh full media. Let cells recover for 24 hours before antibiotic selection.

The backbone of pBabe-PRL-3 and pBabe-PRL-3-PDM was pBabe-puro, which contains a puromycin resistant element. Target cells were selected using puromycin with the concentration of 0.5 μg/ml.

2.3.5 Generation of Cancer Cell Lines Stably Knockdown PRL-3, hVps34, Beclin-1, ATG5, or KRas (lentivirus based method)

The day before transfection, HEK293T were seeded in a 6-well culture plate (5 x 10^5 cells/well, about 50% confluency). Transfection was achieved using JetPRIME transfection reagent according to the manufacturers' instructions similar with the previous section. For each 6-well, mix 250ng pCMV-VSV-G (addgene, #8454), 750ng pCMV-dR8.2 dvpr (addgene, #8455), and 1 μg pLKO.1-puro (addgene, #8453) containing shRNA sequence of indicated genes for transfection. Transfection and virus harvest procedures are similar as previous.

Target cells were seeded 24 hours before infection. Similarly, supernatant containing lentivirus was added to target cells for overnight incubation.

2.4 Quantitative Real Time PCR (qRT-PCR)

2.4.1 RNA Isolation

Cellular RNA was extracted using RNeasy kit (Qiagen, USA). Briefly, cell monolayers (around 80% confluency) were lysed directly in 350 µL of Buffer RLT containing 1% β-mercaptoethanol (v/v). Cell lysates were passed through a QIAshredder spin column in room temperature for homogenization. 350 µL of 70% ethanol (v/v) was added to the homogenized cell lysate, mixing by pipetting up and down. The mixed solution was passed through an RNeasy spin column. After centrifugation in room temperature, RNA will bound to the membrane of the RNeasy spin column. The column was washed by once with 700 µL Buffer RW1, twice with 500 µL Buffer RPE, and spun at full speed for 2 minutes to complete dry it before elusion using 50 µL of RNase-free water. Eluted RNA was quantified using a Nanodrop spectrophotometer (Thermo Fisher Scientific).

2.4.2 cDNA Synthesis

RNA extracted according to the methods above was preceded for cDNA synthesis (Thermo Scientific, RevertAid Reverse Transcriptase, #EP0441) following the manufacturers' manual. Briefly, 1 µg of total RNA sample were first mixed with 100pmol oligo$(dT)_{20}$, and RNase-free water in a 12.5 uL volume and heated at 65°C for 5 min. Subsequently, the mixture was chilled on ice for 2 minutes. cDNA synthesis mix (including: 5X Reaction Buffer, 4 µl; RNase inhibitor (Thermo Scientific RiboLock RNase Inhibitor, #EO0381), 20 u; dNTP Mix with the concentration of 10 mM, 2uL, RevertAid Reverse Transcriptase, 200 u) was added to the pre-chilled mixture of total RNA and Oligo$(dT)_{20}$. Incubate 60 minutes at 42°C, followed by 10 minutes termination a 70°C. Synthesized cDNA can be kept in -20°C or used immediately for Real-Time PCR.

2.4.3 Quantitative Real-Time PCR (qRT-PCR)

For qRT-PCR, 50 ng cDNA was used in each reaction. Commercially optimized TaqMan Gene Expression Assay system was used for qRT-PCR according to the manufacturers' manual. TaqMan Gene Expression Assay mix and primers specific for human PRL-3(PTP4A3) or human GAPDH were all purchased from applied biosystems. To ensure reproducibility and robust statistical significance, biological triplicates were used, with each gene-specific qRT-PCR reaction done in triplicate in an Optical 96-Well Fast Plate (Applied Biosystems, USA).

2.5 Immunoprecipitation (IP)

IP reactions were done in spin columns (Thermo Scientific, USA) according to the manufacturers' manual. Briefly, antibodies (for antibodies from Cell-signaling technologies, 4μL of antibody was used for each reaction) were first bound to 20 μL equilibrated Protein-A/G beads in the coupling buffer (0.01M sodium phosphate, 0.15M NaCl; pH 7.2) for 1 hour at room temperature, with gently rotation. Unbounded antibodies were washed away twice using coupling buffer, followed by centrifugation at 1000g at 4°C. Antibodies were subsequently crosslinked to Protein-A/G beads using 450 μM disuccinimidyl suberate (DSS) in coupling buffer for 45 minutes at room temperature. Low pH elution buffer (0.1 M glycine; pH 2.8) was used to remove unbounded antibodies. IP Lysis/ Wash buffer (0.025M Tris, 0.15M NaCl, 0.001M EDTA, 1% NP-40, 5% glycerol; pH 7.4) was used to equilibrate the antibodies crosslinked beads for optimal binding with the antigens. After washing three times using 400μL of IP Lysis/ Wash buffer, antibodies crosslinked beads were further used for IP.

For each IP reaction, cells grown in 10cm dishes were harvested in 800uL IP Lysis/Wash Buffer with the addition of protease inhibitor and phosphatase inhibitor. Lysates were incubated on ice for 15 minutes before centrifuged for 20 minutes at 16,000 X g at 4°C. Supernatants were collected, quantitated using BCA assay (Thermo Scientific). 1mg protein adjusted to 350~400 μL was used for each IP reaction, and 0.1 mg protein was saved as input control. The protein lysate was added to the agarose beads crosslinked with indicated antibodies for overnight night incubation with gentle rotation at 4°C. Immunoprecipitates were subsequently washed with 1X Tris-Buffered Saline (TBS) (0.025M Tris, 0.15M NaCl; pH 7.2) for 3 times, and once with 100μL of 1X Conditioning Buffer (neutral pH buffer). Elute first with 10 μL Elution buffer (pH 2.8), followed by second elution of 50 μL elution buffer. Lysates aliquots and eluted immunoprecipitates were immediately boiled for 10 minutes after the addition of 6X SDS loading dye. After denaturation, samples were stored in -20°C until use.

2.6 Western Blotting

2.6.1 Standard SDS-PAGE Preparation

Cells were treated as indicated and harvested in RIPA buffer (10 mM Tris-Cl (pH 8.0), 1 mM EDTA, 1% Triton X-100, 0.1% sodium deoxycholate, 0.1% SDS (w/v), 140 mM NaCl) with protease inhibitor (Roche cOmplete Protease inhibitor cocktail tablets #11697498001), and phosphatse inhibitor (Nacalai USA, Phosphatase Inhibitor Cocktail (EDTA free) (100X)) freshly added. Protein amount was quantified using BCA protein assay kit (Thermo Scientific 23225) according to the manufacturer's manual. Home-made acrylamide resolving gels were prepared using 30% Acrylamide/Bis Solution, 37.5:1 (Bio-Rad, 161-0158), 10% sodium dodecyl sulphate (SDS) (w/v), 10% APS (w/v), 1.5M Tris-Cl pH8.8, Milli-Q H_2O, and tetramethylethylenediamine (TEMED). I used 10% or

12.5% gel according to the molecular weight of target protein. For each 10% resolving gel, 3.9 mL H_2O, 3.3 mL 30% bis-acrylamide (Bio-Rad), 2.5 mL 1.5 M Tris-Cl pH 8.8, 100 uL 10% SDS, 100 uL 10% APS, and 10 uL TEMED were gently mixed together, and immediately poured in glass plates with 1.5 mm spacers (Bio-Rad). 2 mL H_2O was layered above the gel to remove the bubbles. Wait for 30 minutes in room temperature for a complete polymerization of the resolving gel. The recipe for each 12.5% gel is as follows: 3.1 mL H_2O, 4.2 mL 30% bis-acrylamide (Bio-Rad), 2.5 mL 1.5 M Tris-Cl pH 8.8, 100 μL 10% SDS, 100 μL 10% APS, and 10 μL TEMED. Water above the resolving gel was removed using paper towels. Stacking gels were prepared according to the following recipes: for each gel, 0.53 mL 30% acrylamide, 1 mL 0.5 M Tris-Cl pH 6.8, 2.4 mL H_2O, and 40 μL 10% SDS, 40μL 10% APS, and 6 μL TEMED were mixed gently, and poured above resolving gels. Combs were immediately placed into the stacking buffer before polymerization. Keep in room temperature for 30 minutes for a complete polymerization before use. Samples with SDS loading buffer were boiled at 100 °C for 10 minutes before loading to each well. Equal amount of protein was loaded to each well of a gel. Gels were run in 1 X SDS-PAGE running buffer (250 mM Tris, 250 mM glycine, 0.1% SDS) at 80V for 20 minutes, followed by 120 V until the dye front reached the bottom of the gel. Protein markers (1^{st}-base) were used as a reference of protein size.

2.6.2 Gel Transfer

SDS-PAGE gels were removed from glass plates and soaked in pre-chilled transfer buffer (25 mM Tris pH 7.3, 192 mM glycine, 20% methanol) prior to transfer. Pre-cut filter paper, nitrocellulose membranes (Pall Corporation) were also soaked in the transfer buffer. The transfer stack was subsequently assembled in ice-cold transfer buffer. The transfer was performed under 100 V in ice-cold transfer buffer for 1.5 hours.

2.6.3 Immunoblotting and Immuno-detection

Membranes were blocked in 5% skim milk (sigma) in TBS-T (50 mM Tris, 150 mM NaCl, 0.05% Tween 20, pH adjusted to 7.5~7.6) for one hour in room temperature, with gentle shaking. For non-phosphorylated antigens, 5% skim milk in TBS-T was also used as buffer to dilute antibodies. Membranes were incubated with diluted primary antibodies overnight at 4 °C. Membranes were subsequently washed 3 times in TBS-T for 15 minutes each before incubating with horse radish peroxidase (HRP)-conjugated secondary antibodies for one hour at room temperature. After that, membranes were washed 3 times again in TBS-T for 15 minutes each. 1:1 SuperSignal West Pico Luminol/Enhancer Solution and SuperSignal West Pico Stable Peroxide Solution were mix freshly (Thermo Scientific, USA). Membranes were incubated with the mixture for 5 minutes in room temperature for 5 minutes with gentle shaking. X-ray films (Fujifilm, Japan) were exposed to the membranes in a dark room before developing in an X-OMAT processor (Kodak, USA). Developed films were scanned using scanner (Epson, USA).

2.6.4 Band Quantification

Band quantification was done using imageJ according to protocols available online (Using ImageJ to Quantify Blots, http://www.di.uq.edu.au/sparqimagejblots)

2.7 Microscopy Analysis

2.7.1 Immunofluorescence Imaging

Cells were seeded on glass coverslips at relatively lower densities (about 20% - 30% confluency) 24 hours before treatment or transient transfection of plasmids. For experiments which requires both transient transfection of EGFP-LC3 and the treatment of CQ, cells were allow growth for 24 hours after the transient transfection before treatment.

After indicated treatments/ transfections, cells were briefly rinsed in PBSCM (DPBS supplemented with 1 mM $CaCl_2$ and 1 mM $MgCl_2$) for 2 minutes, followed by fixation in 4% formaldehyde for 15 minutes at room temperature. The 4% formaldehyde was diluted from methanol free 16% Formaldehyde (Polysciences, Inc. #50-00-0) with Dulbecco's phosphate-buffered saline (DPBS, 2.7 mM KCl, 1.5 mM KH_2PO_4, 136.9 mM NaCl, 8.9 mM $Na_2HPO_4•7H_2O$). Fixed cells were thoroughly washed with PBSCM 3 times, 5 minutes each with gentle shaking. Cells were then permeabilized and blocked using blocking buffer (5 % BSA, 0.3 % Triton-X100 in DPBS) in room temperature for 1 hour. After washed 3 times in DPBS, coverslips were incubated in primary antibodies diluted by antibody dilution buffer (1 % BSA, 0.3 % Triton-X100 in DPBS) overnight at 4 °C. Anti-LC3 antibody (cell signaling technology, #3868) was used at a dilution of 1:200, and anti- PRL-3 antibody (Li et al., 2005) was used at a dilution of 1:400. Coverslips were then washed three times with DPBS again and then incubated with secondary antibody (1:400 dilution; Life Technologies, A10040, A10036) conjugated with appropriate fluorophore for 1 hour at room temperature in the dark. After the incubation of secondary antibodies, coverslips were washed with DPBS for 3 times, 5 minutes each. For F-actin staining, rhodamine-phalloidin (Life technologies) diluted in PBS was added to permeabilized cells for 20 min, followed by washing. Coverslips were wiped at the edges to remove excessive buffers before mounting. Each coverslip was mounted with 8 μL of VECTASHIELD mounting medium (Vector Laboratories, USA) on a slide with correct labeling.

Edges of mounted coverslips were applied a layer of nail polish to avoid dryness, and the smashing between coverslip and the slide. Mounted coverslips were immediately analyzed using an LSM700 confocol microscope (Carl Zeiss AG). The average of LC3 channel pixel intensity value within the cytoplasmic area pre cells was determined using Photoshop (Adobe system). The results were presented as mean ± SD.

2.8 Cell Proliferation Assays

2.8.1 MTT Cell Growth Assay

5000 cells were resuspended in full media (with 10% FBS), seeded triplicate well of a 96-well plate, and allow to attach overnight. The media were replaced with full media / serum free media with different treatments as indicated, and left for incubation. MTT (3-(4,5-Dimethylthiazol-2-yl)-2,5-Diphenyltetrazolium Bromide) reagent (#M5655, Sigma-Aldrich) was added at a final concentration of 0.2mg/mL in each well. After that, cells were incubated in 37 ^{o}C with 5% CO_2 for 3 hours. Media were completely removed and the retained formazan crystals were than dissolved in 150uL DMSO, and the absorbance at 595 nm was measured.

2.8.2 Trypan Blue Viability Assay

A2780 cells were seeded in full media into 6-wellplate and allowed to grow for 24 hours before treatment. Medium with indicated drug was added to each well. Cells treated with indicated drug were put back for incubation in 37°C. Cells were harvested by trypsinization and neutralized using full-medium, before counted with Vi-CELL XR cell viability analyzer (Beckman Coulter). The percentage of viable cell is recorded. Viable cells were distinguished from the dead cells since trypan blue is not able to penetrate the viable cell membrane. Thus, there is an absence of intracellular trypan blue staining in the viable cells.

2.9 ULK1 Activity Assay

Cells were lysed by RIPA buffer and concentration of protein was determined by Coomassie (Bradford) Protein Assay (Thermo-Pierce, Northumberland, UK) against a BSA standard curve. Immunoprecipitation was performed using 1 mg of total protein

lysate. Volume will be adjusted across samples and the samples were then incubated with 2 μg of anti-ULK1 antibody (homemade sheep anti-ULK1 by Dr. James Murray) at 4ºC on a vibrax shaker for overnight. Immunocomplexes were captured by adding 20 μl of a 50% Protein-G Sepharose (GE Lifesciences, Buckinghamshire, UK) bead slurry and incubated for 1 hr at 4 ºC on a vibrax shaker. After incubation, beads were collected by centrifugation at 2,500 x g for 1 min, washed three times in Low Salt Buffer (50 mM Tris-Cl, pH 7.5, 1 mM EGTA, 1 mM EDTA, 0.3 % (w/v) CHAPs, 1 mM sodium orthovanadate, 50 mM sodium fluoride, 5 mM sodium pyrophosphate, 0.27 M sucrose, 0.1 % (v/v) 2-mercaptoethanol) and two times in Assay Buffer (20 mM Hepes, ph 7.5, 150 mM NaCl, 0.1 % β-mercaptoethanol, 25 mM β-glicerophosphate, 100 μM orthovanadate). The beads were collected again, re-suspended in 24 μL of Assay Buffer and processed for ULK1 kinase activity assay.

ULK1 assay was made at 30^0C in Assay Buffer (above), containing immunoprecypitated ULK1, 10 mM MgAc, 3 μg myelin basic protein (MBP), 100 μM [^{32}P] ATP (100-1000 cpm/pmol) in final reaction volume 30 μl. The reaction was quenched after 30 min by addition of 10 μL of 4 x LDS sample buffer and heating samples for 10 min at 70^0C. All samples were loaded on 8 % Bis-Tris gels and resolved in MOPS buffer. The whole gels were transferred onto Immobilon-P (Millipore). The upper part of membrane contained ULK1, was used for Western blot to estimate the level of immunoprecipitated enzyme. The lower part of the membrane, containing phosphorylated MBP substrate was exposed for 24-72 hours to a phosphoimager screen. Incorporated radiolabel was detected by phosphoimager using an FLA-7000 Phosphoimager system (Fujifilm UK, Bedford, Middlesex) and quantified using MultiGuage software. The ULK1 activity was normalized to levels of immunoprecypitated protein detected by immunoblot. Specific activity was expressed as a percent of control and plotted using GraphPad Prism 5.0.

2.10 Soft Agar Assay

The soft agar assay for colony formation tests the anchorage independent growth ability of cells. Briefly, the procedures are as follows. Prepare 2.8 %, and 1.4 % low-melting-point agarose (DNA grade) (Invitrogen) in serum-free media, and autoclave before first use. Heat autoclaved agarose until fully melted before use. Mix 1 mL 2.8 % low-melting-point agarose, 0.9 mL RPMI full-media, and 0.1 mL FBS to make the bottom layer of the agarose (The mixture is 2 mL in total, with 10% FBS, and 1.4 % low-melting-point agarose). 2 mL mixture is enough for one well in a 6-well plate. Put the 6-well plate in 4 ^{o}C until agarose get fully solidified. After the bottom layer of agarose solidified, start to prepare for the top layer of agarose. Mix 1 mL 1.4 % low-melting-point agarose, 0.9 mL full-media resuspending with $2X10^4$ indicated cells, and 0.1 mL FBS to make the top layer of the agarose (the mixture is 2 mL in volume, with 10% FBS, 0.7% low-melting-point agarose, and $2X10^4$ cells resuspending). Gently add the mixture on top of the bottom layer. Put in room temperature for several hours until fully solidified. Add 0.5 mL full-media on top of the agarose, and change fresh media every other day. Observe under microscope every day. Normally it takes one to two weeks to form cell colonies become visible to the naked eyes.

After the formation of these naked-eye-visible colonies, take pictures of single colonies under microscope and picture of the whole well using normal digital camera. Colonies may need to be stained using crystal violet before images capturing by normal digital camera.

Briefly, the processes of crystal violet staining are as follows: remove media and add 1 mL DBPS containing 4% formaldehyde and 0.005% crystal violet to each well. Incubate overnight at 4 ^{o}C. After incubation, pipette off staining media and wash with DPBS gently. Take photos using normal digital camera.

2.11 Human Ovarian Cancer Microarray Dataset Analysis

The biggest Gene Expression Omnibus (GEO) -accessible ovarian cancer database GSE9899 was used in this study. The database consists of microarray and survival data from 285 ovarian cancer patients. The microarray data were pre-processed using RMA algorithm in Bioconductor for normalization. Patients were divided into 4 subgroups based on their PRL-3 mRNA expression using quartiles as the cut-off point. The four groups are weak, moderate, strong, and very strong. For Kaplan-Meier survival analysis, I divided the patients into 2 groups, namely, high PRL-3 group ("very strong" PRL-3 mRNA expression group), and low PRL-3 group ("weak, moderate, and strong" PRL-3 mRNA expression groups). The association between PRL-3 expression and patients' survival and clinical –pathological parameters was tested by Chi-Square, while the association between PRL-3 and patients survival was tested by Kaplan- Meier analysis together with log-rank test. I further divided high / low PRL-3 mRNA expression groups based on their hVps34, Beclin-1, or ATG5 mRNA expression levels using the median value as a cut-off point to distinguish a more autophagy competent subgroup, and a less autophagy-competent subgroup.

2.12 Statistical Analysis

For experiments other than statistical analyses in the clinical data, the Student's *t*-test was used to test for significant differences. For qRT-PCR, the paired t-test was used to analyze the biological triplicates for significance. The statistical analyses in the clinical data were performed using SPSS19.0 software (IBM Corporation). One way ANOVA was performed for comparisons of means between groups. The *P* value for comparison of 2 groups in the same experimental setting was generated by ANOVA post-hoc test, either

Tukey HSD or Games-Howell, depending on the results from the homogeneity test by Levene statistics, where applicable. A p value of < 0.05 was considered as significant in all tests.

CHAPTER 3: PRL-3 IS A NOVEL AUTOPHAGIC SUBSTRATE

3.1 Background

All cellular proteins undergo synthesis and degradation. Such renewal process is necessary for the regulation of protein level in cells, and fulfilling normal metabolism and homeostasis of functional cells. Protein synthesis can be regulated in multiple levels including RNA transcription and protein synthesis. Protein degradation is mediated by two major pathways: lysosomal proteolysis pathway (autophagy) and ubiquitin-proteasome pathway (Korolchuk et al., 2009).

The expression of PRL-3 has to be regulated very precisely since its upregulation may cause cancer by affecting multiple carcinogenesis processes (Al-Aidaroos and Zeng, 2010). Moreover, the upregulation of PRL-3 also correlates with poor prognosis in multiple types of cancers (Al-Aidaroos and Zeng, 2010). Thus, understanding how PRL-3 is regulated may shed lights on unveiling how PRL-3 promotes cancer progression as well as how to target PRL-3 in cancer therapy.

PRL-3 was regulated by genomic amplification (Saha et al., 2001), transcription (Basak et al., 2008), and translation (Wang et al., 2010). Moreover some studies suggest that PRL-3 is degraded through a proteasome pathway under special conditions. For example, Zhou *et al.* showed that Suberoylanilide hydroxamic acid (SAHA) triggers the proteasome degradation of PRL-3. SAHA is a histone deacetylase (HDAC) inhibitor. It has been approved by US Food and Drug Administration (FDA) for the treatment of T-cell lymphoma (Zhou et al., 2011). However, the mechanism of post-translational regulation of PRL-3 remains poorly understood. Lysosomal proteolysis pathway is the alternative post-translational regulation of proteins than proteasome degradation pathway, and autophagy is the major route for delivery of cellular proteins and RNAs into lysosomes for degradation (Dunn, 1994).

The term “autophagy” was derived from Greek, meaning “eating of self”. It was first described by Russell L. Deter and Christian de Duve about 50 years ago. They reported that mitochondria and other intracellular structures were degraded in lysosomes of rat liver (Deter and De Duve, 1967). Indeed, autophagy is an evolutionarily conserved process involved in selective degradation of cellular proteins and damaged organelles by lysosomes (Mizushima, 2007). There are three types of autophagy: micro-autophagy, chaperone-mediated autophagy, and macro-autophagy (Mizushima, 2007). Micro-autophagy is the direct engulfment of cytoplasmic materials into the lysosome (Li et al., 2012). Chaperone-mediated autophagy is a highly selective process, in which heat shock cognate protein of 70 kDa (Hsc70) containing complex recognizes the substrates, and sends them one by one to lysosome for degradation (Kaushik and Cuervo, 2012). Macro-autophagy is the main autophagy pathway occurs in cells, and it is also the best-studied form of autophagy (Mizushima, 2007). In this thesis, I will focus on macro-autophagy, and it is referred to as “autophagy” hereafter.

Although it was first reported almost half a century ago, the mechanisms of autophagy were only started to be revealed in the recent years, when the technique of molecular biology becomes much more advanced. Till now, 32 autophagy-related genes (ATG) have been identified by genetic screening in yeast, many of which are conserved in most eukaryotes, including yeast, plants, worms, flies and mammals. Such conservation suggests that autophagy is important in most living organisms (Nakatogawa et al., 2009).

Autophagy is mainly governed by ATG proteins. The initiation of autophagosome formation starts with the activation ULK1 in mammals (Itakura and Mizushima, 2010). ULK1 is the mammalian ortholog of ATG1 in yeast, and it is a key regulator of autophagy in all eukaryotes (Mizushima, 2010). The formation of autophagosome starts after receiving the initiation signals. There are four steps of canonical autophagosome formation: 1) initiation; 2) nucleation; 3) elongation; and 4) closure. Nucleation, which

requires hVPS34-Beclin-1 complex, happens right after initiation of autophagosome formation. hVPS34 is the catalytic subunit of phosphatidylinositol 3-kinase (PI3K), which belongs to the class III PI3K family, and it phosphorylates PtdIns to generate PtdIns3P, a lipid second messenger essential for autophagosome trafficking (Petiot et al., 2000; Takegawa et al., 1995). Beclin-1 is the mammalian ortholog of yeast Atg6, and its interaction with hVps34 contributes to the recruitment of autophagy proteins to the nucleating phagophore assemble site (PAS) (He and Levine, 2010). This process is followed by autophagosome elongation and closure, in which the soluble LC3-I is conjugated to phosphatidylethanolamine (PE) to form a membrane-bound form of LC3, LC3-II. LC3 is the ortholog of yeast Atg8. This process is termed LC3 conversion, and it is essential for canonical autophagosome formation, which requires ATG5 (Hanada et al., 2007; Weidberg et al., 2011). With all these steps, autophagosome, a double-membrane vesicle wrapping cellular components for degradation, will be formed. However, many studies showed that in some cases, autophagosome formation could also occur independent of some of these genes, or even bypass some of these steps (Codogno et al., 2012). These special autophagosome formation processes are called "noncanonical autophagosome formation". After closure, the complete and newly formed autophagosome, wrapped with all the unwanted organelles and autophagy substrates will fuse with lysosome, forming autolysosme for future degradation (Mizushima, 2007). Recent studies showed that before the formation of autolysosome, endosome might also fuse with autophagosome to form amphisome, suggesting that endosome is also playing a role in autophagy regulation (Cai et al., 2010; Hansen and Johansen, 2011; Razi et al., 2009). Lysozyme in the autolysosme degrades the autophagic substrate, releasing digested short peptides, amino acids, and other nutrients to the cytosol for reuse (Mizushima et al., 2010). The process of canonical autophagy is summarized in **Figure 3.**

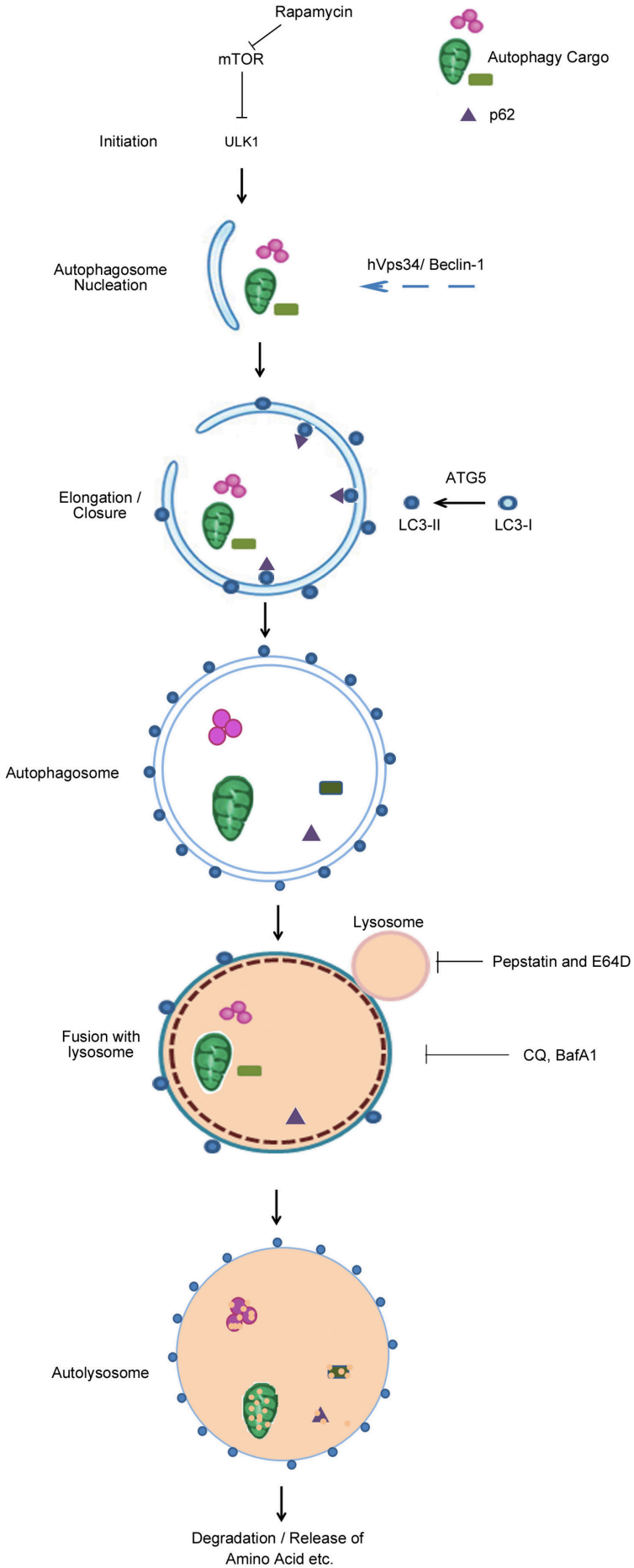
Rapamycin
mTOR
Initiation
ULK1
Autophagy Cargo
p62
Autophagosome
Nucleation
hVps34/ Beclin-1
Elongation /
Closure
ATG5
LC3-II
LC3-I
Autophagosome
Lysosome
Pepstatin and E64D
Fusion with
lysosome
CQ, BafA1
Autolysosome
Degradation / Release of
Amino Acid etc.

Figure 3. Canonical autophagy process. Details of the process were described in the text.

Different chemicals and treatments are used to study autophagy. Since autophagy is initiated by the intracellular signals such as serum and amino acid starvation (He and Klionsky, 2009), Hank's Balanced Salt Solution (HBSS) is broadly used to induce autophagy. HBSS is balanced solution consist of various salts and sugar, which is able to maintain suitable pH and osmotic balance to cells. Chloroquin (CQ), bafilomycin A1 (Baf A1), and the combination treatment of pepstatin and E64D (Pepstatin +E64D) are also widely used in autophagy studies. CQ is a lysosomal acidification inhibitor that blocks autophagic degradation (Amaravadi et al., 2011); Baf A1 functions to prevent maturation of autophagic vacuoles by inhibiting fusion between autophagosomes and lysosomes (Weiss et al., 2012); while pepstatin and E64D are both lysosomal protease inhibitors that inhibit autophagic degradation (Amaravadi et al., 2011). Therefore, these chemicals are all known as inhibitors of the late phase of autophagy. Genetic manipulation of autophagy gene is also commonly used in autophagy studies. Knockdown of autophagy genes such as ATG5 (Mizushima et al., 2001), or Beclin-1 (Mizushima et al., 2001; Yue et al., 2003) leads to autophagy deficiency / reduction.

PRL-3 and PRL-1 are two members of PRL family, which share 79% amino acid identity (Zeng et al., 1998a), and both of them localized to the cytosolic face of the plasma membrane and early endosome in a prenylation dependent manner (Zeng et al., 2000). Endosomes were reported to be involved in regulating autophagy since it may fuse with autophagosome before the fusion of autophagosome to lysosome for degradation (Cai et al., 2010; Hansen and Johansen, 2011; Razi et al., 2009). Thus, PRL-3, as an endosomal protein may also be related to autophagy.

In this chapter, I will focus on autophagy regulation of endosomal protein PRL-3.

3.2 Outline of Experiments

1. To test PRL-3 and PRL-1 localization upon autophagic degradation inhibition, PRL-1 or PRL-3 overexpressing Chinese Hamster Ovary (CHO) cells were treated with autophagic degradation inhibitor CQ for 24 hours, followed by immunofluorescence imaging. PRL-1/ PRL-3 and LC3 were labeled by different fluorescent dye. Results were confirmed in human ovarian cancer cell line A2780, human colorectal cancer cell line DLD-1 and HCT116.

2. PRL-1 and PRL-3 protein level changes after autophagic induction using HBSS were determined by western blotting. p62, a known autophagic substrate was used as a positive control.

3. Autophagy degradation was blocked chemically (CQ, Baf A1 or Pepstatin+E64D) or genetically (autophagy gene knockdown). After that, PRL-3 protein level (both endogenous and exogenous expressed) changes were determined by western blotting, and p62 was used as a positive control.

4. Immunofluorescence imaging was used to test whether PRL-3 and p62 may colocalize upon autophagic degradation inhibition. Immunoprecipitation was used to identify the interaction of PRL-3 and autophagic cargo receptor p62.

3.3 Results

3.3.1 PRL-3 But Not PRL-1 Colocalizes With LC3 Puncta in CHO Cells

To investigate whether endosomal protein PRL-1 or PRL-3 plays a role in autophagy, I co-labeled PRL-1 or PRL-3 together with autophagosome marker LC3. To achieve this goal, I used Chinese Hamster Ovary (CHO) cell line which stably overexpresses either myc tagged PRL-1 (CHO-PRL-1) or myc tagged PRL-3 (CHO-PRL-3). Upon autophagosome formation, the cytosolic form of LC3 (LC3-I) is conjugated to PE to form LC3-II, which is recruited to autophagosome membranes (Tanida et al., 2008). Thus, LC3 positive signal in immunofluorescence imaging has been characterized as a signature of autophagosome (Berg et al., 1998; Kabeya et al., 2000). In order to have stronger signals of LC3, I transiently overexpressed Enhanced Green Fluorescent Protein (EGFP)-tagged LC3 in these two cell lines, and inhibited autophagosome degradation using the treatment of CQ.

With CQ treatment for 24 hours, LC3 puncta accumulated clearly compared to untreated in both CHO-PRL-1 and CHO-PRL-3 cell lines. The localization of PRL-1 protein remained unchanged before and after CQ treatment (**Figure 4A**); however, PRL-3 protein accumulated and colocalized with LC3 positive puncta with CQ treatment (**Figure 4B**). To reaffirm that PRL-3 colocalized with LC3 puncta upon autophagic degradation inhibition, I overexpressed EGFP-tagged version of PRL-3 in CHO cells (CHO-GFP-PRL-3), treated with CQ, and stained with endogenous LC3. Similarly, after CQ treatment, endogenous LC3 also formed puncta, and colocalized with PRL-3 (**Figure 4C**). Thus, PRL-3 but not PRL-1 colocalized with autophagosome upon autophagic degradation inhibition.

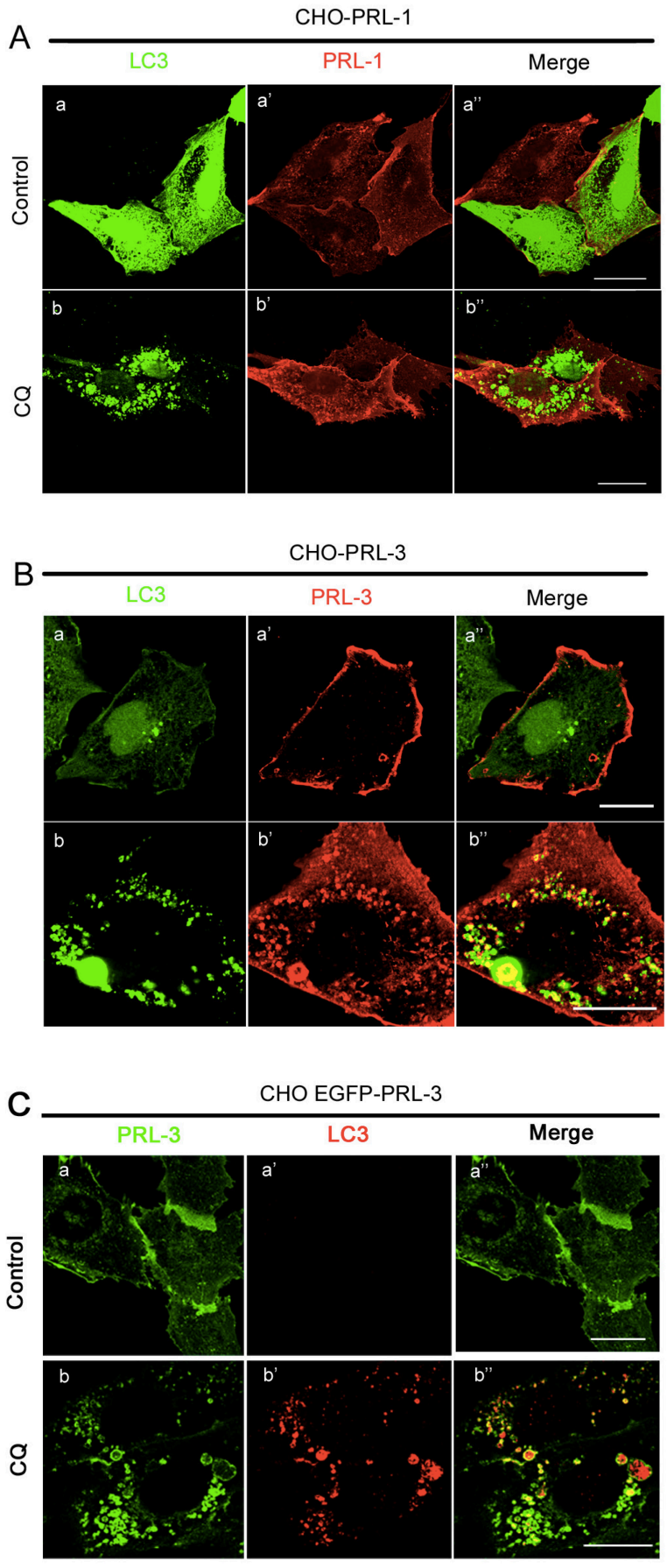
A
CHO-PRL-1
LC3
PRL-1
Merge
Control
CQ
a
a'
a''
b
b'
b''
B
CHO-PRL-3
LC3
PRL-3
Merge
a
a'
a''
b
b'
b''
C
CHO EGFP-PRL-3
PRL-3
LC3
Merge
Control
CQ
a
a'
a''
b
b'
b''

Figure 4. PRL-3 but not PRL-1 colocalized with LC3-positive puncta upon autophagic degradation inhibition in CHO cells. (**A-B**) CHO cells overexpressing (**A**) myc-tagged-PRL-1 (CHO-PRL-1) or (**B**) myc-tagged PRL-3 (CHO-PRL-3) were transiently transfected with EGFP-LC3 construct, and allowed growth for 24 hours. Subsequently, the cells were treated with (CQ)/ without (control) CQ in full media (with 10% FBS) for 24 hours before immunostaining with anti-myc antibody. (Scale bar 20μm). (**C**) CHO cells with EGFP-PRL-3 overexpression were treated with (CQ) / without (Control) CQ for 24 hours, followed by immunostaining with anti-LC3 antibody to show the endogenous LC3 signals (red) in the cells. (Scale bar 20μm)

3.3.2 PRL-3 Colocalizes With LC3 Puncta Independent Of Its Phosphatase Activity And Dependent On Its Prenylation Association Membrane Localization

To gain more insight on the mechanism of the colocalization of PRL-3 and autophagosome, human ovarian cancer cell line A2780 was also used to overexpress EGFP-tag (Vec), EGFP-tagged PRL-3 (PRL-3), EGFP-tagged PRL-3-phosphatase dead mutant (PRL-3-PDM), or EGFP-tagged PRL-3 prenylation mutant (PRL-3-ΔPre). The consensus CAAX sequence in the C-terminal of PRL-3 enables it to be prenylated, where C is cysteine, A is an aliphatic amino acid, and X is any amino acid (Brown and Goldstein, 1993; Moores et al., 1991). To generate PRL-3-ΔPre, the cysteine-170 was replaced with a Serine residue in the C-terminus of PRL-3, and thus disrupts the prenylation. With such disruption of the prenylation, PRL-3 expresses in the nucleus instead of locating in the membrane. I treated the cells with CQ and monitored the immunofluorescence imaging of cells (**Figure 5A-D**). EGFP localized in the cytosol, and the location remains unchanged with or without CQ treatment (**Figure 5A**). Similar with the results obtained in CHO cells, wild type PRL-3 localized in autophagosome upon CQ treatment (**Figure 5B**). PRL-3-PDM had similar localization with wild-type PRL-3 (**Figure 5C**), while, PRL-3-Δ-Pre lost the ability to localize in autophagosome under CQ treatment (**Figure 5D**). The treatment of another late stage autophagy inhibitor Bafilomycin A1 (Baf A1) showed that PRL-3 started to colocalize with LC3 puncta as

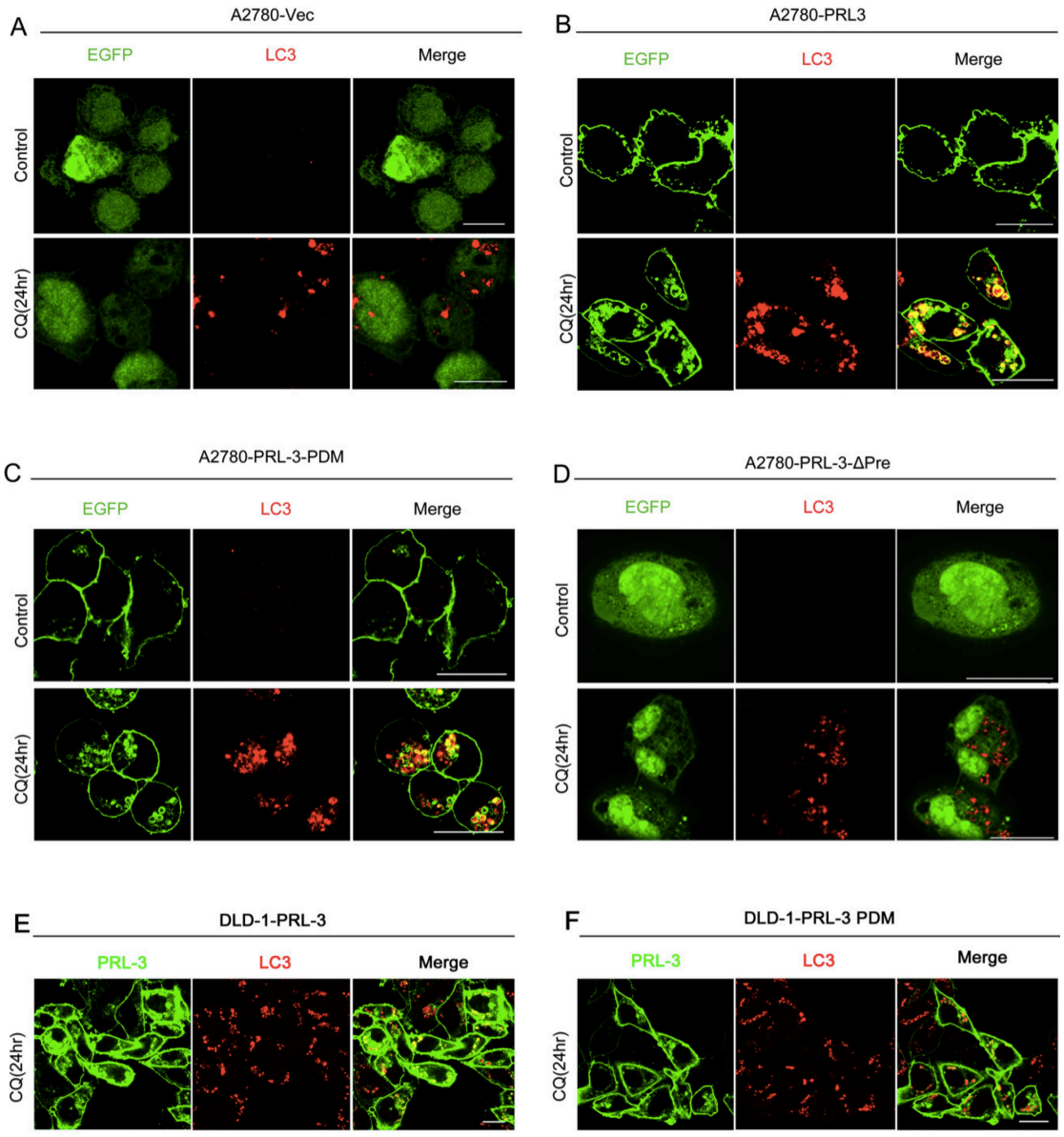

Figure 5. PRL-3 colocalized with LC3 positive puncta in human cancer cell lines independent of its phosphatase activity, and dependent on its prenylation motif. (**A-D**) A2780 cells overexpressing (**A**) EGFP-vector (Vec), (**B**) EGFP-tagged-PRL-3 (PRL-3), (**C**) EGFP-tagged-PRL-3-phosphatase dead mutant (PRL-3-PDM), or (**D**) EGFP-tagged-prenylation domain mutant (PRL-3-ΔPre) were treated with (CQ) / without (Control) CQ for 24 hours before immunostaining with endogenous LC3 (red) respectively. (**E-F**) DLD-1 cells overexpressing (**E**) untagged PRL-3 (DLD-1-PRL-3) or (**F**) untagged PRL-3-phosphatase dead mutant (DLD-1-PRL-3-PDM) were treated with CQ for 24 hours prior to immunofluorescence labeling with PRL-3 (green) and endogenous LC3 (red). (Scale Bar 20 μm)

early as 1 hour (**Figure S1**). The results suggest that the localization of PRL-3 in autophagosome is not a non-specific effect due to prolonged (24 hours) autophagy inhibition.

In order to rule out the effects of epitope tags on PRL-3's localization (EGFP or myc tag), I overexpressed untagged PRL-3 and PRL-3-PDM in a colorectal cancer cell line DLD-1, and then treated with CQ, and co-labeled both PRL-3 and endogenous LC3. Consistently, both untagged PRL-3 and untagged PRL-3-PDM colocalized with autophagosome upon CQ treatment (**Figure 5E-F**). The results had also been confirmed in another human colorectal cancer cell line HCT116 (**Figure S2**). Collectively, my results suggest that PRL-3 colocalizes with LC3 in autophagosome independent of its phosphatase activity, but dependent on its C-terminal prenylation.

3.3.3 PRL-3 is Degraded Specifically Upon Autophagy Induction

The localization of PRL-3 in the autophagosome suggests that PRL-3 may be playing a role in autophagy. One of the possibilities is that by locating to autophagosome, PRL-3 is degraded by autophagy. To test this hypothesis, I treated CHO-PRL-1 and CHO-PRL-3 cells with Hanks' balanced salt solution (HBSS), and checked whether this treatment affect PRL-1 or PRL-3 protein level. HBSS is an amino acid-free media commonly used to create a starvation condition for autophagy induction (Mizushima, 2007). With the treatment of HBSS for 24 hours, PRL-3 protein level decreased dramatically while PRL-1 protein level remained unchanged (**Figure 6A**). To confirm the results, I treated DLD-1 Vector control (DLD-1-Vec) and DLD1 PRL-3 overexpressing cells (DLD-1-PRL-3) with HBSS for 24 hours. Similarly, PRL-3 protein level decreased significantly after HBSS treatment (**Figure 6B**).

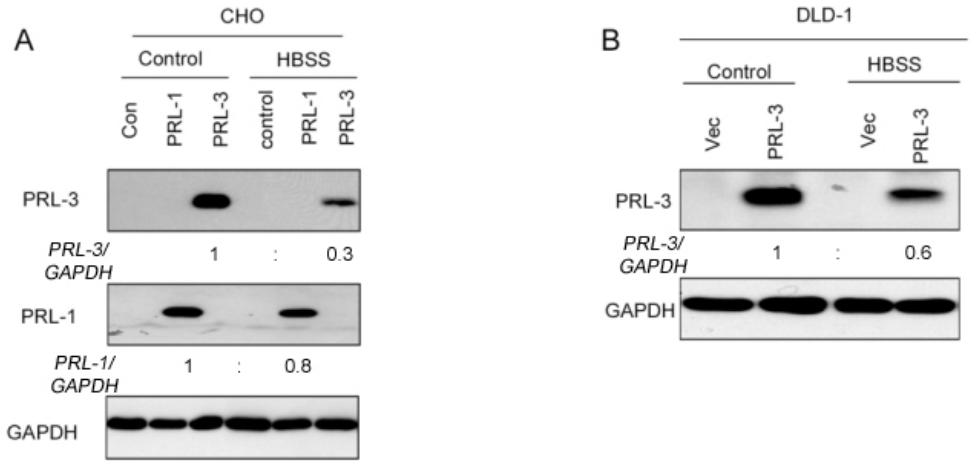

Figure 6. PRL-3 was degraded specifically upon autophagic induction. (**A**) CHO-con, CHO-PRL-1 and CHO-PRL-3 were treated in full media (control) or HBSS as indicated for 24, before lysis for western blotting analysis. PRL-1 and PRL-3 protein levels were checked using antibodies as indicated. GAPDH was used as loading control. (**B**) DLD-1-vector only (Vec) and DLD-1-PRL-3 cells were treated as indicated for 24 hours. Cells were lysed for Western blotting analysis to check the expression level of PRL-3. GAPDH was used as loading control.

3.3.4 PRL-3 Protein Specifically Accumulates Upon Autophagic Degradation Inhibition

CQ blocks autophagic degradation, and thus leads to the accumulation of autophagic substrates. I treated CHO-con, CHO-PRL-1 and CHO-PRL-3 cells with CQ to block autophagic degradation for 24 hours. With such treatment, p62/SQSTM1 (p62) protein accumulated dramatically (**Figure 7A**). p62 is a known autophagic substrate, which is degraded by autophagy (Bjorkoy et al., 2005; Pankiv et al., 2007). Similar with p62, PRL-3 protein also accumulated after CQ treatment. However, PRL-1 protein level remained unchanged (**Figure 7A**). Pepstatin and E64D are lysosomal protease inhibitors, which also inhibit autophagic degradation (Amaravadi et al., 2011). Similar with CQ, the treatment of Pepstatin + E64D also led to an accumulation of p62. Importantly, both CQ and Pepstatain + E64D treatments caused PRL-3 protein accumulation in CHO-PRL-3

cells (**Figure 7B**). The results suggest that similar with p62, PRL-3 is also degraded by autophagy. According to **Figure 5**, PRL-3-PDM localized in autophagosome upon CQ treatment, which is similar with wild-type PRL-3. Next, I investigated whether the PRL-3-PDM can also be degraded by autophagy. I overexpressed wild type PRL-3 or PRL-3-PDM in A2780 and DLD-1 cells respectively, treated with CQ for 24 hours (**Figure 7C**). Similar to p62, exogenous PRL-3 and PRL-3-PDM accumulated with CQ treatment in both A2780 and DLD-1 cells (**Figure 7C**). HCT116 expresses detectable level of endogenous PRL-3, so I used this cell line to investigate whether endogenous PRL-3 is also degraded by autophagy. Similar with CQ, Bafilomycin A1 (Baf A1) is another late stage autophagy inhibitor, which inhibits autophagic degradation (Yamamoto et al., 1998). The treatment of either CQ or Baf A1 led to dramatic accumulation of p62 as well as endogenous PRL-3 protein (**Figure 7D**). Band intensity quantification of PRL-3/ GAPDH was done using imageJ, and showed in the black bar. mRNA levels of the same samples were quantified by RT-qPCR. mRNA levels were shown in the white bar. There is no upregulation of endogenous PRL-3 mRNA after the treatment of either CQ or BafA1. Therefore, endogenous PRL-3 protein level increases upon CQ or BafA1 treatment, and it was due to post-transcriptional regulation.

More specific inhibition of autophagy pathway can be achieved by knockout or knockdown different autophagy genes (ATG) (Mizushima et al., 2010). What is more, it has been confirmed that cells lacking ATG5 (Mizushima et al., 2001) or Beclin-1 (Mizushima et al., 2001; Yue et al., 2003) had a reduced / defective autophagy activity. Thus, I knocked down Beclin-1 using shRNA in A2780-PRL-3, DLD1-PRL-3, and HCT116 cells, and checked PRL-3 protein levels. With the knockdown of Beclin-1, p62 as well as exogenous PRL-3 protein in A2780-PRL-3, DLD1-PRL-3 cells, and endogenous PRL-3 protein in HCT116 cells accumulated (**Figure 7E**). In a complementary approach, I knocked down ATG5 in A2780-PRL-3, DLD-1-PRL-3, and

HCT116 cells. Similar with Beclin-1 knockdown, ATG5 knockdown resulted in increased p62 and PRL-3 protein levels (**Figure 7F**). To sum up, exogenous PRL-3 and PRL-3-PDM, as well as endogenous PRL-3 were all degraded by autophagy. Thus, like p62, PRL-3 is also an autophagic substrate.

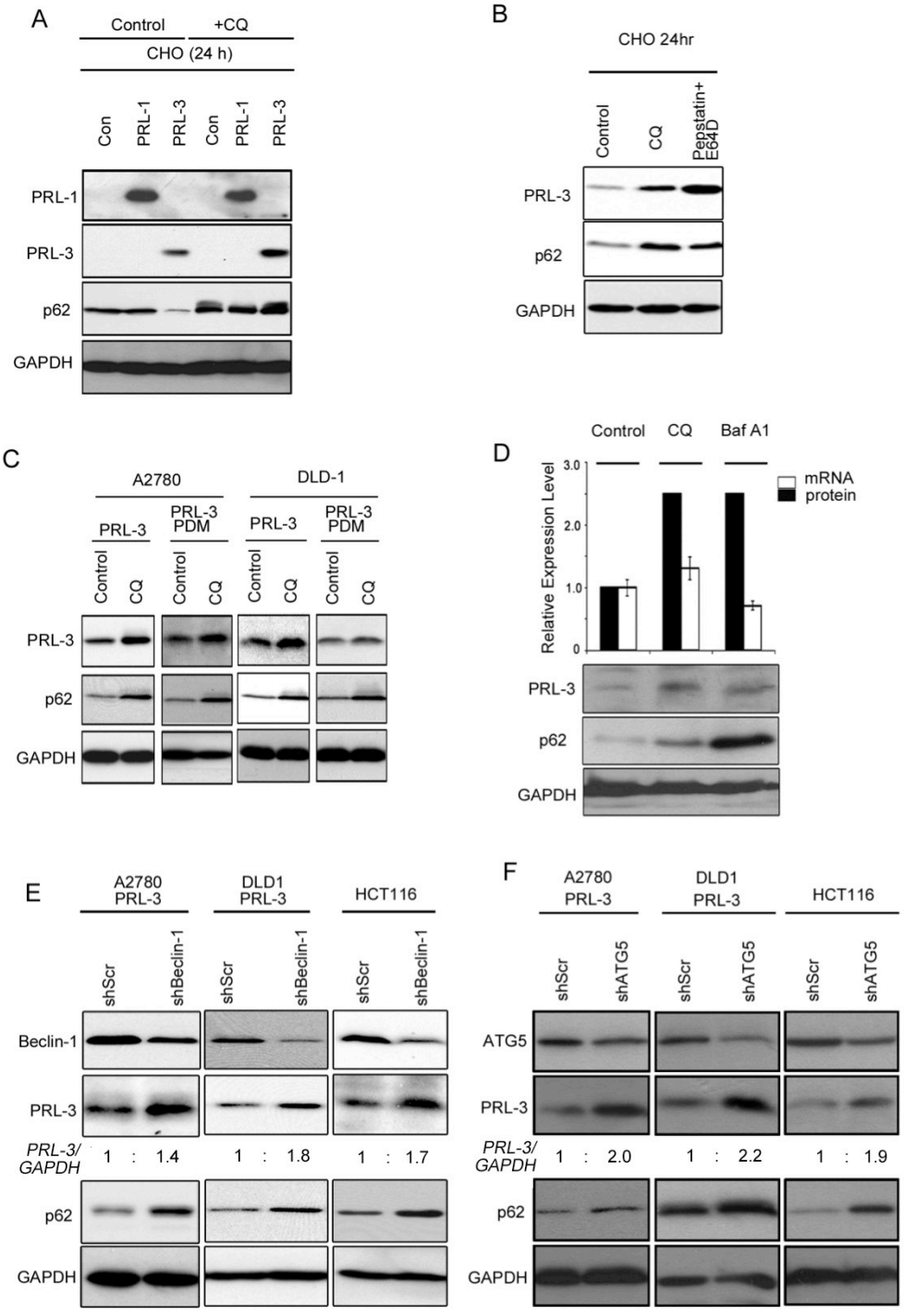

Figure 7. PRL-3 protein specifically accumulated upon autophagic degradation inhibition. (**A**) CHO-con, CHO-PRL-1 and CHO-PRL-3 was treated as indicated for 24 hours, prior to Western blotting analysis. (**B**) CHO-PRL-3 cells were treated in full media (Control), in the presence of CQ (CQ), or the combination treatment of Pepstatin and E64D (Pepstatin + E64D) for 24 hours. Different proteins were analyzed by Western blotting assay. (**C**) A2780-PRL-3, A2780-PRL-3-PDM, DLD-1-PRL-3, and DLD-1-PRL-3-PDM were cultured in full media in the absence of (control), or in the presence of CQ for 24 hours before lysis for western blotting analysis. (**D**) HCT116 cells were cultured in full media in the absence of autophagic inhibitor (control), in the presence of CQ, or in the presence of Baf A1 for 24 hours before lysis for western blotting analysis or RT-qPCR assay. (**E-F**) Exponentially growing A2780-PRL-3, DLD-1-PRL-3 or HCT116 cells transfected with control shRNA (shScr), **(E)** Beclin-1 knockdown shRNA (shBeclin-1), or (**F**) ATG5 knockdown shRNA (shATG5) were lysed for Western blotting analysis, and checked for expression levels of indicated proteins.

3.3.5 PRL-3 Protein Interacts And Colocalizes With p62

p62 is not only a selective substrate that is continuously degraded by autophagy, but also a cargo receptor for selective degradation of other autophagic substrates (Lamark et al., 2009). Thus, one of the possible routes for the autophagic degradation of PRL-3 is through binding to cargo receptor p62.

To test my hypothesis, I transfected CHO-PRL-3 cells with EGFP vector or EGFP-p62, and analyzed GFP immunocomplexes. I found that EGFP-p62 could co-immunoprecipitated PRL-3 under CQ-treated conditions (**Figure 8A**). In a complementary experiment in A2780-GFP-PRL-3 cells, I also found that GFP-PRL-3 could enrich for endogenous p62 (**Figure 8B**). Immunofluorescence data of these cells further supported an interaction between PRL-3 and p62 upon CQ treatment (**Figure 8C**, arrows).

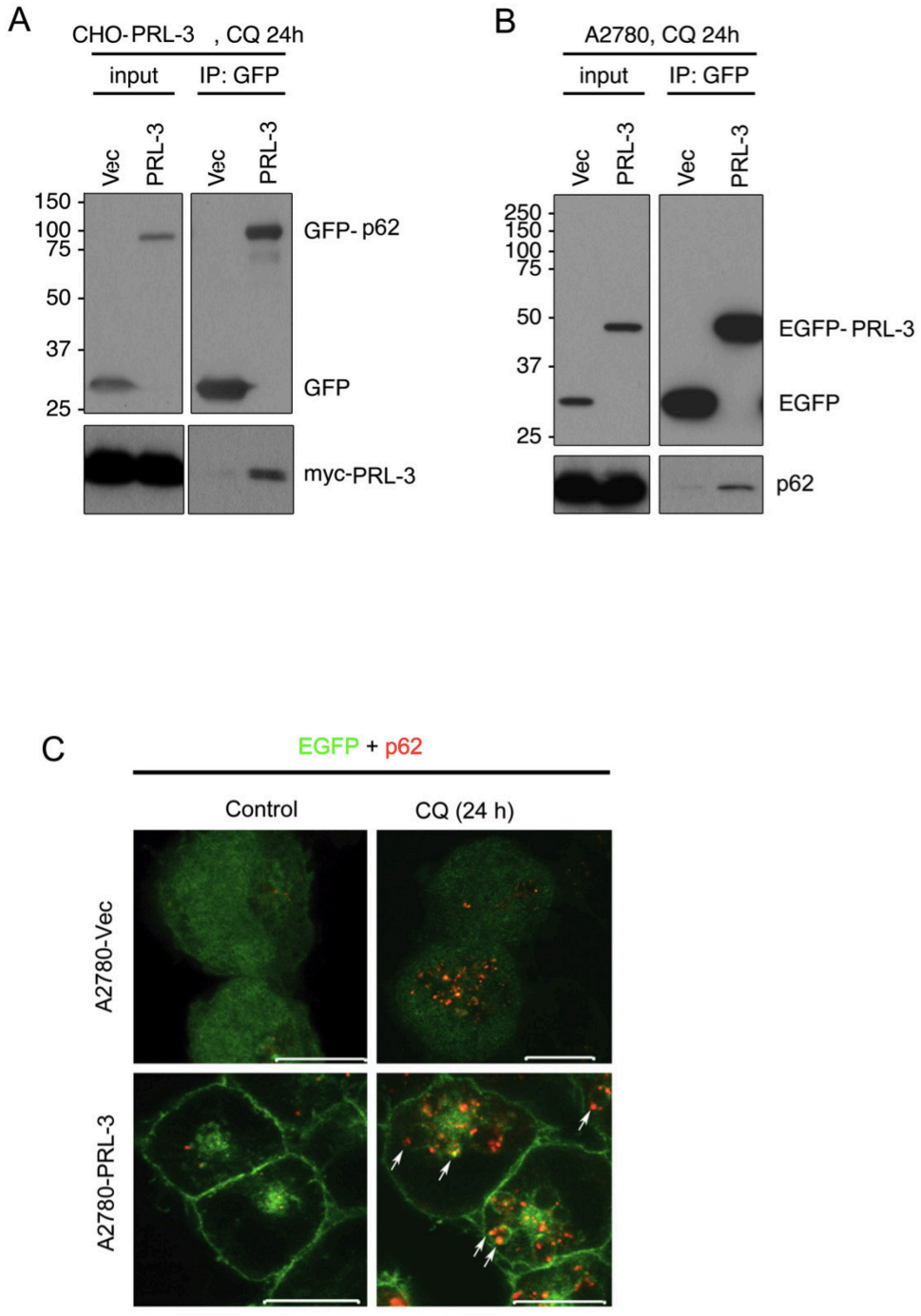

Figure 8. PRL-3 protein was possibly degraded by autophagy through the interaction with p62. (**A**) CHO-myc-PRL-3 cells transfected with pEGFP-C1 vector alone (Vec) or EGFP-p62 (p62) was pretreated with CQ for 24 hours. Anti-EGFP immunoprecipitates from CHO-EGFP-Vec or CHO-EGFP-PRL-3 were probed with antibodies against GFP or PRL-3. (**B**) A2780 transfected with pEGFP-C1 vector alone (A2780-Vec) or pEGFP-PRL-3 (A2780-PRL-3) were pretreated with CQ for 24 hours. Anti-EGFP immunoprecipitates from both cell lines were analyzed by western blotting, and probed with antibodies against EGFP or p62 as indicated. (**C**) A2780-EGFP-Vec and A2780-EGFP-PRL-3 were pretreated in full media with (CQ) / without (control) CQ for

24 hours prior to fixation and immunolabeling with anti-p62 antibody (Red). White arrows show the colocalization of PRL-3 and p62 under CQ treatment.

3.4 Discussion

In the present chapter, I showed that PRL-3, but not PRL-1 localized to autophagosome in a prenylation domain dependent, and phosphatase activity independent manner, after the inhibition of autophagic degradation with CQ treatment. The discovery is surprising, since both of these proteins locate to cytosol membrane and endosome in a prenylation dependent manner, and they share 78% amino acid sequence identity (Zeng et al., 1998a). The results suggest that the autophagosome localization of PRL-3 is not merely caused by its endosomal localization. I did an amino acid sequence alignment of PRL-3 and PRL-1, and found that the biggest amino acid sequence difference between these two genes lies in two clusters (**Figure 9**, red boxes). Interestingly, one of these clusters is between their C-terminal prenylation domain and polybasic domain, and both domains are important for their membrane bound localization. Thus the unique amino acid sequence of PRL-3 here might contribute to its unique localization in autophagosome. However, further studies are still needed to investigate the detailed mechanism of autophagosomal localization of PRL-3.

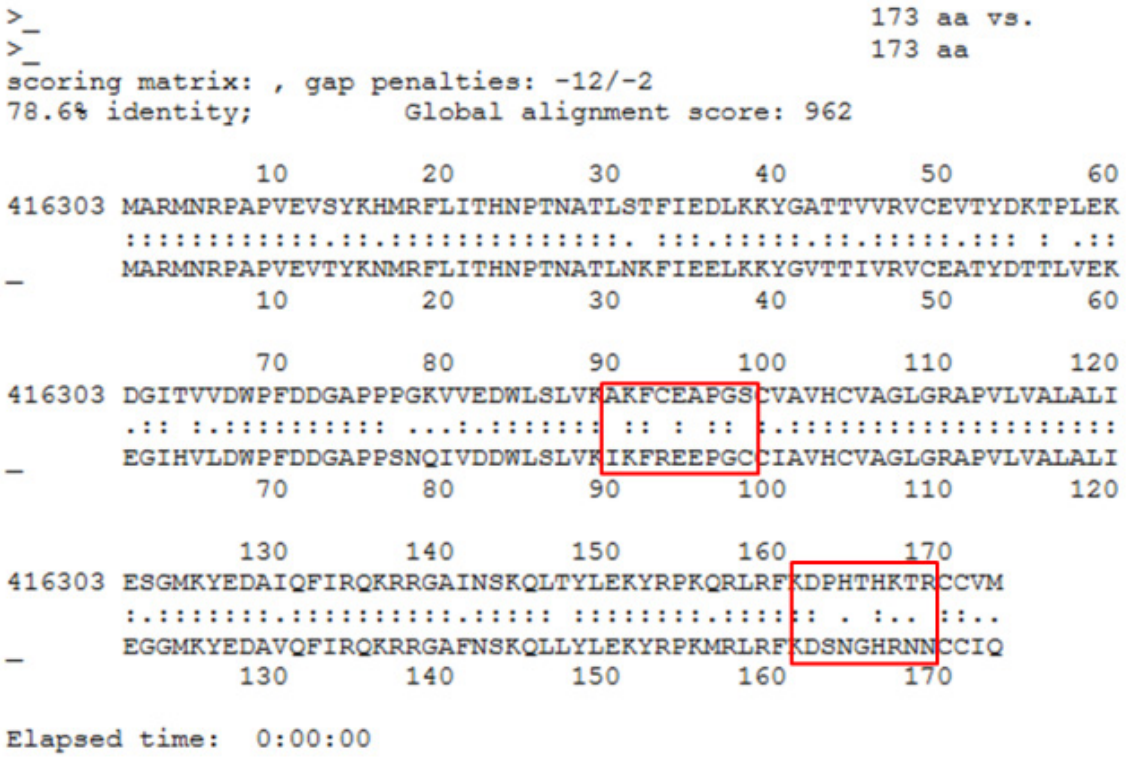

Figure 9. Amino acid alignment of PRL-3 (upper) and PRL-1 (lower). Two dots indicate same amino acid, one dot indicates the two amino acids are from the same group based on their physiochemical properties, and no dots between the two amino acid indicates the two amino acids have distinct properties. Red boxes indicate clusters with biggest difference between the two sequences.

Such autophagosomal localization of PRL-3 strongly indicated that it might play a role in autophagy. p62, as a well-known autophagic substrate, also has autophagosomal localization (Itakura and Mizushima, 2011). Thus, I further investigate whether PRL-3, as an autophagosome protein can also be degraded by autophagy. Again, I used PRL-1, which doesn't localize to autophagosome as a negative control. Unexpectedly, only PRL-3 but not PRL-1 protein accumulated upon autophagic degradation inhibition (**Figure 7**). My results suggest that the localization in autophagosome is needed for protein to get

degraded by autophagy. CQ treatment may cause side effects to the cells other than autophagic degradation inhibition, such as the inhibition of protein synthesis (Ivanina et al., 1989). Thus, I used a more specific method to inhibit autophagy to confirm PRL-3's role as a novel autophagic substrate. Knocking down autophagy genes has been reported to inhibit autophagy activity specifically (Mizushima et al., 2001). Thus, I stably knocked down ATG5 or Beclin-1 in multiple cell lines and checked the expression level of PRL-3. As expected, PRL-3 protein (both exogenous expressed and endogenous expressed), and p62 protein accumulated in multiple cell lines upon autophagy gene knockdown (**Figure 7**). This discovery is important, since the degradation of endogenous PRL-3 by autophagy showed that autophagy is not only degrading PRL-3 due to the clearance of nonspecific affrication of overexpressed proteins (Kopito, 2000). According to my results, I concluded that PRL-3 is a novel autophagy substrate.

Being an autophagic substrate, p62 binds to autophagy regulator LC3 through a region called "LC3-interacting region" (LIR), and this binding is essential for its degradation (Komatsu et al., 2007). What is more, p62 is also an autophagy cargo receptor that regulates the packing and delivery of polyubiquitinated, misfolded, aggregated proteins and dysfunctional organelles for their clearance (Kim et al., 2008; Kirkin et al., 2009; Nezis et al., 2008; Pankiv et al., 2007). Thus, it may bind to other autophagic substrates and target them for degradation. My results suggested that PRL-3 colocalized with, and co-immunoprecipitates with p62 upon CQ treatment (**Figure 8**). The interaction between PRL-3 and p62 may unveil a possible mechanism for how PRL-3 is degraded by autophagy specifically. Despite these data suggesting that PRL-3 binds to p62, it is notable that the interaction appears rather weak (**Figure 8**). It suggests that the two proteins might interact at low stoichiometry and/or that the interaction is transient. Alternatively, other autophagy cargo receptors such as NBR1 or VCP might play a role in

targeting PRL-3 for autophagic degradation. Thus, it is an interesting frontier for future study.

Although the detailed study is still needed, my study firstly showed that PRL-3 is a substrate specifically degraded by autophagy. Autophagy has been shown to suppress tumor formation by removing damaged organelles and unwanted proteins (Mathew et al., 2007). Such mechanisms might be utilized by normal tissues to remove excessive PRL-3, in order to maintain normal tissue homeostasis.

CHAPTER 4: THE ROLE OF AUTOPHAGY IN PRL-3-DRIVEN CANCER PROGRESSION

4.1 Background

Autophagy is an evolutionary conserved catabolic pathway where cells deliver their own cytoplasmic materials or organelles to lysosomes for degradation. After degradation, energy and nutrients are returned to the cytoplasm to be reused for vital biosynthetic reactions in the cell. (Mizushima et al., 2010). Autophagy is important in normal development and cell homeostasis, and thus, autophagy dysregulation has been shown to correlate with different diseases including cancer, diabetes, and neurodegeneration. In this chapter, I will discuss the novel correlations of autophagy and PRL-3, and their correlations in ovarian cancer progression.

Nowadays, most researchers believed that autophagy is playing dual roles in cancer progression depending on genetic background and tumor stage (Janku et al., 2011; Morselli et al., 2009). In some cases, autophagy functions to promote tumor progression. With the accumulation of mutations, tumors may be formed (Loeb et al., 2003). The fast growing tumor tissues consume great amount of oxygen and nutrients. When the tumor tissues reach a certain size, the oxygen and nutrient supply become insufficient, especially for interior of these tissues. Therefore, autophagy is needed for these tissues to reuse energy and nutrients before the formation of new blood vessels. Indeed, it is documented that cells in the tumor interior, where oxygen and nutrients are more likely to be insufficient, has an increased autophagy activity compared to the tumor margins (Degenhardt et al., 2006). Thus, the activation of autophagy contributes to the survival of cancer tissues in extreme conditions. Other than promoting tumor progression, autophagy activation has also been shown to enable tumor cells survive anti-cancer treatment. Anti-cancer treatment creates stress to induce cell death or inhibit cell survival. Autophagy, which attempts to maintain/ restore metabolic homeostasis, may help cancer cells to cope

with therapeutic stresses upon anti-cancer treatment. Some studies showed that inhibition of autophagy sensitizes tumor cells to anti-cancer therapies (Chen and Debnath, 2010; Morselli et al., 2009) For example, chloroquine (CQ) and hydrocholoroquine (HCQ) are drugs that block lysosomal acidification and degradation of autophagosomes (Glaumann and Ahlberg, 1987; Poole and Ohkuma, 1981). Both drugs showed efficacy in combination with other anti-cancer drugs in preclinical models, and both of them are under clinical trials (Janku et al., 2011). Taken together, autophagy supports tumor progression by enabling tumor tissues survive in metabolic and therapeutic stresses.

However, autophagy has also been shown to have a tumor suppressing function. Autophagy is able to clear unwanted protein and damaged organelles in the cells. The accumulation of these unwanted proteins and damaged organelles leads to an increased metabolic stress and chronic tissue damage, which, consequently, results in genetic instability (Janku et al., 2011). Genetic instability refers to a high frequency of mutations within the genome, which may contribute to carcinogenesis process. Thus, by clearing damaged and unwanted organelles, autophagy maintains genetic stability and suppresses cancer. Indeed, Beclin-1, an essential factor for autophagosome nucleation, is also a tumor suppressor gene. Clinical data showed that Beclin-1 is deleted in 75% of ovarian cancer, 50% of breast cancer as well as some cancer cell lines (Aita et al., 1999). Beclin-1 functions as a tumor suppressor has also been proven in *in vitro* models as well as in animal models. Thus, autophagy also has an anti-cancer role (Eskelinen, 2011).

To sum up, autophagy plays either tumor suppressing or tumor promoting role depending on cancer types and genetic backgrounds. In the previous chapter, when I analyzed the data of LC3 and PRL-3 colocalization, I found that CHO-PRL-3 has more LC3 puncta compared to CHO-PRL-1 cells, which may represent an increased number of autophagosome in CHO-PRL-3 cells. Moreover, both PRL-3 and autophagy are playing important roles in cancer progression. Thus I proceeded to investigate:

i) Whether PRL-3 has any effect on autophagic flux;

ii) Whether PRL-3 regulates autophagy through the canonical pathway; and

iii) What is the correlation of PRL-3 and autophagy in cancer progression.

4.2 Outline Of Experiments

1. Quantitation of LC3 puncta intensity of A2780-Vec, A2780-PRL-3 and A2780-PRL-3-PDM by immunofluorescence.

2. Quantitation of LC3 puncta intensity of A2780-Vec, A2780-PRL-3 and A2780-PRL-3-PDM by immunofluorescence after knockdown of Beclin-1 and hVps34.

3. Analysis of LC3 protein levels by Western blotting with or without CQ treatment in CHO and A2780 cells with / without the overexpression of PRL-3 to investigate autophagic flux

4. Analysis of SQSTM1/p62 protein levels by western blotting upon CQ treatment in CHO and A2780 cells as an alternative readout of autophagic flux

5. The effect of autophagy on PRL-3 mediated cell proliferation increase was investigated using MTT assays in A2780-Vec, and A2780-PRL-3, with or without autophagy inhibition

6. To identify the clinical correlation of my in vitro discovery, I analyzed the GSE9899 ovarian cancer patient cohort for the relationship between PRL-3, autophagy genes and survival.

4.3 Results

4.3.1 PRL-3 But Not PRL-1 Promotes Autophagosome Formation Dependent On Its Phosphatase Activity

The fact that PRL-3 colocalized with LC3 (autophagosome) implicated that PRL-3 might play a role in regulating autophagy. More importantly, in the previous experiments, I noticed that CHO-PRL-3 contained more endogenous LC3 puncta quantity compared to CHO-PRL-1. LC3 puncta indicate the location and amount of autophagosome, and thus the increased LC3 puncta may suggest an increased autophagosome number. I stained endogenous LC3 (green) and used actin (red) to mark the cell boundary in CHO-con, CHO-PRL-1 and CHO-PRL-3 cells after the treatment of CQ for 24 hours, and used Photoshop software to quantify the LC3 puncta intensity per cell, which is an indicator for autophagosome number (**Figure. 10 A-B**). Quantification of LC3 puncta intensity confirmed a significantly higher LC3 puncta intensity per cell in CQ-treated CHO-PRL-3 compared to CQ-treated CHO-con or CHO-PRL-1 cells (**Figure.10 B**, $p < 0.01$), meaning more autophagosome were formed in CHO-PRL-3 cells than CHO-con or CHO-PRL-1. The results suggest that PRL-3 but not PRL-1 overexpression promotes autophagosome formation in CHO cells.

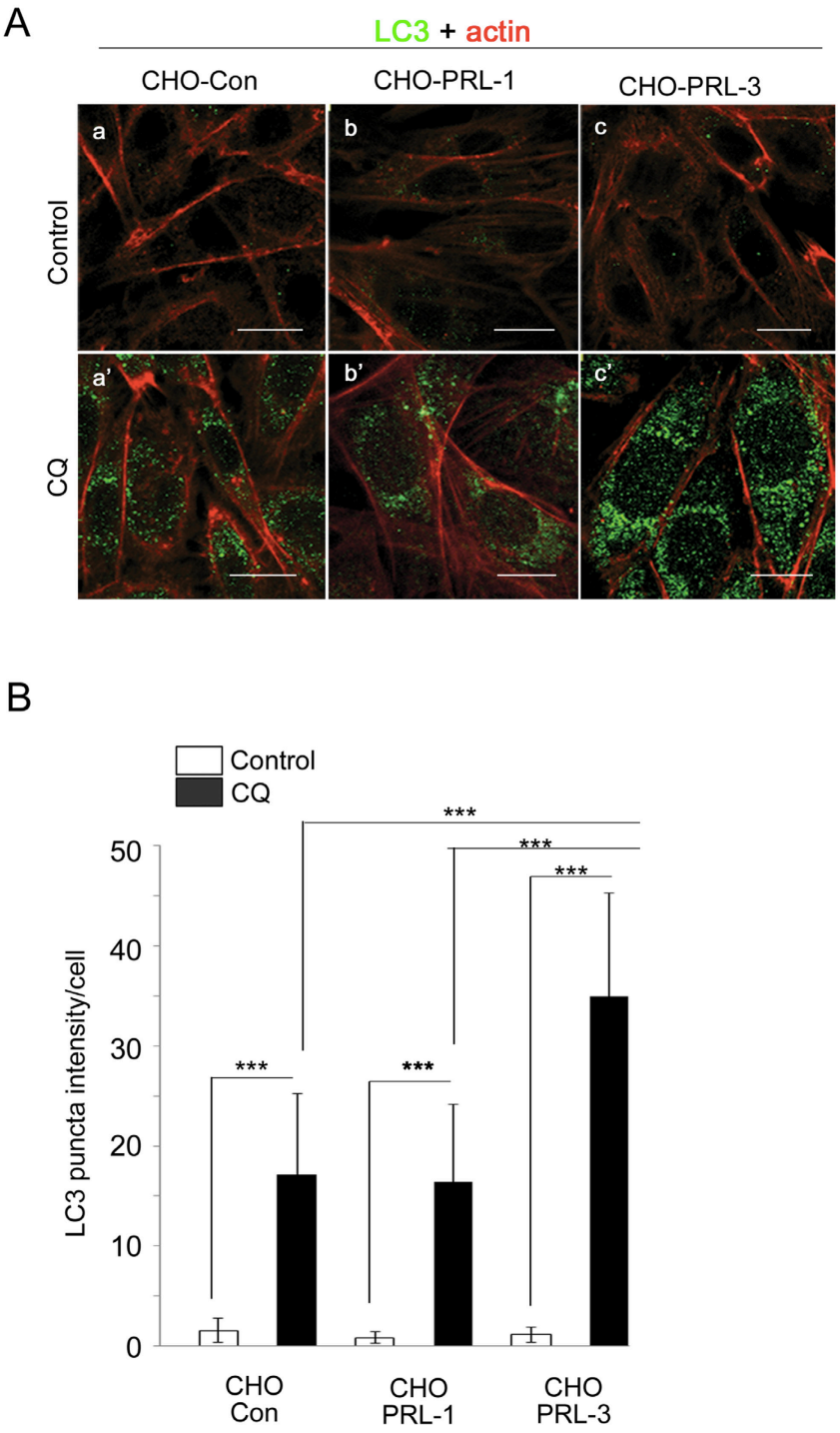

Figure 10. PRL-3 but not PRL-1 promotes autophagosome formation. (**A**) CHO control (CHO-con), CHO-PRL-1, and CHO-PRL-3 were treated without (Control) / with CQ for 24 h prior to immunostaining for LC3 (green) and actin (red). Representative images are shown (scale bar: 20 μm). (**B**) LC3 puncta intensity per cell were quantified and presented as a histogram in (mean ± S.D.). ***$p < 0.001$.

To confirm the results, I treated A2780-Vec, A2780-PRL-3, and A2780-PRL-3-PDM with CQ for 24 hours, and quantified LC3 puncta in these three cell lines (**Figure 11 A-B**). LC3 signal is almost absent without CQ treatment, and this phenomenon may be due to the fast degradation of newly formed autophagosome (images not shown). Since autophagosomes are not degraded in the presence of CQ, the number of LC3 puncta indicates the autophagosome formed during period with CQ treatment. More importantly, A2780-PRL-3 cells had significantly more endogenous LC3 puncta than A2780-Vec or A2780-PRL-3-PDM (**Figure 11B**, black columns, $p < 0.01$). Although PRL-3-PDM still colocalized with LC3 upon CQ treatment, it lost the ability to promote autophagosome formation compared to wild type PRL-3. The results suggest that in addition to localization, phosphatase activity is required for PRL-3 to promote autophagosome formation.

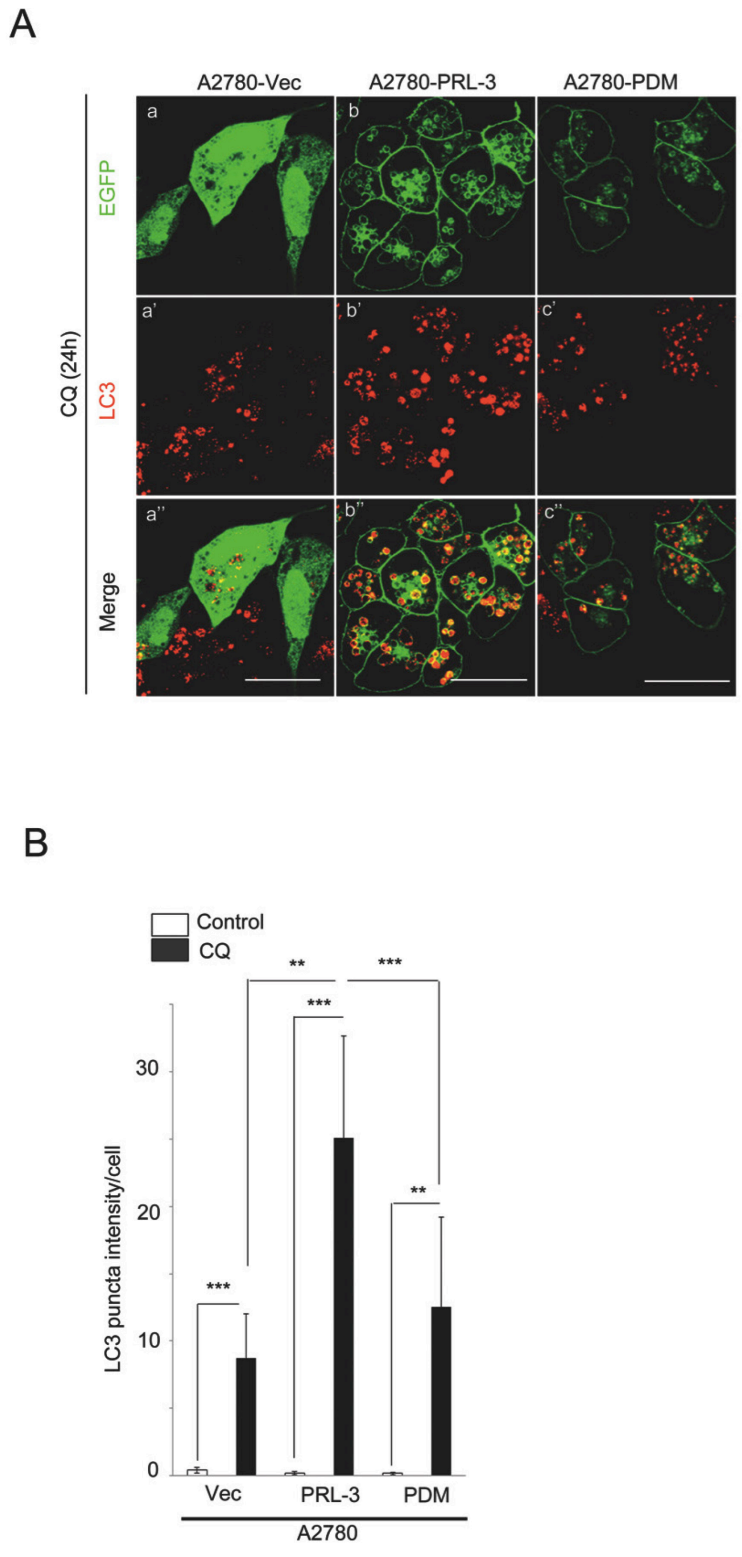

Figure 11. PRL-3 promotes autophagosome formation dependent on its phosphatase activity. (**A**) A2780-EGFP (Vec), A2780-EGFP-PRL-3 (PRL-3), and A2780-EGFP-PRL-3-PDM (PDM) cells were treated with CQ for 24 h before immunostaining with an anti-LC3 antibody. (**B**) LC3 puncta intensity value were quantified and presented as a histogram (mean ± S.D.) (***$p < 0.001$, **$p < 0.01$).

4.3.2 PRL-3 Promotes Autophagosome Formation Through The Canonical hVps34-Beclin-1 Pathway

To study whether PRL-3 promotes autophagosome formation through the canonical autophagy pathway, I stably knocked down hVps34 or Beclin-1, which are two upstream regulators of canonical autophagosome formation pathway (Russell et al., 2013) in A2780-Vec A2780-PRL-3 and A2780-PRL-3-PDM cells. The knockdown efficiency is shown in **Figure 12A**. The indicated cell lines were treated with CQ for 24 hours followed by immunofluorescence imaging (**Figure 12B-D**). LC3 puncta quantification was also performed by Photoshop software (**Figure 12E**). In agreement with my earlier results, significantly more LC3 puncta intensity per cell was observed in A2780-PRL-3 cells with CQ treatment in the control knockdown group (shScr) (**Figure 12E**, first 3 columns). Knockdown of either hVps34 or Beclin-1 abolished the LC3 puncta intensity difference between A2780-PRL-3 and A2780-Vec or A2780-PRL-3-PDM upon CQ treatment (**Figure 12E**, last 6 columns, difference not significant).

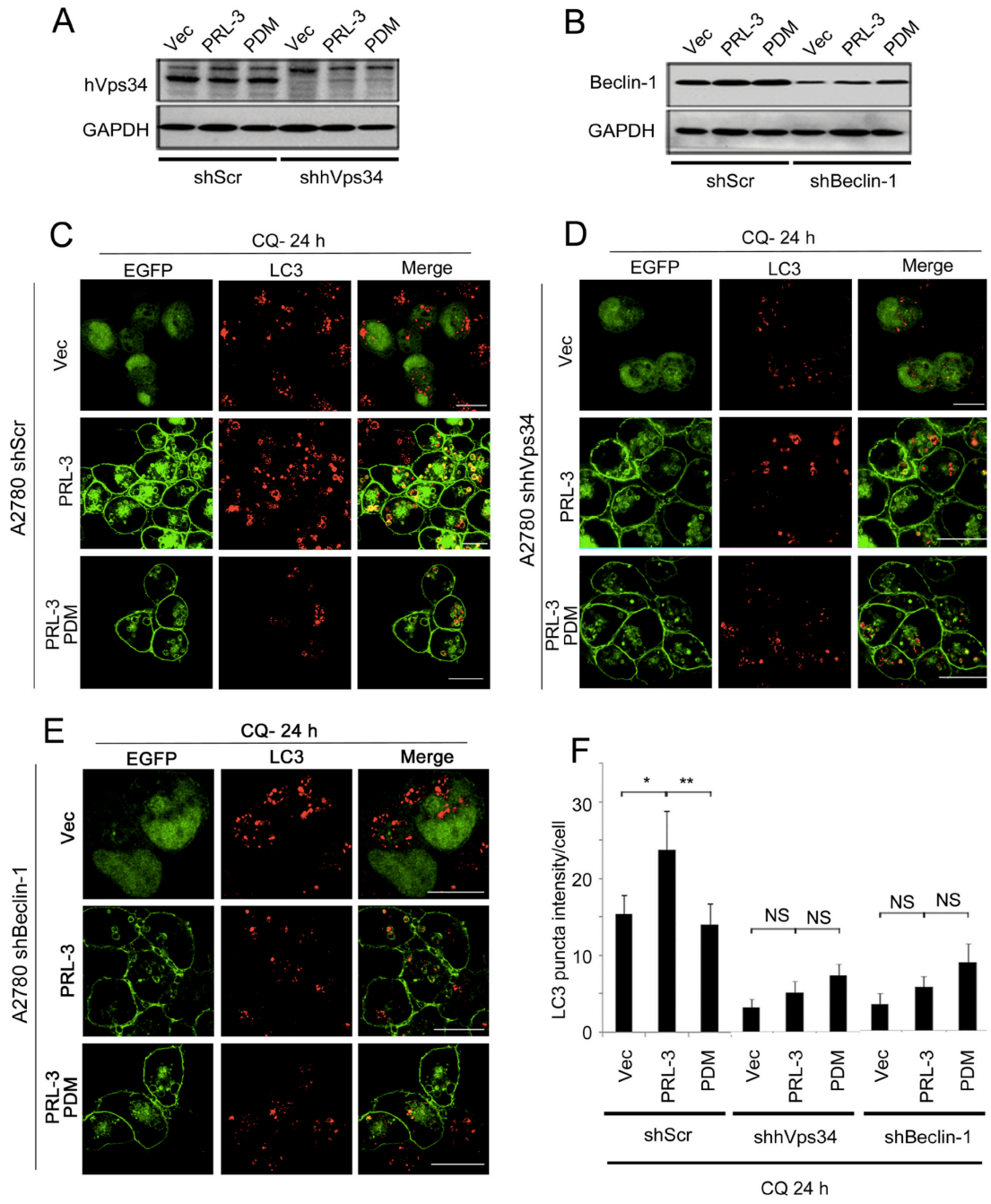

Figure 12. PRL-3 promotes basal autophagosome formation through the canonical hVps34-Beclin-1 pathway. (**A-B**) A2780-Vec, A2780-PRL-3, and A2780-PDM cells were infected with shRNA knockdown constructs with either a "scrambled" sequence against non-specific targets (shScr), (**A**) hVps34 (shhVps34), (**B**) or Beclin-1 (shBeclin-1). After stable selection, exponentially growing cells were lysed for Western blotting analysis for indicated proteins. (**C-E**) Indicated cell lines were treated with CQ for 24 hours prior to immunostaining with an anti- LC3 antibody (Red). Representative images are shown. (**F**) LC3 puncta intensity per cell quantified and presented as a histogram (mean ± S.D.) $^{**}p < 0.01$, $^{*}p < 0.05$, NS (not significant) $p > 0.05$

A key autophagy regulator, mammalian target of Rapamycin (MTOR), can be inhibited by the treatment of Rapamycin (Jung et al., 2010). MTOR inhibits autophagy, while the treatment of Rapamycin relieves suppression of autophagy by MTOR. Immunofluorescence was done after the combination treatment of Rapamycin and CQ for 4 hours in the cell lines indicated (**Figure 13A-C**). Similar with CQ treatment alone, combined treatment of Rapamycin and CQ led to autophagosome accumulation (increased LC3 puncta intensity). According to the quantification of LC3 puncta, I found that the LC3 puncta accumulation was faster in A2780-PRL-3 cells than A2780-Vec or A2780-PRL-3-PDM (**Figure 13D**, first three columns). The knockdown of hVps34 or Beclin-1 abolished the LC3 puncta intensity difference between A2780-PRL-3 and A2780-Vec or A2780-PRL-3-PDM (**Figure 13D**, last 6 columns, difference not significant). My results suggest that PRL-3 activates autophagosome formation dependent on hVps34 and Beclin-1 through the canonical pathway. More importantly, since PRL-3 is able to enhance autophagosome formation upon Rapamycin inhibition of MTOR, it might affect autophagy pathway downstream of MTOR.

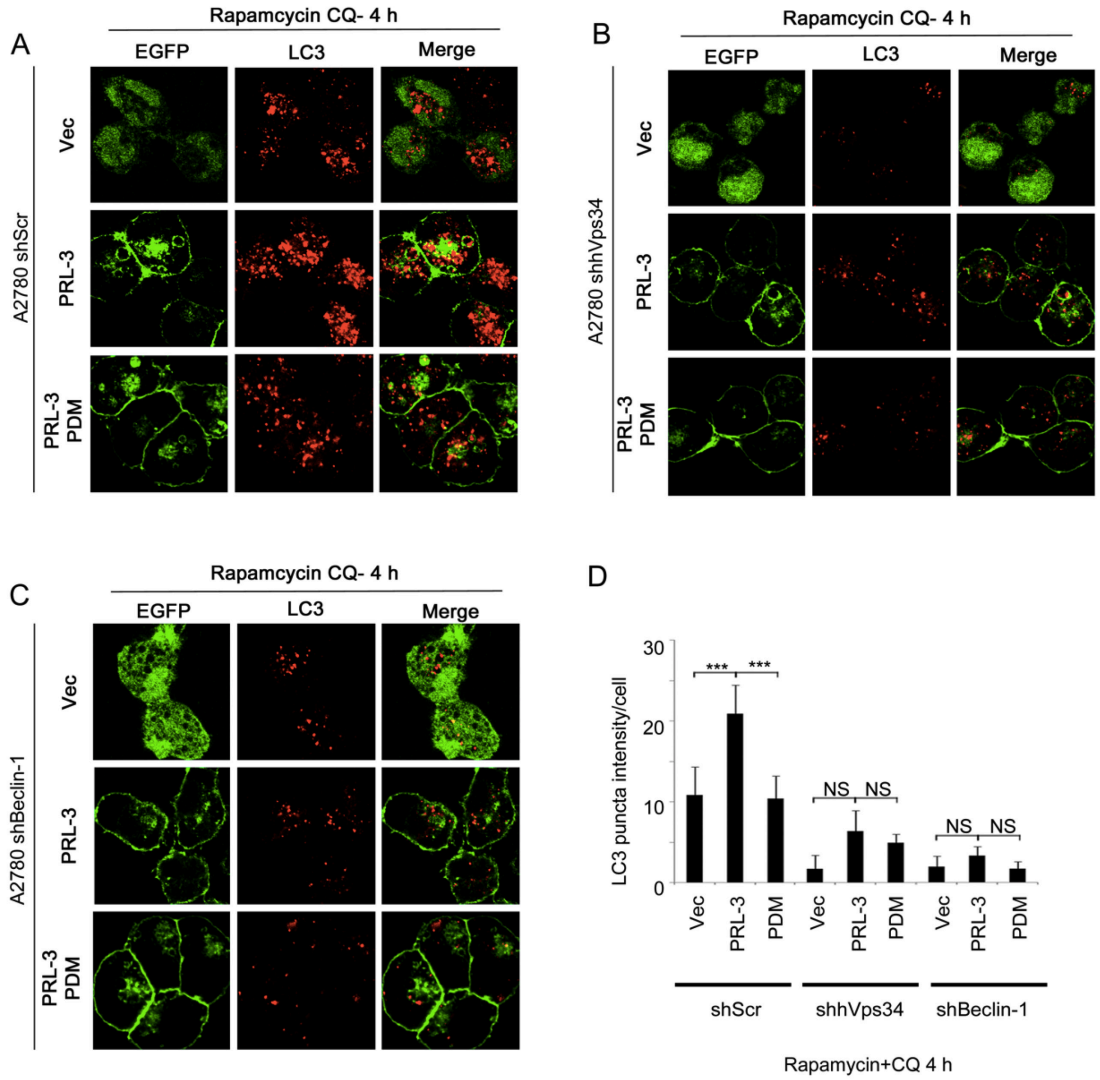

Figure 13. PRL-3 promotes Rapamycin induced autophagosome formation through the canonical hVps34-Beclin-1 pathway. (A-C) Indicated cell lines were treated with Rapamycin and CQ for 4 hours prior to immunostaining with an anti- LC3 antibody (Red). Representative images are shown. (**D**) LC3 puncta intensity per cell were quantified using photoshop and presented as a histogram in the right panel (mean ± S.D.). ***$p < 0.001$, NS (not significant) $p > 0.05$.

4.3.3 PRL-3 Overexpression Promotes Autophagy Flux Dependent On ATG5 Expression

The lipidation of soluble LC3-I to membrane bound LC3-II is associated with autophagosome elongation and vesicle completion (Mizushima, 2007). Hence, LC3 conversion is used as another marker of autophagosome generation and accumulation (Meijer and Codogno, 2004).

Immunoblotting was used to detect 'autophagic flux' by comparing LC3 conversion in cells treated with or without lysosomal inhibitor (I used CQ in this study). When cells are treated with CQ, LC3-II degradation is blocked, and it leads to LC3-II accumulation (Tanida et al., 2005). Thus, the differences in the LC3-II level with or without CQ treatment represents the amount of LC3-II that is delivered to lysosome for degradation during the treatment period (Mizushima et al., 2010). After CQ treatment for different time points (2 hours and 24 hours), LC3-II increased robustly. Moreover, the increase of LC3-II in CHO-PRL-3 cells was much more significant compared to CHO-con or CHO-PRL-1 cell line (**Figure 14A**, lane 1 – 6; lane 7 – 12, red boxes), which indicated a faster autophagic flux in CHO-PRL-3 cell than CHO-con and CHO-PRL-1 cells. With the treatment of Rapamycin and the combined treatment of Rapamycin and CQ, LC3-II level was higher in CHO-PRL-3 cells than CHO-con or CHO-PRL-1. Thus, there was also a faster rapamycin induced autophagy flux in CHO-PRL-3 cells (**Figure 14A**, lane 7 - 18). My results suggest that the overexpression of PRL-3 (but not PRL-1) promotes both basal and rapamycin-induced autophagy flux.

In the previous section, I showed the phosphatase activity of PRL-3 was not needed for its localization in the autophagosome, whereas prenylation dependent membrane association was. To examine whether the catalytic activity of PRL-3 is necessary in promoting autophagic flux, I treated A2780-Vec, A2780-PRL-3, and A2780-PRL-3-PDM with CQ, and found that A2780-PRL-3 had a higher LC3-II protein level than the other two cell

lines (**Figure 14B**, lane 1 – 6, red box). Rapamycin induced autophagy level was also examined in these three cell lines. LC3-II protein increased significantly in the combination treatment of rapamycin and CQ compared to rapamycin alone, and within the three cell lines, A2780-PRL-3 has the highest LC3-II level upon rapamycin CQ combined treatment in both 2 hours and 4 hours (**Figure. 14B**, lane 7 – 18, red boxes). Notably, PRL-3 also promoted autophagy flux under starvation condition (HBSS) in both CHO and A2780 cells (**Figure S3**).

As predicted, A2780-PRL-3-ΔPre, which failed to localize in autophagosome, failed to promote autophagy flux (**Figure S4**). Thus, PRL-3 overexpression promotes basal as well as rapamycin and starvation induced autophagy flux, and this effect is dependent on its phosphatase catalytic activity and prenylation dependent membrane localization.

ATG5 is an autophagy regulator, which plays an important role in LC3 lipidation and autophagosome formation (Kirisako et al., 2000). I stably knocked down ATG5 in A2780-Vec, A2780 -PRL-3 and A2780 –PRL-3-PDM. In cells with ATG5 knockdown, PRL-3 lost the ability to promote LC3 lipidation compared to Vec or PRL-3-PDM in A2780 cells with the treatment of CQ, Rapamycin, or the combination treatment of Rapyamycin and CQ (**Figure 14C,** red boxes vs blue boxes). Thus, my results show that the promotion of autophagic flux by PRL-3 is dependent on the expression of ATG5.

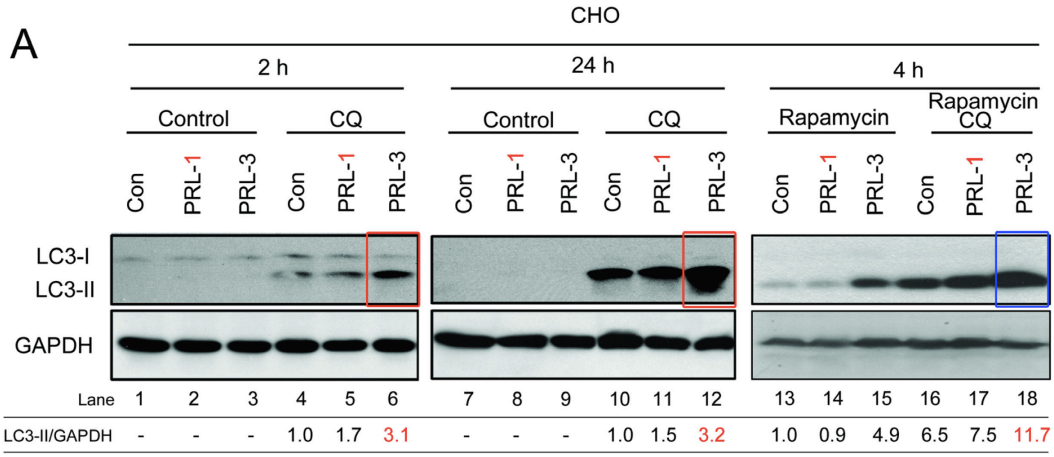
A
CHO
2 h
24 h
4 h
Control
CQ
Control
CQ
Rapamycin
Rapamycin CQ
Con
PRL-1
PRL-3
LC3-I
LC3-II
GAPDH
Lane 1 2 3 4 5 6 7 8 9 10 11 12 13 14 15 16 17 18
LC3-II/GAPDH - - - 1.0 1.7 3.1 - - - 1.0 1.5 3.2 1.0 0.9 4.9 6.5 7.5 11.7

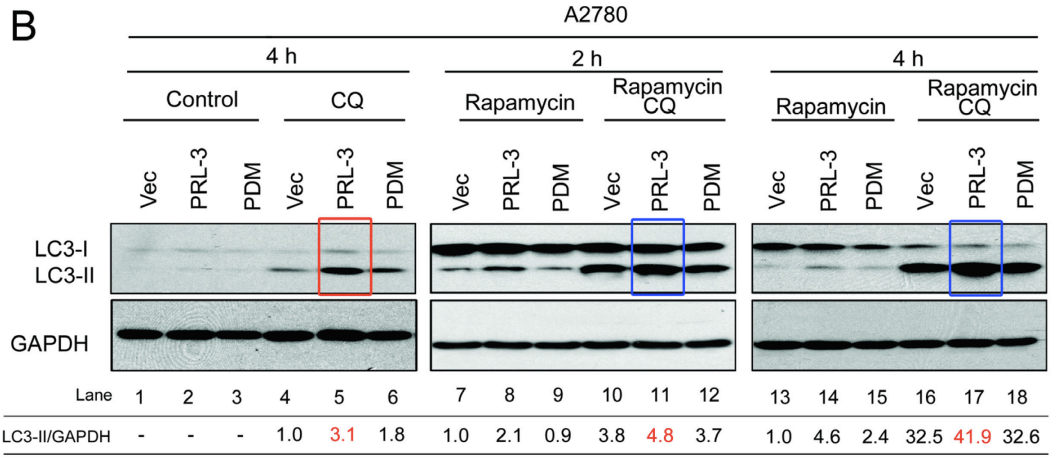
B
A2780
4 h
2 h
4 h
Control
CQ
Rapamycin
Rapamycin CQ
Rapamycin
Rapamycin CQ
Vec
PRL-3
PDM
LC3-I
LC3-II
GAPDH
Lane 1 2 3 4 5 6 7 8 9 10 11 12 13 14 15 16 17 18
LC3-II/GAPDH - - - 1.0 3.1 1.8 1.0 2.1 0.9 3.8 4.8 3.7 1.0 4.6 2.4 32.5 41.9 32.6

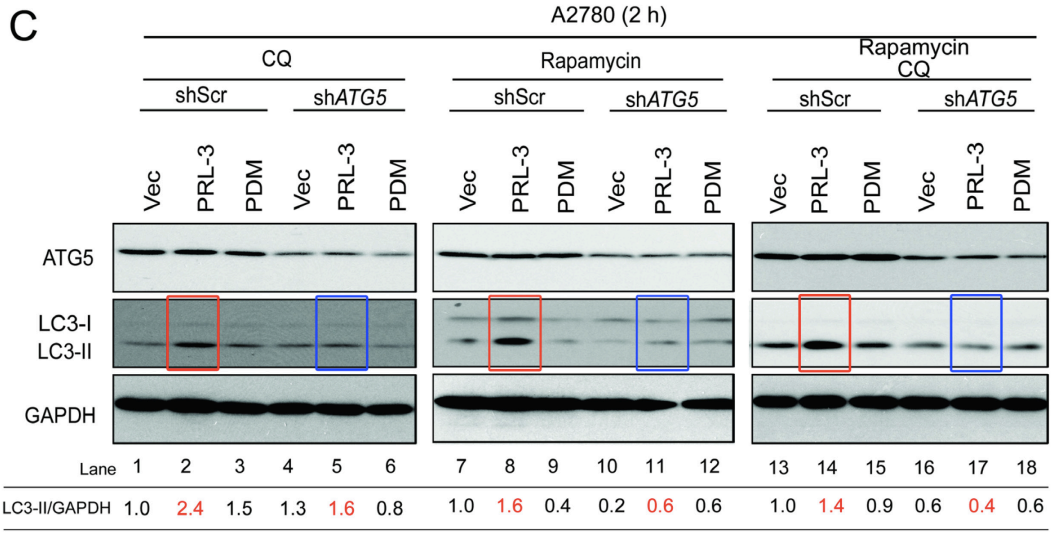
C
A2780 (2 h)
CQ
Rapamycin
Rapamycin CQ
shScr
shATG5
Vec
PRL-3
PDM
ATG5
LC3-I
LC3-II
GAPDH
Lane 1 2 3 4 5 6 7 8 9 10 11 12 13 14 15 16 17 18
LC3-II/GAPDH 1.0 2.4 1.5 1.3 1.6 0.8 1.0 1.6 0.4 0.2 0.6 0.6 1.0 1.4 0.9 0.6 0.4 0.6

Figure 14. PRL-3 overexpression promotes autophagic flux dependent on ATG-5 expression. (**A**) CHO-con, CHO-PRL-1, and CHO-PRL-3 cells were cultured in full medium with indicated treatment for the indicated durations before lysis for Western blotting analysis. (**B**) A2780-Vec, A2780-PRL-3, and A2780-PDM cells were treated as indicated before lysis for Western blotting analysis. (**C**) A2780-Vec, A2780-PRL-3, and A2780-PDM cells stably expressing control shRNA (shScr) or ATG5 shRNA (shATG5) were treated as indicated, and lysed for western blotting analysis. All band quantifications of LC3-II/GAPDH were done using ImageJ.

4.3.4 PRL-3 Promotes Autophagic Flux Through Increasing The Kinase Activity Of ULK1

Atg1 is the first autophagy gene identified in yeast, and it is a protein kinase that receives signals of cellular nutrients status, and recruits downstream ATG proteins to the autophagosome formation site to induce autophagy (Nakatogawa et al., 2009). There are two orthologs of Atg1 in mammals, namely UNC-51-like kinase-1, and -2 (ULK1, and ULK2). ULK1 acts downstream of MTOR complex, and initiates autophagy when activated. The role of ULK2 is less clear (Mizushima, 2010; Young et al., 2006).

In A2780 cells, PRL-3 overexpression resulted in increased ULK1 phosphorylation in Ser555 site, while PRL-3 knockdown resulted in decreased ULK1 phosphorylation in Ser555 (**Figure 15A**), indicating a positive correlation between ULK1 Ser555 phosphorylation and PRL-3 expression level. The phosphorylation of Ser555 of ULK1 is positively correlated with its kinase activity, and is required for autophagy induction (Meijer and Codogno, 2011). Indeed, I found that ULK1 purified from PRL-3 overexpressing cells had higher in vitro kinase activity than that ULK1 purified from control cells (**Figure 15B**). These results suggest that ULK1 might be an important node in regulation of autophagy by PRL-3, although much future work is needed to address the molecular detail regarding the activated phosphorylation of ULK1 in response to increased PRL-3 levels.

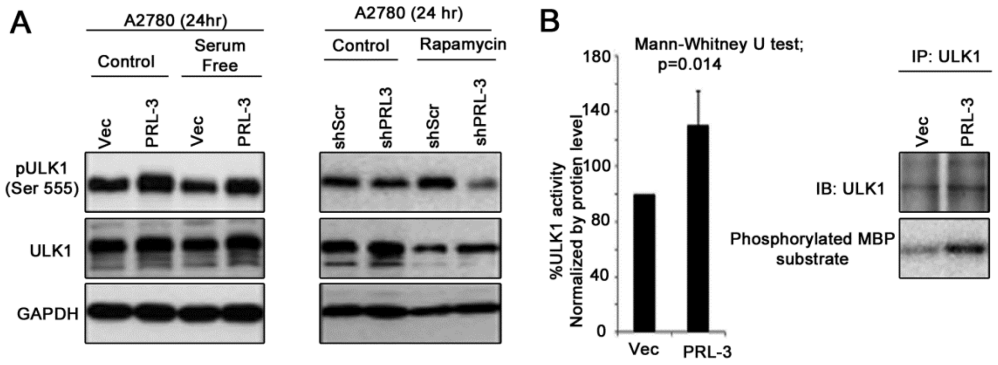

Figure 15. PRL-3 regulates ULK1 activity. (**A**) pULK1 (Ser 555) is increased in A2780-PRL-3 cells and (**B**) decreased in A2780-shPRL-3 cells compared to control cells when autophagy is induced. (**C**) ULK1 activity measured by ULK1 pull-down, and MBP substrate phosphorylation by immunoprecipitated ULK1. Right: mean ULK1 activity, Left: a representative Western blot (Top) and a phospho-image (Bottom).

*Figure 15B is contributed by Dr. James Murray

To confirm the role of ULK1 in PRL-3 promoted autophagy flux, I knocked down ULK1 in A2780-Vec and A2780-PRL-3 cells. I treated the cell lines indicated with Rapamycin and CQ for 6 hours, and did Western blotting to detect LC3 protein levels (**Figure 16**). Similar with the results from **Figure 13**, in shScr cells, A2780-PRL-3 had a higher level of LC3-II compared to A2780-Vec. The knock down of ULK1 decreased LC3-II protein level under combination treatment of Rapamycin and CQ. Significantly, the difference between LC3-II levels in A2780-Vec and A2780-PRL-3 was abolished upon the knockdown of ULK1 (**Figure 16,** red box). The results indicated that PRL-3 promotes autophagy flux dependent on ULK1.

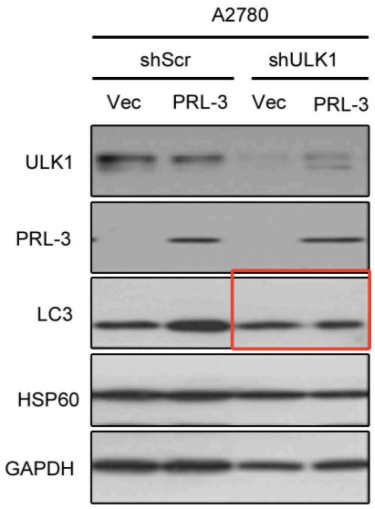

Figure 16. Knockdown of ULK1 abolished the LC3 conversion rate promoted by PRL-3. A2780-Vec and A2780-PRL-3 cells stably expressing knockdown constructs against nonspecific targets (shScr) or ULK1 (shULK1) were treated with Rapamycin in combination with CQ for 6 hours before lysis for western blotting analysis.

4.3.5 The Overexpression Of PRL-3 Promotes Autophagic Degradation Of p62

Being an autophagic substrate, p62 protein level accumulates when autophagy is inhibited, and decreases when autophagy is induced (Bjorkoy et al., 2005; Pankiv et al., 2007). Hence, p62 degradation is widely used as a marker to study autophagy flux (Bjorkoy et al., 2005). To study whether PRL-3 protein level affects p62 degradation, I stably knocked down PRL-3 in A2780 cells using shRNA. A2780-shPRL-3 showed an increase of p62 level compared to A2780-shScr cells (**Figure 17A**). I treated these two cell lines with CQ for different durations. p62 protein level increased upon CQ treatment in a time dependent manner. More importantly, the different p62 protein level was abolished with CQ treatment beyond 8 hours (**Figure 17B**, lane 9-12).

Moreover, I also found that CHO-PRL-3 had lower p62 protein level compared to CHO-con or CHO-PRL-1 cells (**Figure 17C**). With the treatment of CQ for 2, 4 or 24 hours,

p62 protein accumulated in all three cell lines in a time dependent manner. More importantly, the different level of p62 between CHO-PRL-3 and CHO-con or CHO-PRL-1 was abolished after CQ treatment (**Figure 17D**). Band intensity of p62/GAPDH in Figure 17D with 24 hours treatment was quantified using imageJ (**Figure 17E**, columns show the results of 3 independent biological repeats). These results indicate a faster autophagic degradation rate in CHO-PRL-3 cells than CHO-con or CHO-PRL-1. The combination treatment of pepstatin and E64D, functions to inhibit lysosomal protease, is also widely used to inhibit autophagic degradation (Amaravadi et al., 2011).

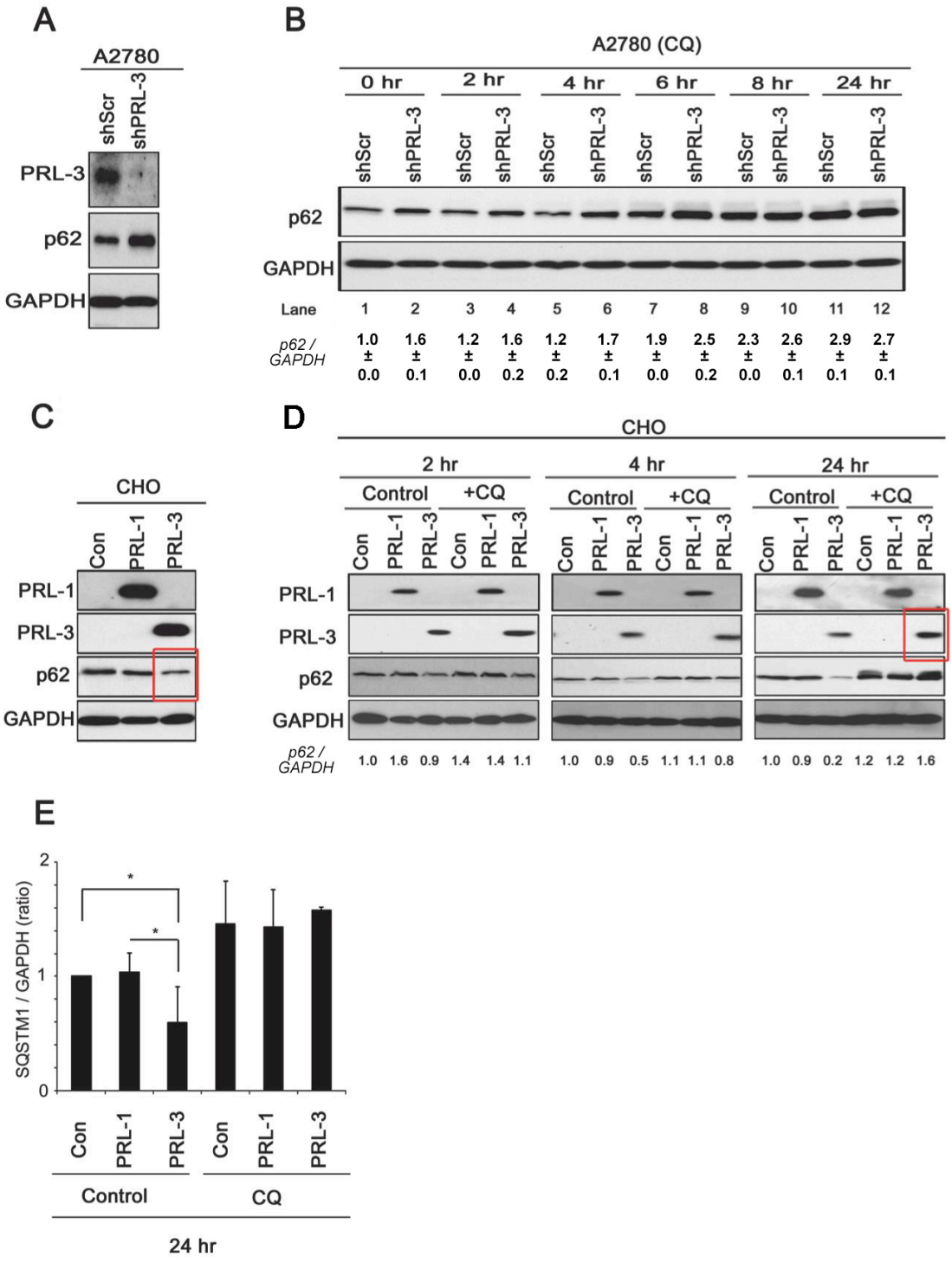

Figure 17. PRL-3 promotes autophagic degradation of p62. (**A**) A2780 cells stably expressing shRNA knockdown constructs against nonspecific targets (shScr) or PRL-3 (shPRL-3) were lysed and analysed for stable-state p62 and PRL-3 expression levels by western blotting assay. (**B**) A2780-shScr and A2780-shPRL-3 cells were treated with CQ for indicated durations before lysis for western blotting analysis. The band intensity of p62/GAPDH was quantified using imageJ. (**C**) Exponentially growing CHO-Con, CHO-PRL-1, and CHO-PRL-3 stable cells were lysed for western blotting to analyse the stable

state p62 expression. (**D**) CHO-Con, CHO-PRL-1, and CHO-PRL-3 cells were cultured in full medium in the absence (control) or presence of CQ for indicated time points before lysis for western blot analysis. (**E**) The band intensity of p62/GAPDH for 24 hours treatment in (**D**) was quantified using imageJ, and presented as a histogram. The results were from three biological repeats, and presented as mean ± S.D..

According to the results, I proposed a model on how PRL-3 functions in canonical autophagy pathway as follows: 1) PRL-3 is an activator on canonical autophagosome formation dependent on hVps34-Beclin-1 complex; 2) PRL-3 promotes LC3-I to LC3-II conversion dependent on ATG5; 3) PRL-3 increases ULK1 activity; 4) PRL-3 promotes autophagic substrate p62 degradation; 5) PRL-3 itself functions as a novel autophagic substrate (results from the last chapter), thus forming a negative feedback loop to fine tune autophagy activity (**Figure 18**).

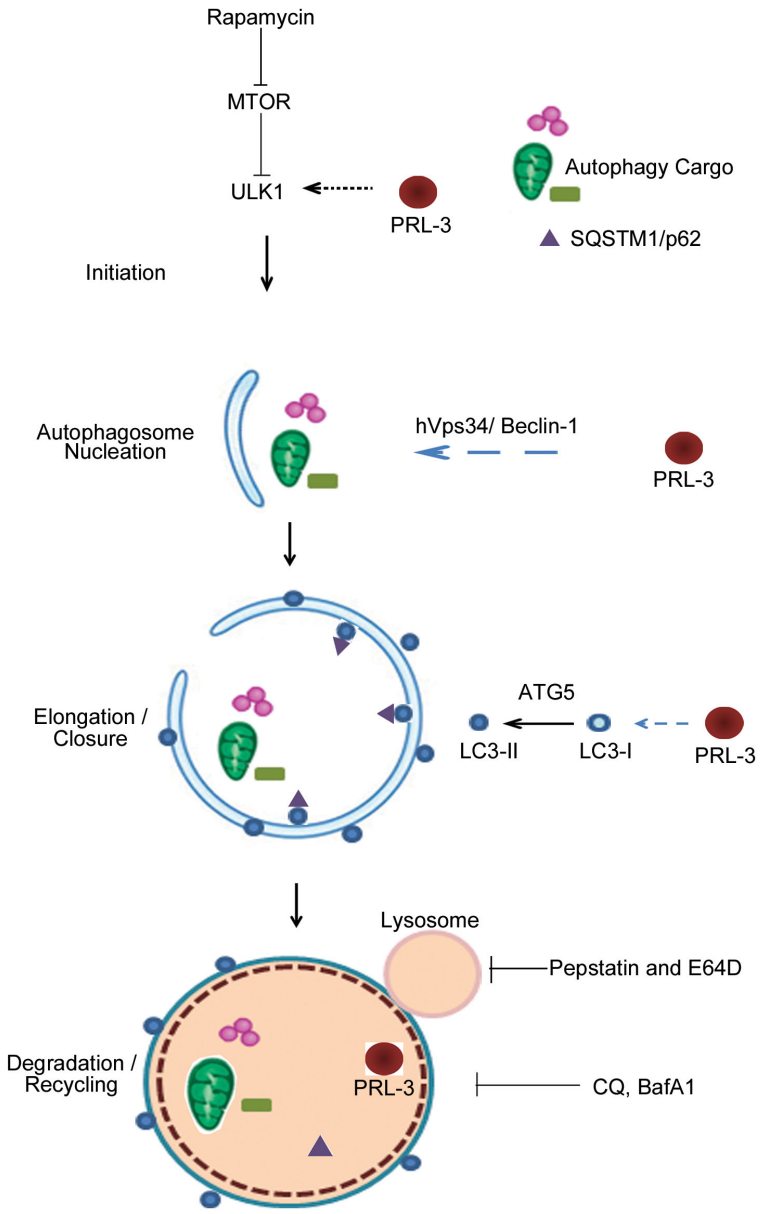

Figure 18. A model illustrates the involvement of PRL-3 in multiple steps of canonical autophagy pathway. 1) PRL-3 activates autophagy independent of MTOR and via activating ULK1; 2) PRL-3 promotes autophagosome formation in an hVps34-Beclin-1 dependent manner; 3) PRL-3 accelerates LC3 conversion dependent on ATG5; 4) PRL-3 enhances p62 degradation, and p62 is a key autophagy substrate; 5) PRL-3 itself is a novel autophagic substrate. Sites of action of chemicals used in the experiments (rapamycin, pepstatin and E64D, CQ, Baf A1) are also indicated.

4.3.6 PRL-3 Utilizes Autophagy To Promote Ovarian Cancer Cell Proliferation

As an oncogene, PRL-3 promotes multiple process of cancer progression including cell growth, migration, invasion, angiogenesis as well as metastasis depending on genetic background and cancer types (Al-Aidaroos and Zeng, 2010). More specifically in ovarian cancer, PRL-3 has been proven to increase cell growth (Polato et al., 2005). Since my data suggested that PRL-3 could promote autophagic activity, and autophagy has been reported to play either tumor-promoting or tumor-suppressing role depending on cellular context (Janku et al., 2011), I further investigated the role autophagy plays in PRL-3 mediated cancer cell proliferation.

First of all, the proliferation of A2780-Vec and A2780-PRL-3 following shRNA knockdown of hVps34, Beclin-1, and ATG5 was compared. In control knockdown cells (shScr), PRL-3 overexpression promoted an increase in cell proliferation measured by MTT assay (**Figure 19A-C**, black lines). The knockdown of hVps34, Beclin-1 or ATG5, which results in an inhibition of autophagy, also leads to a decrease of proliferation in A2780-PRL-3 cells (**Figure 19A-C**, red vs. black dashed lines; $p < 0.001$). However, the knockdown of these genes had no significant effect on the proliferation rate of A2780-Vec cells (**Figure 19A-C**, red vs. black solid lines, $p > 0.05$). My results are consistent with the previous finding that ovarian cancer cell line A2780 is not sensitive to autophagic inhibition in serum-replete condition (Zhang et al., 2012b). Thus, my results suggest that the inhibition of autophagy by knocking down autophagy genes inhibit cell proliferation promoted by the overexpression of PRL-3 in A2780 cells.

Autophagy enables cells to grow in starvation conditions. I next tested the ability for cells overexpressing PRL-3 to survive and grow under serum and amino acid starvation condition. A2780-PRL-3 cells were able to survive and continue growth in the absence of serum and glutamine supplementation; in contrast, A2780-Vec cells could not (**Figure 19D-F**, black lines; $p < 0.001$). Importantly, the knock down of hVps34, Beclin-1 or

ATG5 significantly reduced the proliferation of A2780-PRL-3 cells in serum and amino acid starvation (**Figure 19D-F**, red vs. black dashed lines. $p < 0.001$). However, autophagy genes knock down doesn't have a significant effect on A2780-Vec cells (**Figure 19D-F**, red vs. black solid lines, $p > 0.05$). Thus, the overexpression of PRL-3 promoted A2780 growth in serum replete as well as serum-depleted conditions in an autophagy dependent manner.

To confirm the results, I chemically inhibited autophagy using lysosomal degradation inhibitor CQ. Consistently with my knockdown results, A2780-PRL-3 cells proliferate much faster than A2780-Vec in full media (**Figure 19G**, black lines). The treatment of CQ leads to a significant decrease of proliferation in both cell lines (**Figure 19G**, red lines). Critically, the enhanced cell proliferation by overexpression of PRL-3 was abolished by the treatment of CQ (**Figure 19G**, red lines). The results suggest PRL-3 overexpressing cells are more sensitive to chemically autophagic inhibitor CQ treatment.

PRL-3 enhances AKT activity by upregulating the phosphorylation on its Serine 473 site (Al-Aidaroos and Zeng, 2010; Wang et al., 2010). I found AKT-Ser473 phosphorylation (pAKT) level is higher in A2780-PRL-3 compared with A2780-Vec (**Figure 19G**, right panel, lanes 1-2). Significantly, CQ resulted in decreased pAKT level in A2780-PRL-3 but not in A2780-Vec cells (**Figure 19G**, right panel, lanes 3-4). Similarly, A2780-PRL-3 cells are able to survive and proliferate for up to four days in serum free media, while A2780-Vec cells cannot (**Figure 19H**, black lines). The addition of CQ also abolished the proliferation difference between the two cell lines in serum free condition (**Figure 19H**, red lines; $p > 0.05$). Again, I tested whether pAKT level was involved in PRL-3 overexpressing cells in sustaining proliferation in serum deprived condition. Indeed, A2780-PRL-3 did have a higher pAKT level than A2780-Vec in serum free condition, while the addition of CQ reduces the pAKT level difference between the two cell lines (**Figure 19H,** right panel).

Both decreased proliferation and increased apoptosis may contribute to a decreased MTT growth curve. To confirm whether CQ treatment affected cell proliferation but not apoptosis, I analyzed cellular viability under treatments in full medium or serum-free conditions shown in **Figures 19G** (**Figure S5**). According to the results, there was no loss of A2780 cell viability upon CQ treatment in the presence of serum, Thus, CQ treatment in A2780 cells mainly affected cell proliferation but not cell death.

In summary, my data suggest that overexpression of PRL-3 upregulated autophagic flux, providing the cells with a growth advantage regardless of the presence of growth factor or amino acid, and this growth advantage can be diminished by the inhibition of autophagy, either genetically or chemically.

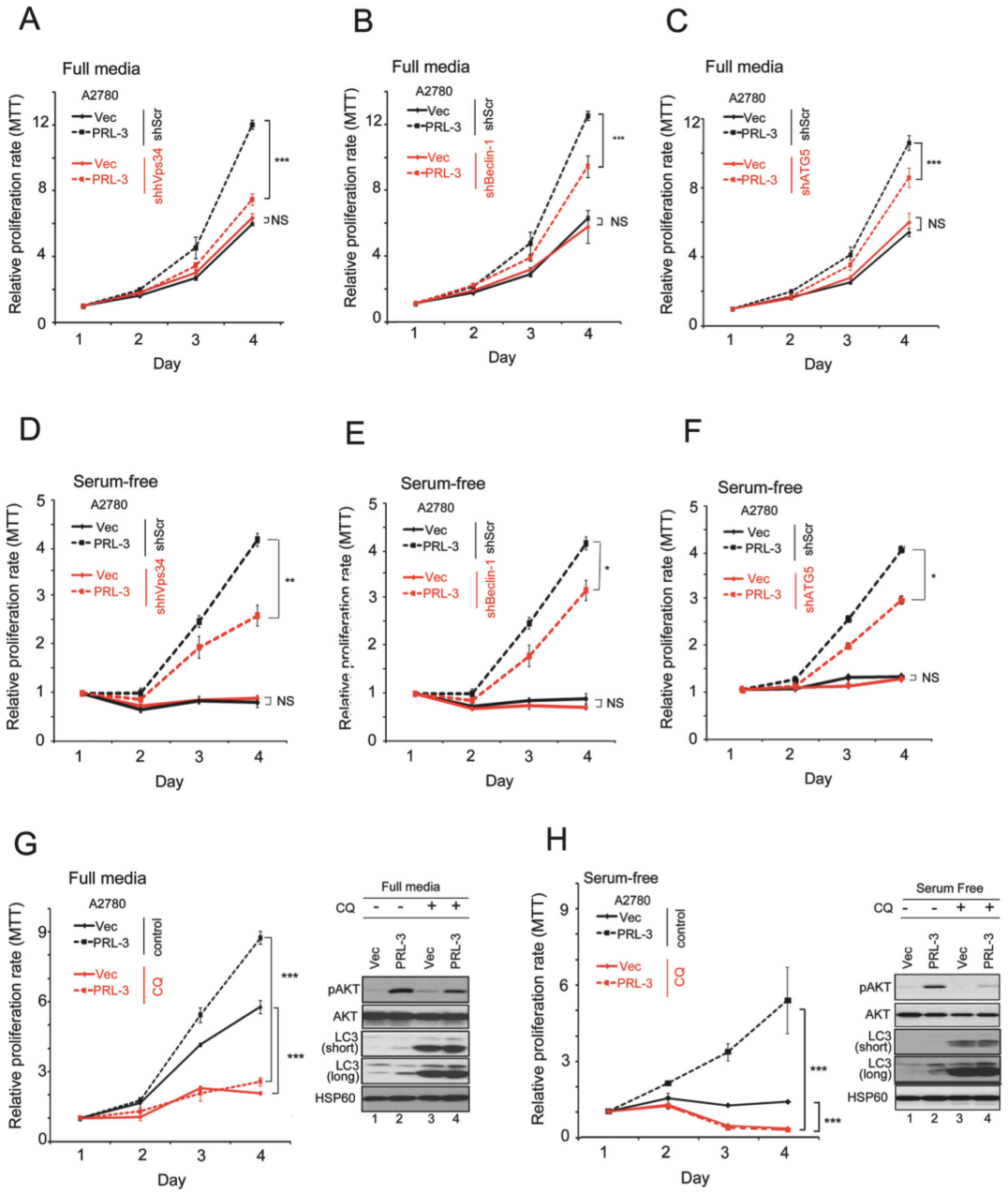

Figure 19. Overexpression of PRL-3 promotes cell proliferation in A2780 cells dependent on autophagy. (**A–C**) A2780-Vec and A2780-PRL-3 cells stably expressing shRNA against non-specific target (shScr), (**A**) hVps34 (shhVps34), (**B**) Beclin-1 (shBeclin-1), or (**C**) ATG5 (shATG5) were cultured in full media. Relative proliferation rates were measured using MTT assay. (**D** and **E**) Cell lines used in (**A–C**) were cultured in serum-free and amino acid free RPMI media for an MTT assay. (**G** and **H**) A2780-Vec and A2780-PTP4A3 cells were cultured in (**G**) full media or (**H**) serum-free meida in the absence (control) or presence of CQ. Similarly treated cells were analyzed (48 h treatment) in parallel by western blotting for indicated protein levels, HSP60 is used as loading control (right panel). All results were shown as mean ± S.D. (NS $P > 0.05$, *$P < 0.05$, **$P < 0.01$, ***$P < 0.001$)

4.3.7 PRL-3-Mediated Non-Adherent Growths of CHO Cells in Soft Agar Are Diminished Upon Autophagy Inhibition

Our group previously showed that PRL-3 overexpression resulted in transformation of CHO cells, leading to an increase in anchorage-independent cell growth (Guo et al., 2004b). Notably, Akt activation is critical for anchorage-independent cell growth (Liu et al., 2001; Nakanishi et al., 2002). In soft agar colony formation assays, I found that the ability of CHO-PRL-3 cells to form colonies could be abolished by CQ treatment (**Figure 20A-B**).

Importantly, the increase in pAkt level in PRL-3 overexpressing CHO cells in nutrient-deprived conditions compared to control CHO cells was also abolished when autophagy was inhibited following CQ treatment (**Figure 20C**). Thus, in line with our earlier observations, PRL-3 is likely to promote anchorage-independent cell growth via Akt activation through increased autophagy.

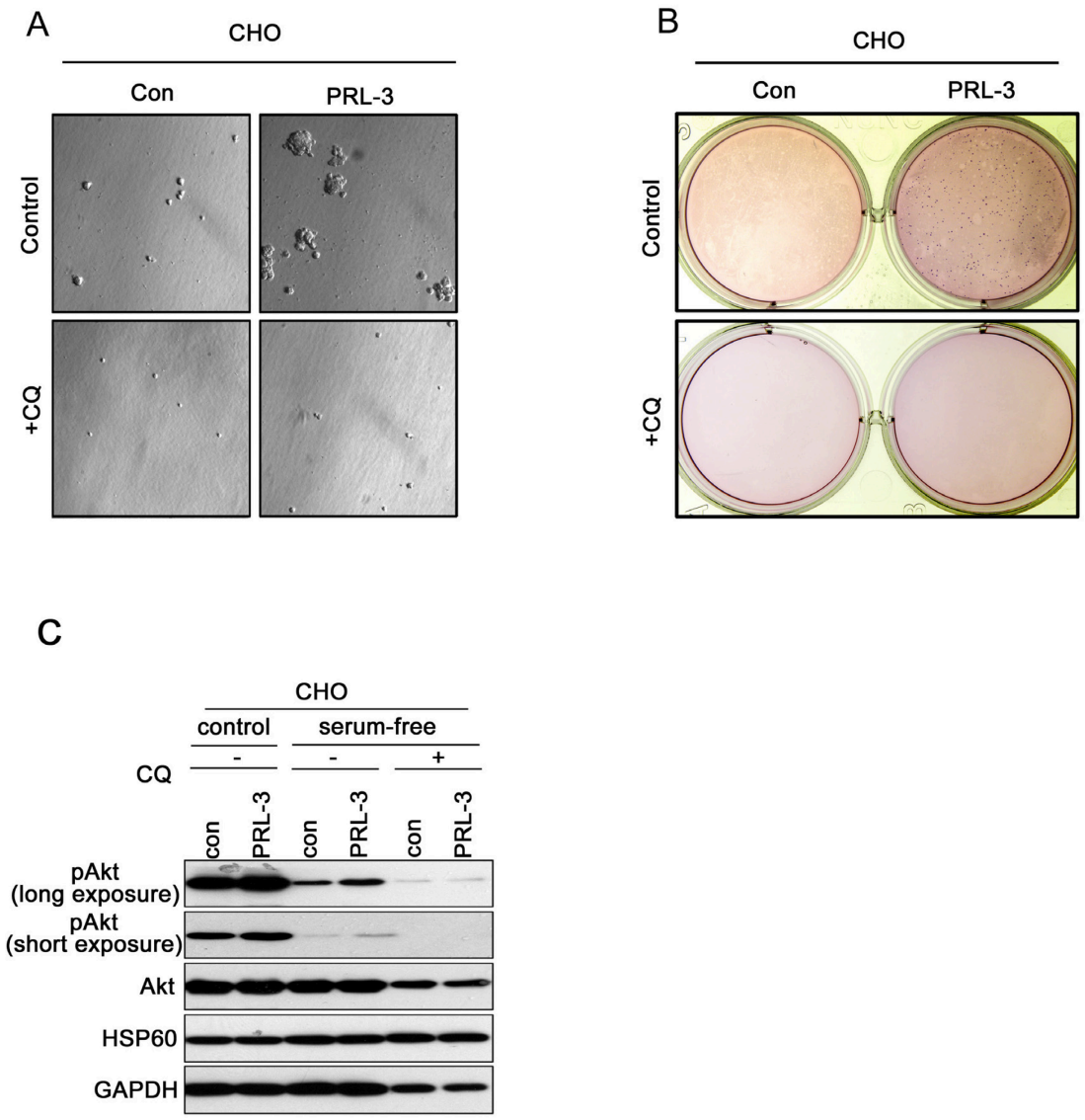

Figure 20. PRL-3-promoted non-adherent growth of CHO cells in soft agar is diminished by inhibition of autophagy. (A-B) CHO-Con and CHO-PRL-3 cells were grown with or without the treatment of CQ. (**A**) Images were taken under phase-contrast microscope. (**B**)Images were taken after crystal violet staining using digital camera. (**C**) Indicated cells were treated as indicated for 24 hours before lysis for western blotting analysis.

4.3.8 PRL-3 Correlates With Ovarian Cancer Patient Survival In An hVps34, Beclin-1 And ATG5-Dependent Manner

I showed that PRL-3 promoted proliferation in A2780 cells and anchorage-independent cell growth in CHO cells dependent on autophagy. To find out the clinical relevance of my *in vitro* findings obtained from CHO and A2780 ovarian cell lines, I extracted microarray and clinico-pathological data from an ovarian cancer patient cohort (GSE 9899), the largest ovarian cancer dataset (n = 285) currently available in the GEO database. I found that mRNA expression level of PRL-3 in ovarian cancer specimens correlated with higher malignant potential compared to those with lower malignant potential (**Figure S6A**; $p < 0.001$). Moreover, increased PRL-3 mRNA expression was associated with not only higher histological grade (**Figure S6B**; $p = 0.001$), but also pathological stage (**Figure S6C**; $p = 0.006$), and shorter recurrence free survival in this cohort (**Figure S6D**; Kaplan-Meier analysis, log-rank test, $p = 0.007$). By Cox-regression analysis, increasing expression of PRL-3 mRNA was significantly associated with higher risk of recurrence-associated death (HR = 1.223, 95% CI = 1.051 – 1.424, $p = 0.009$). It is consistent with previous studies that PRL-3 overexpression promotes ovarian cancer progression (Kraft et al., 2012).

To investigate the role of autophagy in the prognostic effect of PRL-3 in this ovarian cancer patient cohort, I stratified the patients into two groups by using the median mRNA expression of hVps34 as cut-off points. In patients with a higher level of hVps34 mRNA level, higher PRL-3 mRNA level was significantly associated with pathological stage III and IV (**Figure 21A**; $p = 0.002$), histological grade 3 (**Figure 21B**; $p < 0.001$) and shorter recurrence-free survival (**Figure 21C**; $p = 0.003$). In contrast, with a lower level of hVps34 mRNA expression, PRL-3 mRNA level was not significantly associated with any of these clinco-pathological parameters (**Figure 21D-F**; $p > 0.05$). Cox-regression analysis revealed that increasing mRNA expression of PRL-3 was significantly associated

with a higher risk of recurrence-associated death only in patients with a higher level of hVps34 expression (**Table 1**).

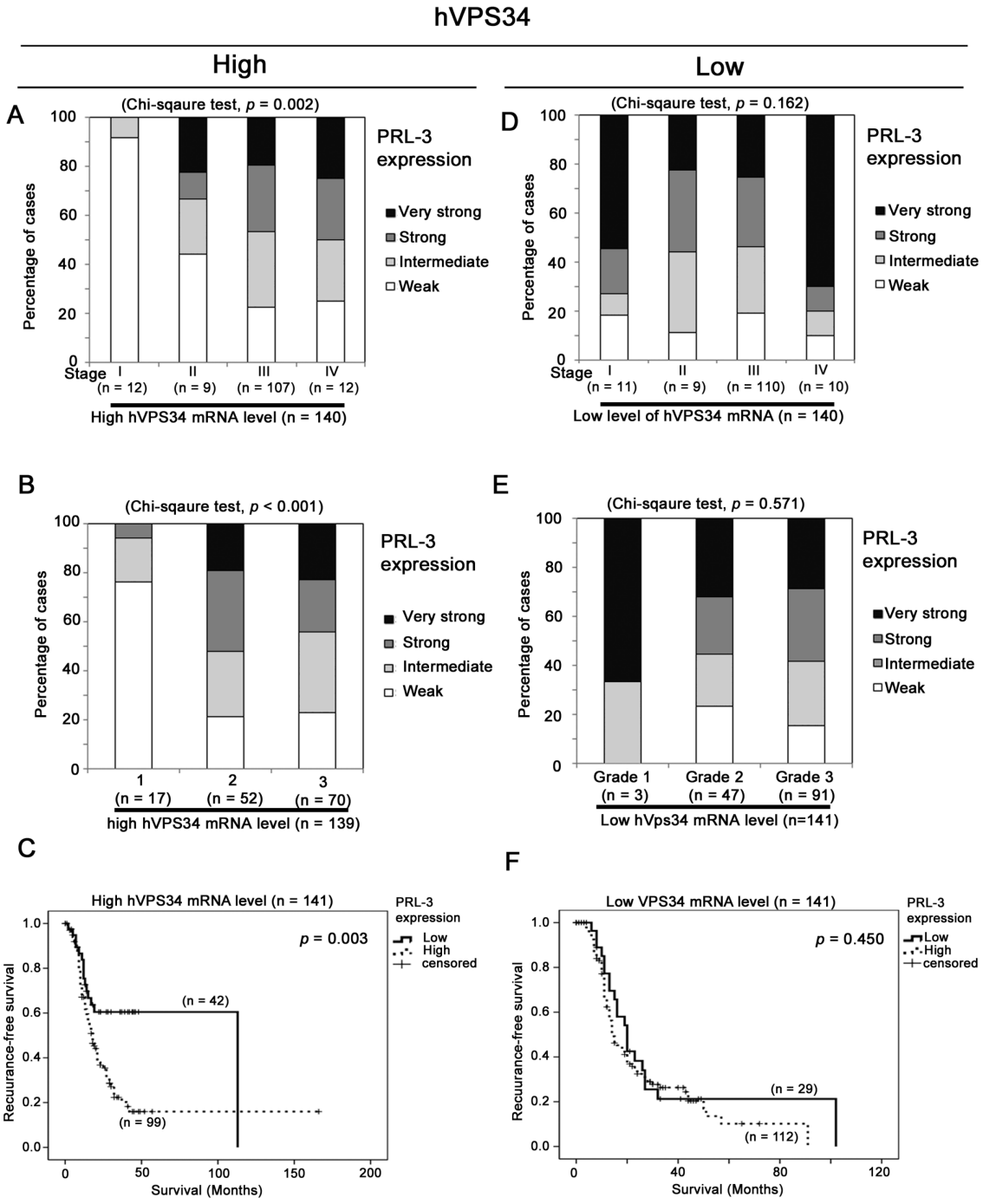

Figure 21. High PRL-3 expression levels predict poorer survival of ovarian cancer patients coexpressing high levels of hVps34. (**A-C**) In patients with higher levels of hVps34, higher PRL-3 expression levels were significantly correlated with (**A**) later pathological stage ($p = 0.002$), (**B**) higher histological grade ($p < 0.001$), and (**C**) shorter

recurrence-free survival (p = 0.003). (**D-F**) In patients with lower levels of hVps34, higher PRL-3 expression levels were not significantly correlated with (**D**) later pathological stage (p = 0.162), (**E**) higher histological grade (p = 0.571), or (**F**) recurrence-free survival (p = 0.450).

Similarly, when Beclin-1 mRNA level was used to stratify the patients into higher Beclin-1 mRNA level group, and lower Beclin-1 mRNA level group, higher PRL-3 mRNA level was only significantly associated with later pathological stage, higher histological grade and shorter recurrence-free survival in the higher Beclin-1 mRNA level group (**Figure 22A-C**), but not in the lower Beclin-1 mRNA level group (**Figure 22D-F**). In addition, Cox-regression analysis revealed that increasing mRNA expression of PRL-3 was significantly associated with a higher risk of recurrence-associated death only in patients with a higher level of Beclin-1 expression (**Table 2**).

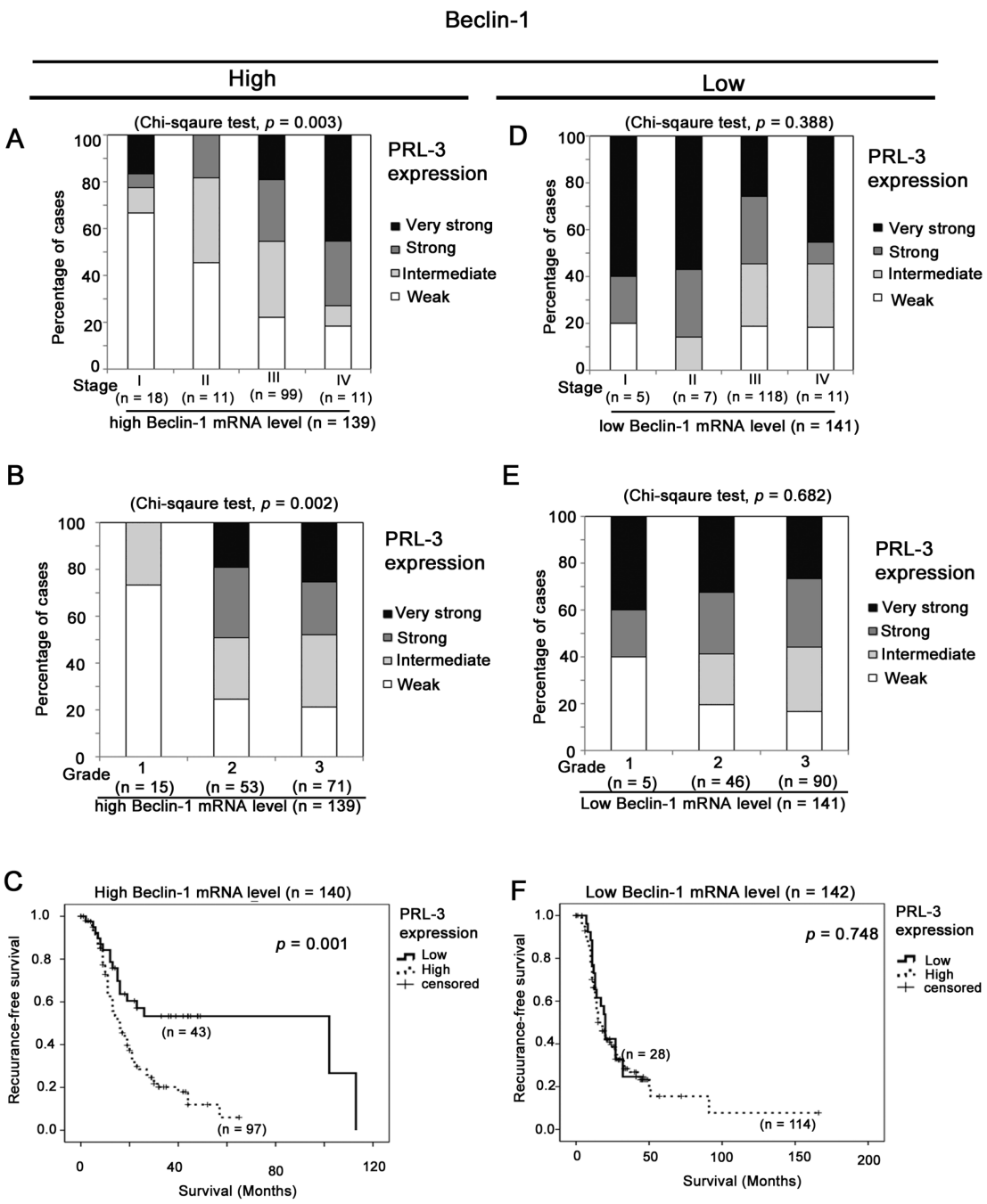

Figure 22. High PRL-3 expression levels predict poorer survival of ovarian cancer patients coexpressing high levels of Beclin-1. (**A-C**) In ovarian cancer patients with higher levels of Beclin-1, higher PRL-3 expression levels were significantly correlated with (**A**) later pathological stage (p = 0.003), (**B**) higher histological grade (p = 0.002), and (**C**) shorter recurrence-free survival (p = 0.001). (**D-F**) In ovarian cancer patients with lower levels of Beclin-1, higher PRL-3 expression levels were not significantly correlated with (**D**) later pathological stage (p = 0.388), (**E**) higher histological grade (p = 0.682), and (**F**) shorter recurrence-free survival (p = 0.748).

Stratifying patients into ATG5-high and ATG5-low groups resulted in a similar observation where a significant association between PRL-3 expression and patient recurrence-free survival was obtained in ATG5-high group patients but not in ATG5-low group patients (**Figure 23**). However, the mRNA expression level of hVps34, Beclin-1, or ATG5 alone is not able to predict patient prognosis in this cohort (**Figure S7**).

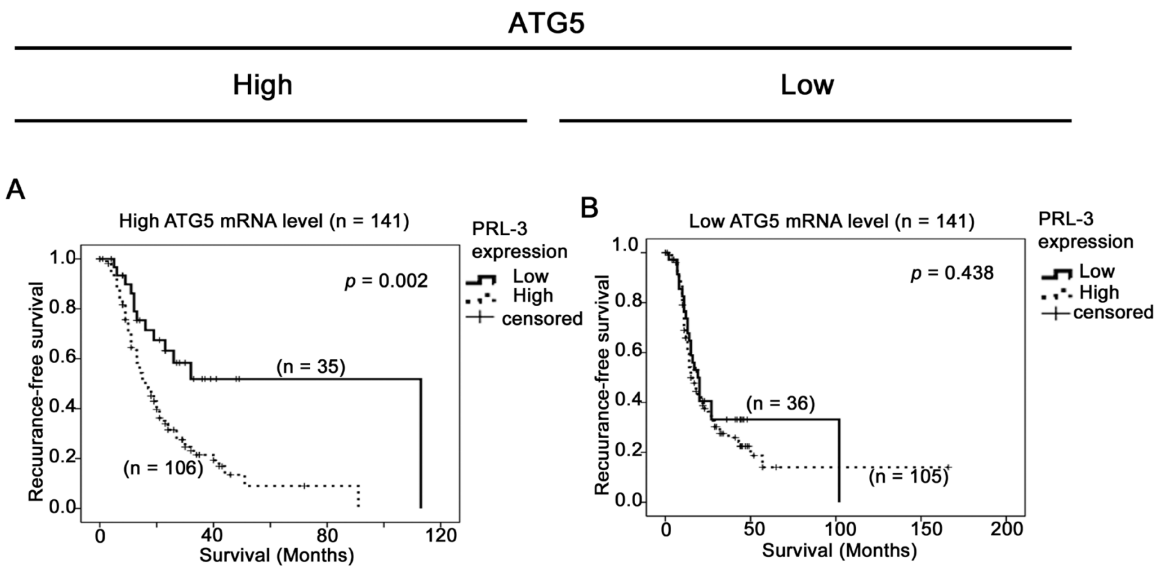

Figure 23. High PRL-3 expression levels predict poorer survival of ovarian cancer patients coexpressing high levels of ATG5. (**A**) In ovarian cancer patients with higher levels of ATG5, PRL-3 expression levels were significantly correlated with recurrence-free survival (p = 0.002) (**B**) In the same cohort with lower expression level of ATG5, PRL-3 expression levels were not significantly correlated with recurrence-free survival (p = 0.438).

Taken together, my results strongly suggest that that the prognostic significance of PRL-3 in ovarian cancer patients is highly dependent on the autophagy competency of the primary tumors, in which the associations between PRL-3 expression and clinico-pathological parameters can only be significantly detected in patients with higher levels of expression of autophagy-related genes.

Table 1. Cox regression analysis of patient survival for PRL-3 stratifying patients by their hVPS34 mRNA expression

		HR	95%CI	P-value
hVPS34 mRNA levels				
Lower	Low	1.235	0.921 – 1.657	0.159
Quartile	High	1.207	1.008 – 1.446	0.041
Median	Low	1.182	0.941 – 1.485	0.150
	High	1.228	0.997 – 1.512	0.053
Higher	Low	1.067	0.888 – 1.283	0.488
Quartile	High	1.722	1.214 – 2.441	0.002

Table 2. Cox regression analysis of patient survival for PRL-3 stratifying patients by their Beclin-1 mRNA expression

		HR	95%CI	P-value
Beclin-1 mRNA levels				
Lower	Low	1.051	0.759 – 1.457	0.764
Quartile	High	1.277	1.079 – 1.513	0.005
Median	Low	1.060	0.837 – 1.342	0.627
	High	1.347	1.110 – 1.633	0.002
Higher	Low	1.129	0.947 – 1.347	0.177
Quartile	High	1.557	1.142 – 2.124	0.005

4.4 Discussion

This is the first study showing a novel correlation between autophagy, a dual player in cancer, and PRL-3, a multifunctional oncogene. In this study, I demonstrated that endosomal phosphatase PRL-3, which also localize in the autophagosome, upregulates autophagy activity in multiple levels dependent on the activation of ULK1: 1) PRL-3 promoted canonical autophagosome formation dependent on hVps34-Beclin-1 complex; 2) PRL-3 increased LC3 conversion dependent on ATG5 expression; 3) PRL-3 promoted p62 degradation (summarized in **Figure 18**).

I found that phosphorylation of Serine 555 site of ULK1 was increased with the overexpression of PRL-3 in A2780 cells (**Figure 15**). The Phosphorylation of ULK1 at Ser555 is critical for starvation-induced autophagy, and also positively correlated with the kinase activity of ULK1 (Meijer and Codogno, 2011). ULK1 is an upstream activator of autophagy, which is under the regulation of many regulators including MTOR and AMP-activated protein kinase (AMPK) (Alers et al., 2012). PRL-3 functions as a phosphatase, which can dephosphorylate its substrate. Thus, its overexpression is likely to increased pULK1-Ser555 in an indirect way, perhaps by directly dephosphorylating an upstream inhibitor of ULK1, and consequently, increases pULK1-Ser555 level, to upregulate its activity. Since MTOR is one of the best-studied upstream regulators of ULK1, I checked the activity of MTOR and its downstream effectors. However, there was no significant activity difference of MTOR and its downstream effectors between A2780 control cells and A2780 PRL-3 overexpressing cells (data not shown). Rapamycin (MTOR inhibitor) treatment was not able to abolish PRL-3 promoted autophagy flux (**Figure 14**), confirming the finding that PRL-3 unregulated autophagy flux and ULK1 activity independent of MTOR. The activity of AMPK, another upstream regulator of ULK1, has also been checked. No significant difference in Phospho-AMPKα (Thr172), the essential activation site of the catalytic subunit of AMPK (Shaw et al., 2004), was found between

A2780-Vec and A2780-PRL-3 cells (data not shown). Thus, further studies are still needed to find out the direct effector of PRL-3 that induces an activation of autophagy.

Interestingly, I previously showed that PRL-3 locates in autophagosome and it is specifically degraded by autophagy. Such regulation of PRL-3 and autophagy forms a highly tuned negative feedback mechanism: PRL-3 protein level accumulation leads to an enhanced autophagy activity, which accordingly contributes the degradation of PRL-3 itself. As a results, autophagy activity and PRL-3 protein level is regulated to a homeostatic functional state. This may be utilized by normal tissue to maintain a steady functional state of autophagy activity as well as PRL-3 protein level. Indeed, ULK1 as an autophagy activator can also be degraded by autophagy (Yang et al., 2011). Such negative feedback loop of ULK1 and autophagy fine-tunes ULK1 protein level and autophagy activity, preventing constitutive progressive consumption of cellular components by prolonged over-activation of autophagy, which might lead to autophagic cell death (Guo et al., 2011a). My findings here suggest that PRL-3 may contribute to maintain a moderate level of autophagy, which supports tumor tissues through starvation; and prevents autophagic cell death caused by unrestrained autophagy (Guo et al., 2011a).

More importantly, inhibition of autophagy chemically by CQ reduced the cell proliferation promotional effect of PRL-3 in ovarian cancer cell A2780, as well as its effect in enhancing Akt phosphorylation, suggesting that autophagy plays an important role in PRL-3 mediated cancer progression (**Figure 19**). Moreover, genetic inhibition of autophagy by knockdown of autophagy genes (including hVps34, Beclin-1 and ATG5) also effectively crippled the ability of PRL-3 to drive ovarian cancer cell proliferation. My results are supported by previous studies, showing that apoptosis and clonogenic potential of A2780 cells are not affected by treatment with CQ (Zhang et al., 2012b). In addition, in the same study, they showed that Beclin-1 or ATG5 knockdown also did not affect the clonogenic potential of A2780 cells. These results suggest that autophagy is not

the key pathway for survival of A2780 cells under normal conditions, an observation in line with my results. However, in my study, I report the novel finding that PRL-3 overexpression increased the proliferation of A2780 cells in an autophagy-dependent manner. I did not observe increased proliferation upon autophagy gene knockdown in A2780 cells, despite my data showing that such knockdown would promote PRL-3 protein accumulation. Here, I propose that PRL-3 requires fully functional, uninhibited autophagy to effect and support increased proliferation in the A2780 cell line. Physiologically, PRL-3 requires a higher autophagy activity to promote ovarian cancer progression. Significantly, I showed that clinical data support my finding. I found that higher expression level of PRL-3 predicts poorer prognosis only when autophagy genes (hVps34, Beclin-1, or ATG5) expressions are high. Taken together, my results suggest that autophagy plays a crucial role in PRL-3 mediated ovarian cancer progression and that autophagy inhibition may be a novel therapeutic target for PRL-3-positive ovarian cancer. Paradoxically, since autophagy is playing dual roles in cancer progression depending on genetic background, both inhibition and activation of autophagy have been documented to have positive effects on cancer therapy. Recently, there are more approximately 20 ongoing clinical trials in multiple types of cancers (Mancias and Kimmelman, 2011). The identification of PRL-3 as a biomarker to predict favorable prognostic effect of autophagy inhibition is of significant clinical utility.

PRL-3 has been reported to have multiple functions in cancer progression (Al-Aidaroos and Zeng, 2010). It functions to promote multiple carcinogenesis processes including proliferation, cell survival, angiogenesis, and metastasis. My study here shows another aspect of PRL-3 in fine-tuning the ability of cells to utilize energy and resource through autophagy. Moreover, PRL-3 depends on autophagy to promote carcinogenesis process in ovarian cancer. The study contributed to a better understanding of PRL-3 in cancer

progression, and also suggested that inhibition of autophagy may have positive effect on cancer patients with PRL-3 overexpression.

Recently, activated KRas has been shown to increase tumorigenesis dependent on autophagy. In this case, there are several similarities between PRL-3 and KRas. 1) both PRL-3 and KRas function as oncogenes; 2) autophagy activation by PRL-3 or KRas are both critical for cancer cell proliferation under starvation condition; 3) both proteins are able to activate receptor tyrosine kinase signaling; 4) both proteins have similar membrane targeting domain -- polybasic domain and prenylation domain which locates in the C-terminus of the protein, which might lead to similar localization of both these two proteins. These striking correlations prompted me to study the possible relationships between the two genes further, and form the core of my focus in the next chapter.

CHAPTER 5: CONSTITUTIVELY ACTIVATED KRAS (G13D, G12V) UPREGULATES PRL-3 PROTEIN LEVEL

5.1 Background

The Ras superfamily includes over 150 members with GTPase activity. Based on similarities in sequences and functions, the Ras superfamily is further categorized into different subfamilies. Within the Ras subfamily, KRas is the best studied member due to the correlation of its mutations with human cancers (Wennerberg et al., 2005).

The full name of KRas is V-Ki-ras2 Kirsten rat sarcoma viral oncogene homolog, and it is encoded by the KRAS gene in human (McGrath et al., 1983). It functions as a molecular switch in the cells, and its activity depends on whether it is binding to a guanosine triphosphate (GTP) or guanosine diphosphate (GDP). KRas is activated when bound to GTP, whereas it stays inactive when bound to GDP. KRas itself has low intrinsic GTPase activity. Therefore, the exchanging of bound nucleotide (GTP or GDP) is facilitated by guanine nucleotide exchange factors (GEFs) and GTPase activating proteins (GAPs). GAP binds to KRas, and functions to stimulate GTPase activity of KRas. GEF catalyzes the release of GDP from KRas, which stimulates the exchange of GDP for GTP (Vigil et al., 2010). Thus, with the help of GAP and GEF, KRas is able to circle rapidly between their active GTP-bound and inactive GDP-bound status according to its upstream regulators (Schubbert et al., 2007).

KRas functions downstream of several receptor tyrosine kinases (RTKs), including Epidermal Growth Factor Receptor (EGFR), Platelet Derived Growth Factor Receptor (PDGFR), and Vascular-Endothelial Growth Factor Receptor (VEGFR) (Wilhelm et al., 2004). Ligand binding to the extracellular domain of these RTKs results in receptor dimerization and the phosphorylation of its intracellular domains. As a consequence, KRas gets GTP bound and activated. RAF proto-oncogene serine/threonine-protein

kinase (RAF) binds to GTP bound KRas specifically, and thus it is translocated to the plasma membrane (KRas itself has a membrane associated localization due to the C-terminus prenylation) where it can be phosphorylated by different protein kinases. Phosphorylated RAF is fully activated to phosphorylate its downstream effectors (Marais et al., 1998). Activated RAF phosphorylates Mitogen/Extracellular signal-regulated Kinase 1/2 (MEK1/2), subsequently leading to the phosphorylation of ERK1/2. ERKs, as proline-directed protein kinases, phosphorylate proline-neighboring serine or threonine residues (Tanoue et al., 2000). Activated ERK regulates growth factor-responsive targets in the cytosol and also translocates to the nucleus where it phosphorylates a number of transcription factors (Wortzel and Seger, 2011). By phosphorylating their substrates, ERKs modulate a wide variety of stimulated cellular processes, mainly including proliferation, differentiation, survival, as well as apoptosis and stress response (Chambard et al., 2007; Wortzel and Seger, 2011). Dysregulation of the ERK signaling is known to result in various pathologies, inducing neurodegenerative diseases (Kim and Choi, 2010), developmental diseases (Tidyman and Rauen, 2009), diabetes (Tanti and Jager, 2009), as well as cancer. (Dhillon et al., 2007). Another important downstream effector regulated by KRas is PI3K. Activated GTP-bound KRas has been shown to bind to and activate PI3K directly (Castellano and Downward, 2011). With the activation of PI3K, PI(4,5)P2 is phosphorylated to generate PI(3,4,5)P3, leading to an activation of AKT, which also plays important roles in KRas-mediated cell survival and proliferation (Jancik et al., 2010; Vivanco and Sawyers, 2002). The two main signaling pathways downstream of KRas are summarized in **Figure 24**. The dysregulation of both pathways may contribute to cancer progression (Marc, 2012).

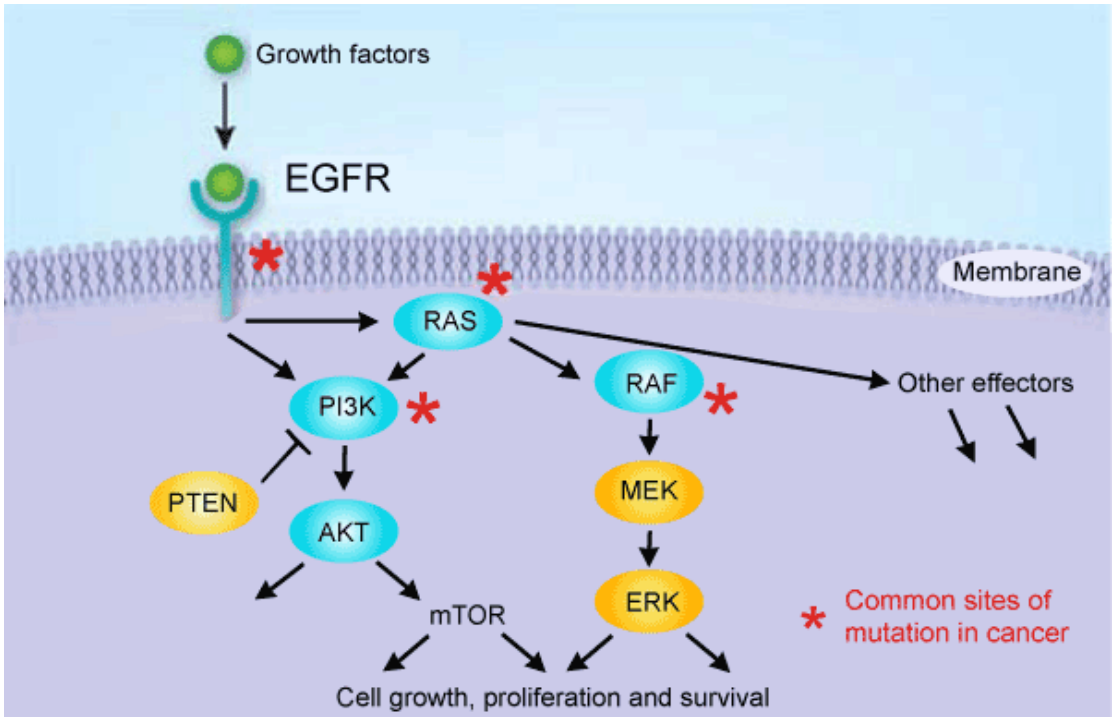

Figure 24. The two main downstream pathways of KRas. Figure Adapted from Marc Pusztaszeri (Marc, 2012). PI3K-AKT, and RAF-MEK- ERK are the two main downstream pathways of KRas.

Indeed, mutations in some certain sites of KRas result in amino acid substitutions that reduce its intrinsic GTPase activity. Such mutations disable KRas to hydrolyze the GTP, therefore locks KRas in an activated GTP-bound state, regardless of the status of its upstream pathways. The constitutively activated mutation of KRas may result in the development of many human cancers (Jancik et al., 2010). Thus, KRas is a proto-oncogene, and it is one of the most frequently mutant genes in human cancers. The majority of the KRas mutations in cancers are in codons 12, 13 (exon 2), and codon 61 (exon 3) (Bos, 1989). Different KRas mutation variants show different preferences on the activation of its downstream effectors. For example, KRas-G12D, the most common KRas mutation in colon and pancreatic cancers (Brink et al., 2003; Kim et al., 2011; Neumann et al., 2009), primarily activates PI3K- AKT signaling pathway (Cespedes et

al., 2006; Ihle et al., 2012), and causes constitutive PI3K-mTOR activation, without affecting the activity of the RAF-MEK-ERK pathway (Cespedes et al., 2006). However, KRas-G12V, the second most common KRas mutation in colon cancers predominately functions on RAF-MEK-ERK pathway but not the PI3K-AKT pathway (Ihle et al., 2012). In addition, different mutations of KRas also have different oncogenic potentials. KRas-G12V is associated with more aggressive cancer behavior and has more oncogenic potential than KRas-G12D (Andreyev et al., 1998; Cespedes et al., 2006). KRas-G13D is the third most common KRas mutation in colon cancers (Brink et al., 2003; Neumann et al., 2009). Colon cancer cells with the expression of this mutant form of KRas show anchorage-independent growth, and increased expression of growth promoting genes c-myc (Shirasawa et al., 1993), but less oncogenic potential than mutations in codon 12 (Guerrero et al., 2000). Notably, activating mutations of KRas are commonly found in multiple cancers including: pancreatic cancers (95%), thyroid cancers (55%), colorectal cancers (35%), and lung cancers (35%), and often constitute essential steps in cancer development (Kranenburg, 2005; Shirasawa et al., 1993).

Interestingly, there are some similarities between KRas and PRL-3. Functionally, both of them are strong oncogenes that contribute to cancer progression. Also, both proteins have been shown to activate ERK and AKT to promote cell proliferation and inhibit apoptosis (Al-Aidaroos and Zeng, 2010). Structurally, both proteins have a polybasic domain followed by a prenylation domain in the C-terminus, contributing to membrane association localization. It is highly possible that their similar localization may enable them to interact or crosstalk with each other. According to the previous chapters, PRL-3 is specifically degraded by autophagy, and PRL-3 requires autophagy activity to promote cancer progression. Interestingly, similar with PRL-3, activated KRas mutation has been shown to require autophagy to maintain its tumorigenesis ability (Guo et al., 2011a).

However, correlations between these two important oncogenes PRL-3 and KRas are still lacking, and therefore I will present some data related to the aspects in this chapter.

5.2 Outline Of Experiments

1. To test the correlations between constitutive activated KRas and PRL-3, I obtained 2 pairs of isogenic cell lines, with KRas status being the only difference between each pair. I checked PRL-3 protein levels in these cell lines.

2. I stably knocked down KRas in HCT116 (KRas-G13D) and DLD1-PRL-3 (KRas-G13D) cells, and check the changes of PRL-3 protein level as well as KRas downstream effectors. mRNA level of PRL-3 were also checked.

3. KRas-G12V, one of most oncogenic KRas mutation was overexpressed in HCT116 and Hkh-2 cells. PRL-3 protein levels and mRNA level changes were determined by Western blotting and RT-qPCR.

4. MEK inhibitors U0126 and PD98059 were used to investigate the role of RAF-MEK-ERK pathway in KRas mediated upregulation of PRL-3 protein level.

5.3 Results

5.3.1 The Knockout Of Constitutively Activated Kras-G13D Mutation Reduces Endogenous PRL-3 Protein Level

Our group found that PRL-3 induced EGFR activation (Al-Aidaroos et al., 2013). KRas is an important downstream factor of EGFR. In order to investigate whether there are any other links among EGFR, KRas and PRL-3 activity / expression levels, the experiments below were performed.

To investigate the correlation between KRas and PRL-3, I used two pairs of isogenic cell lines: DLD-1 and DKO-3; together with HCT116, and Hkh-2 (Shirasawa et al., 1993). A point mutation that converts Glycine (G) to Aspartic acid (D) in codon 13 (G13D) of KRas is present in one allele of DLD-1. Such amino acid replacement mutation reduces the intrinsic GTPase activity of KRas, and thus locked KRas in a GTP-bound status. Consequently, KRas is constitutively activated in DLD-1 cells. DKO-3 is an isogeneic counterpart of DLD-1, in which the constitutively activated KRas was disrupted by homologous recombination. Similarly, HCT116 also harbors a constitutively activated KRas-G13D mutation. Hkh-2 is its KRas wild-type isogeneic counterpart. Either DLD-1 and DKO-3, or HCT116 and Hkh-2 are paired cell lines with identical genetic background, and different KRas status. The KRas status of these cell lines is summarized in a cartoon (**Figure 25A)**.

Western blottings were performed to examine and compared the endogenous PRL-3 protein level among the four cell lines (**Figure 25B**). Consistent with our previous finding (Wang et al., 2010), endogenous PRL-3 protein was not expressed in DLD-1 cells, while there was relatively high expression level of endogenous PRL-3 protein in HCT116 cells. Significantly, Hkh-2 had lower endogenous PRL-3 protein level than its KRas mutant

counterpart HCT116. The results indicated that constitutively activated KRas might contribute to an upregulation of endogenous PRL-3 protein level.

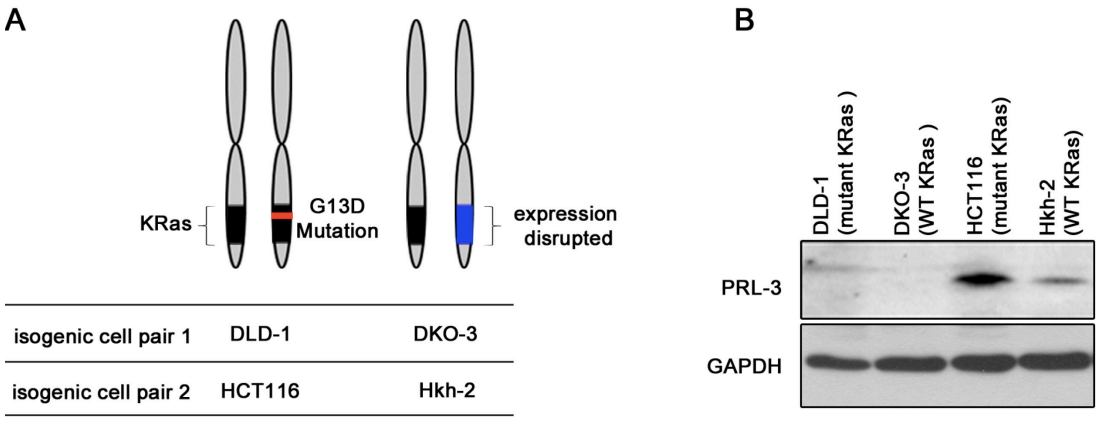

Figure 25. The knockout of constitutively activated KRas-G13D mutation reduced endogenous PRL-3 protein level. (**A**) KRas status of DLD-1, DKO-3, HCT116 and Hkh-2 cells. (**B**) Exponentially growing cells of indicated cell lines were lysed for Western blotting analysis for the expression level of endogenous PRL-3. GAPDH was used as loading control.

5.3.2 The Knockdown of KRasG13D Decreases PRL-3 Protein Level

To confirm the results acquired from **Figure 25**, I constructed two shRNAs specifically against KRas, and infected HCT116 cells with these shRNAs. Exponentially growing cells were lysed for Western blotting analysis after stable selection (**Figure 26A**). Phospho-ERK1/2 (Thr202/Tyr204) (pERK1/2), levels were checked in these cell lines, and decreased significantly with the knockdown of KRas (**Figure 26A**). Endogenous PRL-3 protein levels in HCT116 were downregulated upon the knockdown of KRas. Band intensity of PRL-3/GAPDH was quantified using imageJ according to Materials and Methods, and showed in white bar in the right panel (**Figure 26B**, white columns). RT-qPCR was performed to check the transcript level of PRL-3 in these cell lines, and

GAPDH was used as the internal control. Transcript levels of PRL-3 are shown in the right panel (**Figure 26B**, black columns). The difference between the mRNA and protein levels of PRL-3 suggests that the regulation of PRL-3 by KRas knockdown is not due to the regulation of transcription (**Figure 26B**, white columns V.S. black columns).

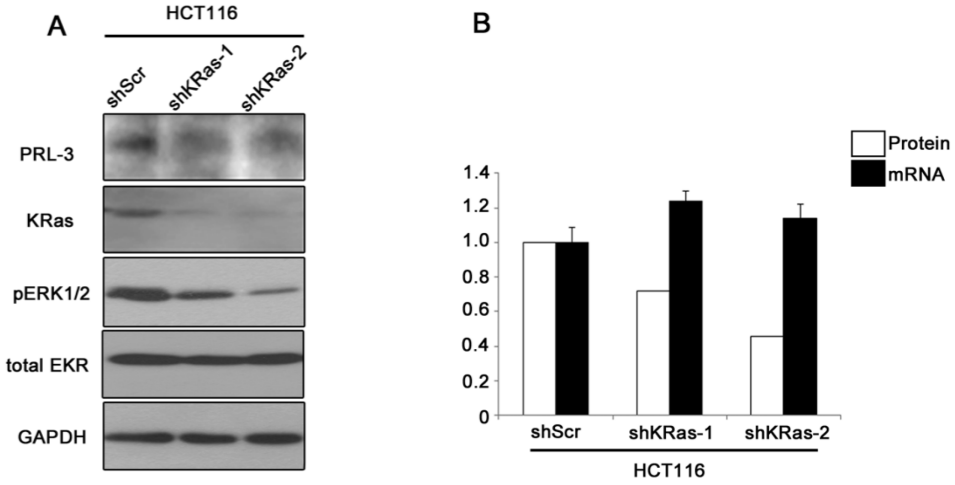

Figure 26. KRas knockdown led to downregulation of endogenous PRL-3 protein levels. (**A**) HCT116 cells were stably infected with shRNA against nonspecific target (shScr), or KRas (shKRas-1, or shKRas-2) as indicated. Exponentially growing cells were lysed for Western blotting analysis for indicated proteins. (**B**) the ratios of PRL-3/ GAPDH from (A) were quantified as described in materials and methods (white columns). mRNA levels of PRL-3 of indicated cell lines were quantified by RT-qPCR, and presented as a histogram as mean±S.D. (black columns).

Since DLD-1 (KRas-G13D) showed undetectable endogenous PRL-3 protein levels, I stably overexpressed PRL-3 in this cell line. After stable selection, PRL-3 protein can easily be detected in DLD-1-PRL-3. Similarly, the knockdown of KRas significantly downregulated exogenous PRL-3 protein levels but left mRNA level unchanged in DLD-1-PRL-3 cells (**Figure 27A-B**). My results suggest that constitutively activated mutation of KRas upregulates PRL-3 in a post-transcriptional level.

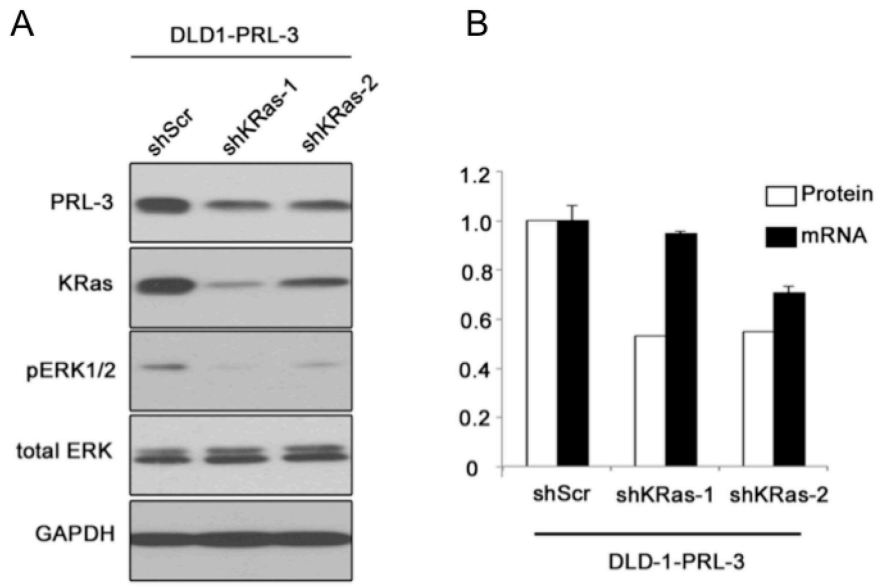

Figure 27. KRas knockdown led to downregulation of exogenous PRL-3 protein level.

(**A**) DLD-1-PRL-3 cells were stably infected with shRNA against nonspecific target (shScr), or KRas (shKRas-1, or shKRas-2). Exponentially growing cells were lysed for western blotting analysis for indicated proteins. (**B**) the ratios of PRL-3/ GAPDH from () were quantified as described in materials and methods (white columns). mRNA levels of PRL-3 of indicated cell lines were quantified by RT-qPCR, and presented as a histogram as mean±S.D. (black columns).

5.3.3 Overexpression of constitutively activated KRas-G12V leads to upregulation of endogenous PRL-3

In the previous section, I found that KRas-G13D, the third most common KRas mutation in colorectal cancer, positively correlated with PRL-3 protein levels by KRas knockout or knockdown approaches. Among the top three most common KRas mutations, KRas-G12V has the highest oncogenic potential (Guerrero et al., 2000). Thus, I further investigate whether this KRas mutation is also positively related with PRL-3 protein levels.

I overexpressed KRas-G12V in HCT116 (KRas-G13D) and Hkh2 (KRas wild type) cells. After stable selection, exponentially growing cells were lysed for western blotting analysis. Endogenous PRL-3 protein level, pERK1/2, and pAKT(S473) levels were checked in these cell lines (**Figure 28A**). The KRas overexpression in HCT116 cells is not as clear as that in Hkh-2 cells, and this may be due to a high endogenous KRas level in HCT116 cells. The overexpression of KRas-G12V led to an upregulation of pERK1/2 level in both cell lines, while pAKT levels remained unchanged. As introduced before, although both PI3K-AKT and RAF-MEK-ERK are both downstream pathways regulated by KRas, KRas-G12V affects RAF-MEK-ERK pathway more predominantly (Ihle et al., 2012). Importantly, endogenous PRL-3 protein levels increased in Hkh-2 cells with the overexpression of KRas-G12V. The increase of PRL-3 endogenous protein level in HCT116 is not as clear as that in Hkh-2 cells, and this may be due to the originally existing KRas-G13D in HCT116 cells.

To investigate if such regulation of PRL-3 is due to transcription level, RT-qPCR of these cell lines was performed (**Figure 28B**, black columns). The mRNA levels of PRL-3 were not significantly different between these four cell lines. Thus, the overexpression of KRas-G12V did not significantly affect PRL-3 transcript level, despite an increase in protein levels. My results suggest a post-transcriptional regulation of PRL-3 by KRas-G12V.

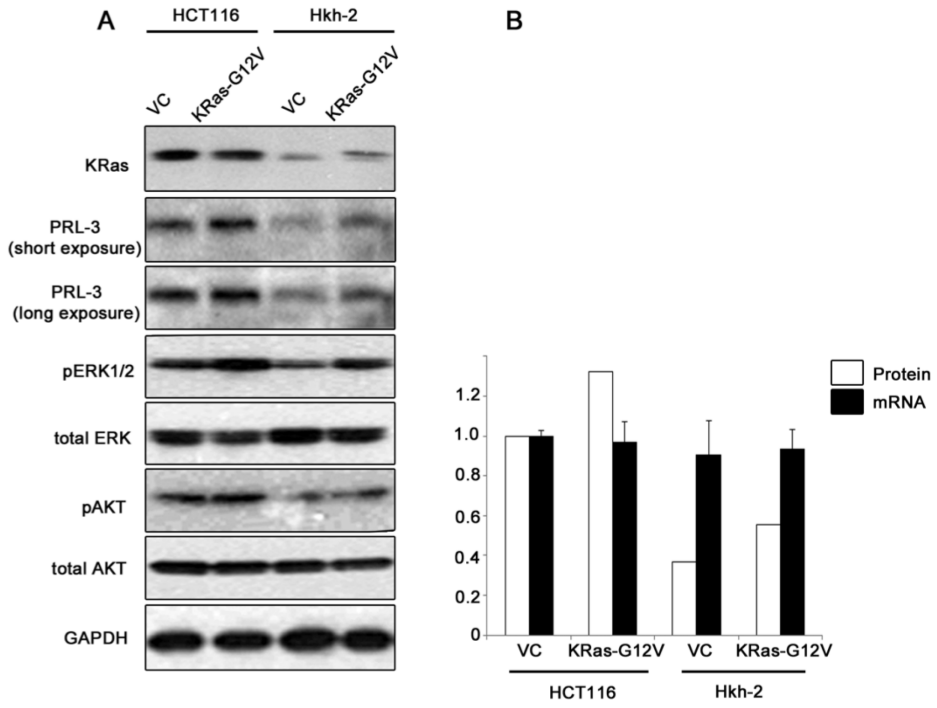

Figure 28. Overexpression of constitutively activated KRas-G12V upregulated endogenous PRL-3 protein levels. (**A**)KRas-G12V was stably overexpressed in HCT116 or Hkh-2 cells. Indicated cells were lysed for Western blotting analysis for indicated proteins. (**B**) The ratio of PRL-3/ GAPDH from (A) were quantified as descripted in materials and methods (white columns). mRNA levels of PRL-3 of indicated cell lines were quantified by RT-qPCR, and presented as a histogram as mean±S.D. (black columns).

5.3.4 Inhibition of MEK activity downregulates PRL-3 protein level

My previous results suggested a positive correlation of PRL-3 expression level and pERK1/2 level. To investigate whether mutation of KRas upregulates PRL-3 protein level through RAF-MEK-ERK pathway, I used two MEK inhibitors, U0126 and PD98059, for further experiments. U0126 is a highly selective inhibitor of MEK1 and MEK2. MEK1/2, also called MAP Kinase or ERK kinase, activates ERK by phosphorylating its activation site (Cobb and Goldsmith, 1995). Thus, the treatment of U0126 leads to inhibition of pERK1/2 level as well as ERK1/2 activity. Similarly, PD98059 is a MEK1 inhibitor that

binds to the inactive forms of MEK1 and prevents its activation, and the treatment of PD98059 similarly leads to the inhibition of ERK activity (Mandic et al., 2001).

DLD-1-PRL-3 cells were treated with U0126 or PD98059 for indicated concentration and durations, before lysis for Western blotting analysis (**Figure 29**). The treatment of U0126 with different concentrations (from 1 μM to 20 μM) for different durations (from 2 hours to 48 hours) led to a reduced pERK1/2 level, while left pAKT level unchanged (**Figure 29A**). Importantly, the prolonged treatment of U0126 for 24 hours or 48 hours resulted in significantly downregulation of PRL-3 protein level, in a dose dependent manner (**Figure 29A**, red boxes). Similarly, treatments of PD98059 for different durations resulted in a significant downregulation of pERK1/2 level in a dose dependent manner (**Figure 29B**). Importantly, prolonged high dose treatment (24 and 48 hours) of PD98059 downregulated PRL-3 protein level (**Figure 29B**, red boxes). My results here suggest that PRL-3 is downregulated with the inhibition of RAF-MEK-ERK pathway.

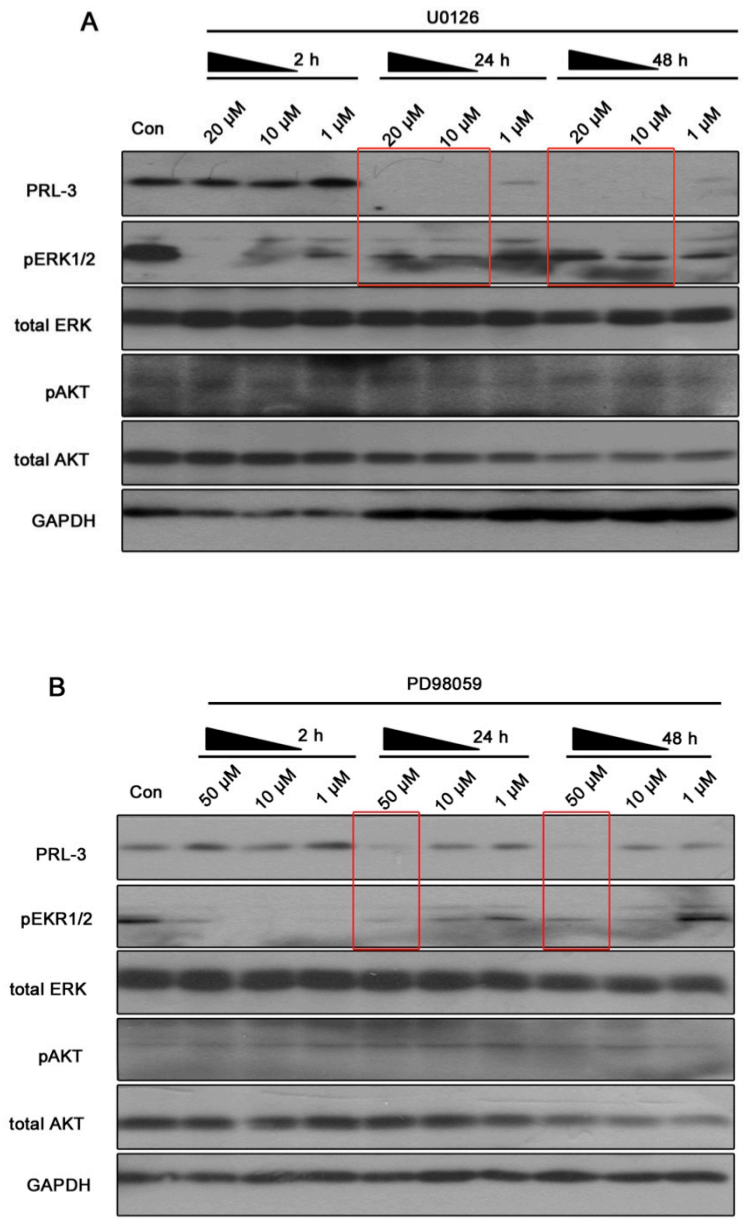

Figure 29. Inhibition of MEK activity downregulated PRL-3 protein levels.

(**A**) DLD-1-PRL-3 cells were treated with/ without (Con) MEK inhibitor U0126 for indicated concentrations and durations before lysis for Western blotting analysis for indicated proteins. (**B**) DLD-1-PRL-3 cells were treated with/ without (Con) MEK inhibitor PD98059 for indicated concentrations and durations before lysis for Western blotting analysis for indicated proteins.

5.4 Discussion

In this chapter, I found that the expression of constitutively activated mutant KRas (G13D/G12V) positively correlated with the up regulation of PRL-3 protein, without any effect on PRL-3 mRNA expression level. This is in accordance with an increase in RAF-MEK-ERK signaling. ERK inhibition suppressed the upregulation of PRL-3 by mutant KRas. My results pointed to a novel post-translational regulation of PRL-3 by the Ras-RAF- MEK-ERK pathway.

Approximately 17% - 25% human cancers are known to have a mutated KRAS allele (Kranenburg, 2005). Moreover, KRas mutation predicts poorer prognosis of patients with multiple cancers (Kranenburg, 2005). Thus, KRas plays a very important role in human cancers. Besides being a signal transduction switch that modulates the activity of various cellular signaling pathways, KRas also regulates the expression of many proteins. For instance, ERK, as a downstream effector of Ras genes (HRas, KRas and NRas), may translocate to the nucleus when activated, and therefore phosphorylates and activates different transcription factors. Thus, KRas is able to regulate a variety of proteins transcriptionally (Zuber et al., 2000). In addition, KRas also regulates protein levels by post-transcriptional mechanisms. Firstly, KRas-G12V upregulates basal autophagy (Guo et al., 2011a). However, it is unlikely that constitutively activated KRas mutation regulates PRL-3 protein level through increased basal autophagy activity, as my results show PRL-3 is an autophagic substrate. Secondly, KRas-G13D has been shown to activate ERK to protect $p21^{Waf1/Cip1}$ from proteasome degradation through transcriptionally upregulation of cyclin D1. Specifically, increased ERK activity promotes cyclin D1 transcription, thereby increasing cyclin D1 binding and stabilization of $p21^{Waf1/Cip1}$ from proteasome degradation by masking the $p21^{Waf1/Cip1}$ proteasome-binding motif (Coleman et al., 2003). A similar mechanism may be relevant in the case for activated KRas- RAF- MEK- ERK pathway upregulating PRL-3 protein level.

Indeed, PRL-3 was degraded by proteasome with SAHA (an HDAC inhibitor) treatment (Zhou et al., 2011). Therefore, it is possible that the status of ERK signaling determines whether PRL-3 is degraded by proteasome or not. Specifically, when ERK activity is low, PRL-3 gets degraded by proteasome and autophagy pathways; while with over activated ERK; PRL-3 is only degraded by autophagy but not proteasome, leading to an increase of PRL-3 protein level. Such transition may be fulfilled by a stabilizing modification of PRL-3 by over-activated ERK directly or indirectly. Further experiments are still needed to investigate how PRL-3 is upregulated by the activation of RAF-MEK-ERK pathway, including the knockdown of ERK itself. Understanding the mechanism of Ras-mediated stabilization of PRL-3 could reveal novel targets for inhibition of oncogenic PRL-3 accumulation in cancers.

It has been documented that PRL-3 upregulates the phosphorylation level of ERK (Liang et al., 2007; Park et al., 2013). Thus raises an intriguing possibility that PRL-3 and ERK activity might form a positive feedback loop. PRL-3 is a strong oncogene that contributes to multiple aspects of tumor progression (Al-Aidaroos and Zeng, 2010). RAF-MEK-ERK pathway is activated in more than 30% of human cancers, and the aberrant regulation of this pathway promotes cancers (Hatzivassiliou et al., 2012). Such a positive feedback loop of PRL-3 and ERK activity might strengthen the tumorigenic properties of each other. However, such feedback loop may also provide new targets for cancer therapy. For example, cancer patients with KRas mutations may have an over-activation of RAF-MEK-ERK pathway, which may result in an upregulation of PRL-3 protein level. The upregulated PRL-3 may in turn, functions to further enhance ERK activity. If so, patients might be expected to be more sensitive to targeted therapy against PRL-3 or RAF-MEK-ERK pathway due to addiction to such positive feedback loops.

EGFR inhibitors such as Cetuximab and Panitumumab are widely used in colorectal cancer therapy (Adams and Weiner, 2005). However, patients with KRas mutations

respond poorly to EGFR inhibition (Amado et al., 2008), as oncogenic KRas lies downstream of this receptor. In contrast, inhibition of MEK and PI3K, which lies downstream of KRas, shows good therapeutic effect in cancers with KRas mutation (Engelman et al., 2008). Since my results suggest that PRL-3 also lies downstream of KRas, it is plausible that PRL-3 inhibition may likewise be a good target for cancer patients with KRas mutations. Importantly, our group showed that PRL-3, as an intracellular protein, is targetable by specific antibody (Guo et al., 2011b). Although further *in vivo* experiments are still needed to study the utility of PRL-3 inhibition in KRas mutant cancers, my study might shed light on new therapeutic approach for cancer patients with activating KRas mutations.

CHAPTER 6: CONCLUSION

In this thesis, I described three novel findings on PRL-3 (PTP4A3) metastatic phosphatase: First, PRL-3 promoted canonical autophagy flux, and it depends on autophagy to promote cancer progression in ovarian cancer cells. Second, PRL-3 was specifically degraded by autophagy especially upon starvation conditions. Third, I also showed some important observations that PRL-3 protein levels were increased by constitutively activate KRas mutation (KRas-G13D or G12V).

I further illustrate the detailed results in below cartoon (Figure 29). To activate autophagy activity, PRL-3: (1) upregulates the activity of ULK1, which is a key initiator of autophagy; (2) promotes hVps34-Beclin-1-dependent autophagosome formation; (3) accelerates LC3-I to LC3-II conversion in an ATG5-dependent manner, and (4) enhances the degradation of p62, a key autophagy substrate (related regulations of 1, 2, 3, and 4 are also labeled in Figure 29). These functions of PRL-3 are dependent on its catalytic activity and prenylation-dependent membrane association. Following autophagy activation, PRL-3 unexpectedly serves as a novel autophagic substrate (No.5 in **Figure 29**). It was specifically degraded by autophagy especially upon starvation condition thereby establishing a negative feedback-loop that may be required to fine-tune autophagy activity. The correlation between KRas and PRL-3 are also summarized in **Figure 29**, constitutively activate KRas mutation (KRas-G13D or G12V) stabilized PRL-3 protein through RAF-MEK-ERK kinase cascade (No. 6 in **Figure 29**). In the contrary, PRL-3 has been documented to upregulate the activity of ERK (Liang et al., 2007; Park et al., 2013). Thus, PRL-3 and ERK may form a positive feedback loop.

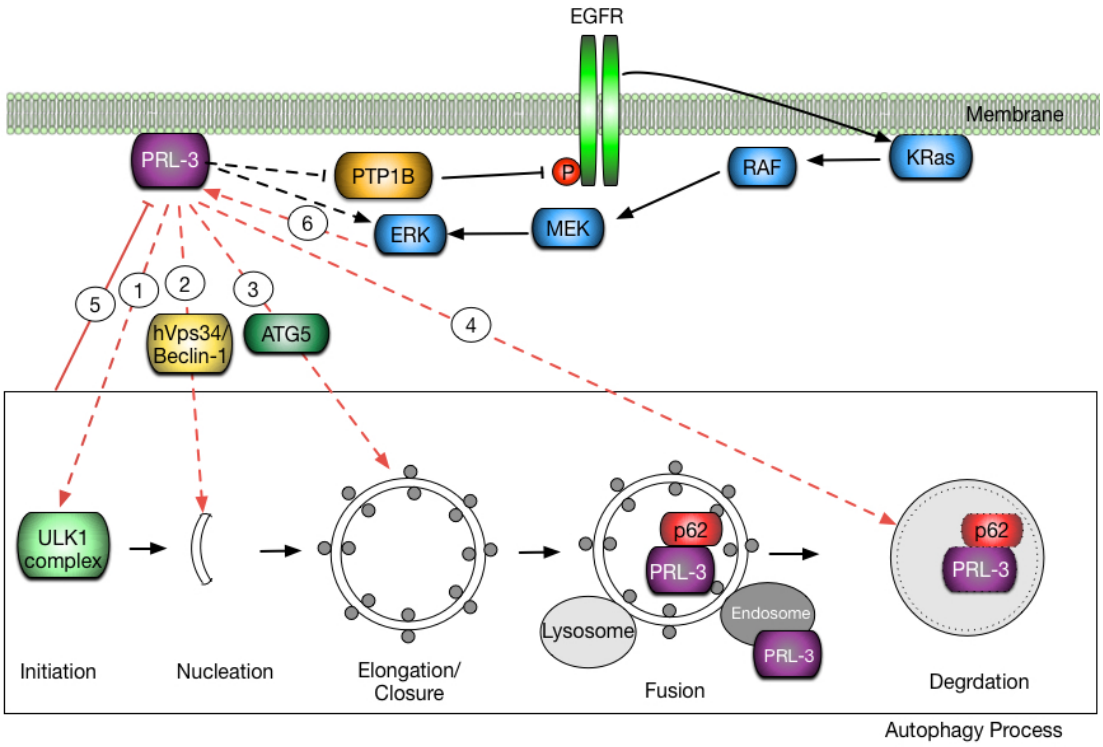

Figure 30. A proposed model of coverage between PRL-3, KRas signaling, and autophagy signaling. PRL-3 activates autophagosome formation and is also degraded by autophagy. Constitutively active mutation of KRas stabilizes PRL-3 through the RAF/MEK/ERK kinase cascade. Solid lines indicate direct regulation, while dotted line indicated indirect regulation. Black lines are based on existing literature, and red lines show novel finding in this study.

My study unveils a picture correlating PRL-3, autophagy, and the KRas pathway, as well as their roles in cancer. PRL-3 and KRas have several similarities including similar mechanism of membrane-associated localization; similar downstream effectors (AKT, ERK1/2); and a common role in promoting cancer progression. Similar to my observation where PRL-3 not only enhanced autophagy flux, but also promoted cancer progression dependent on autophagy activity in ovarian cancer cells, constitutively activate KRas was also shown to accelerate basal autophagy activity, and promoted cancer progression in an autophagy-dependent fashion (Guo et al.,

2011a). Indeed, knocking down autophagy genes such as ATG5 or ATG7 abolishes the tumor promoting effect of mutant KRas (Guo et al., 2011a). There may be several possible explanations for this similarity between PRL-3 and mutant KRas. Mutant KRas triggers changes in metabolism to facilitate its cell transforming activities (Bryant et al., 2014). In this situation, autophagy providing new energy resources, might contribute to survival of cells with KRas mutations (Bryant et al., 2014). Given the similarities between PRL-3 and KRas, it may be interesting to study whether PRL-3 may also cause changes in cellular metabolism to achieve its oncogenic effect.

A previous study from our group showed that PRL-3 activates EGFR, an upstream regulator of KRas through downregulation of protein-tyrosine phosphatase 1B (PTP1B), an EGFR phosphatase. Taken together with my results showing that constitutively activated mutations in KRas can stabilize PRL-3 protein, it is likely that a positive feedback mechanism may exist between these oncogenes. Since PRL-3 itself was upregulated by constitutively activated KRas mutant, upregulating the expression level of PRL-3 might serve as an alternative route for mutant KRas to accelerate autophagy flux. Moreover, since the blockage of autophagy inhibits tumorigenesis effects of both constitutively activated KRas mutation and PRL-3 overexpression, it may also be possible that PRL-3 functions as an effector of mutant KRas to promote cancer progression. Further studies are warranted to find out the role of PRL-3 in constitutively activated KRas mutation in promoting cancer progression.

KRas, HRas and NRas are three closely related genes in Ras subfamily. They are highly homologous, engage a common set of downstream effectors, and are able to exhibit oncogenic activity especially when mutant (Prior et al., 2012). Indeed, oncogenic mutations of KRas, HRas and NRas are frequently found in human cancers derived from different origins (Prior et al., 2012). Thus, it is of significant interest to

investigate whether the constitutive activate mutations in HRas and NRas may also cause upregulation of PRL-3. Investigate the correlations between PRL-3 and KRas, HRas and NRas, may help us understand the regulation of PRL-3 in cancers. In addition, given the large number of clinical studies underway targeting Ras signaling networks, establishing the importance of PRL-3 as an oncogenic Ras effector would potentially unravel new targets for therapy.

SUPPLEMENTARY FIGURES

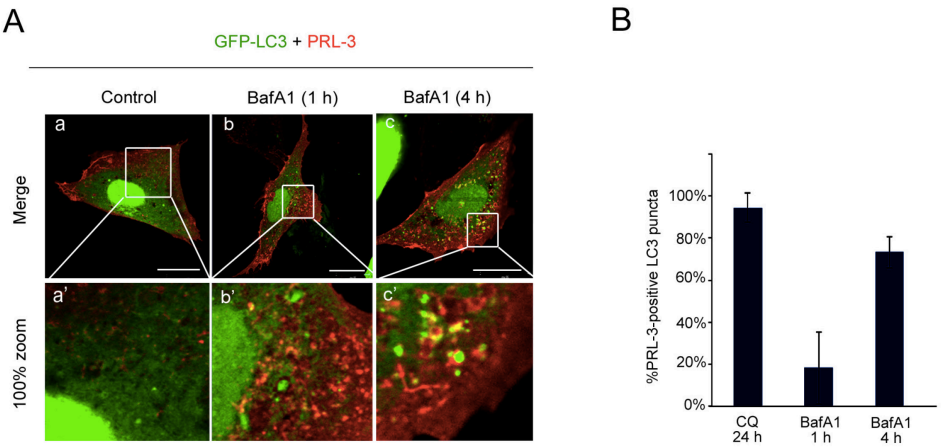

Figure S1. Localization of PRL-3 with Baf A1 treatment for shorter durations. CHO-PRL-3 cells were transiently overexpressed with GFP-LC3, and let grow for 24 hours before treatment and immunofluorescence assay. (**A**) Representative images with CHO cells treated for different time points. (**B**) Percentage of PRL-3 positive LC3 puncta were quantified manually in at least 20 cell, and shown as a histogram (mean± S.D.)

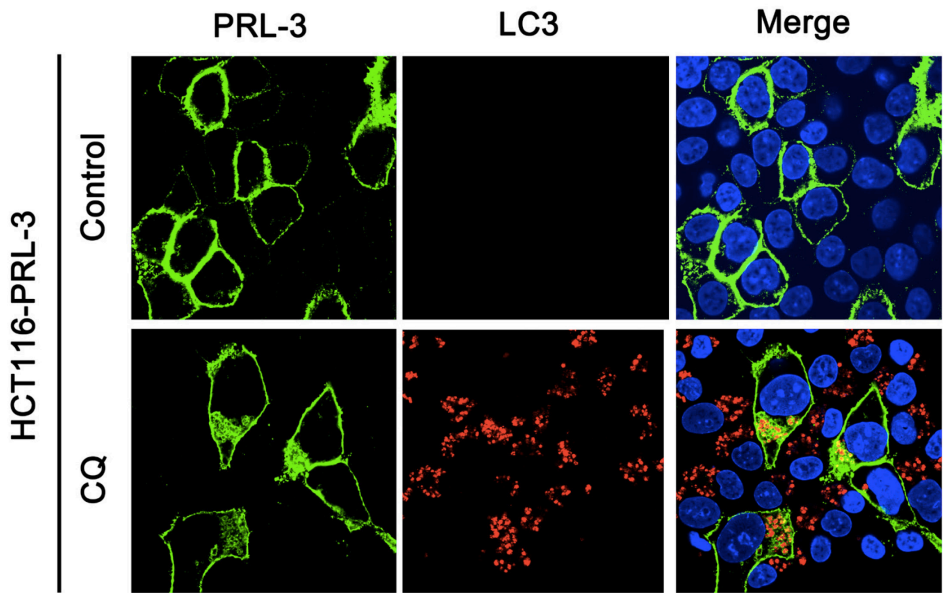

Figure S2. PRL-3 colocalized with LC3 upon CQ treatment in HCT116 cells. HCT116 cells overexpressed with PRL-3 (HCT116-PRL-3) were treated as indicated, before immunolabeling with PRL-3 and LC3.

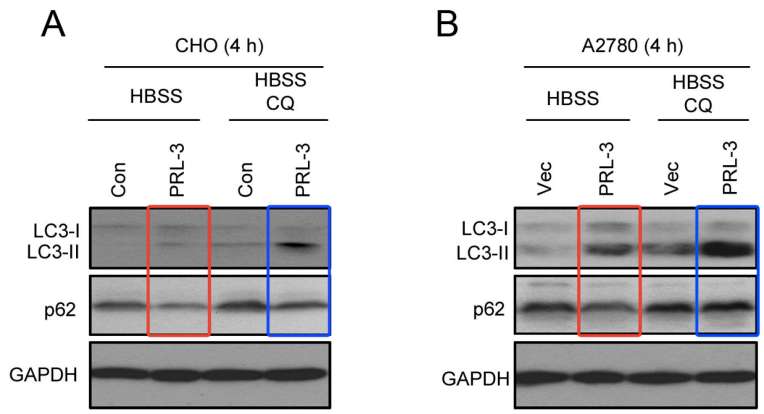

Figure S3. PRL-3 overexpression promoted HBSS induced autophagy flux. Indicated cell lines were treated as indicated before the lysis for Western Blotting analysis.

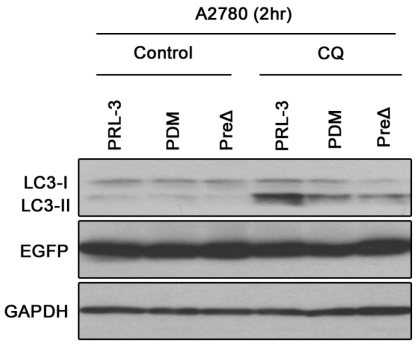

Figure S4. PRL-3 promoted autophagy flux dependent on its phosphatase activity as well as its prenylation domain. Indicated cell were treated with (CQ) or without CQ (Control) before lysis for Western blotting analysis.

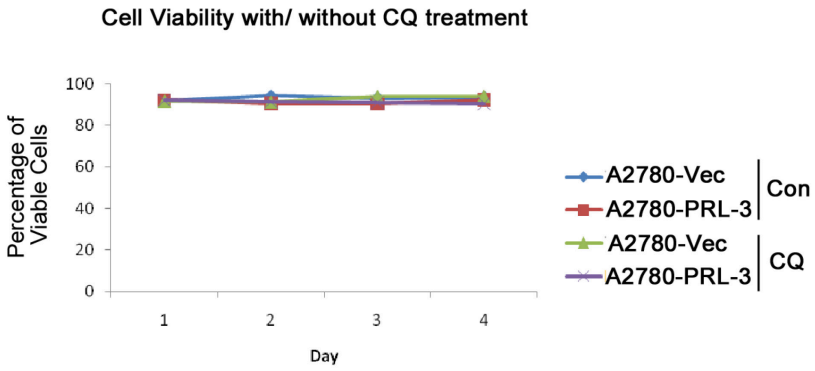

Figure S5. A2780 Cell viability is not much affected upon prolonged CQ treatment in A2780 cells. Cells with the same treatments in Figure 19G were counted after the trysin blue staining.

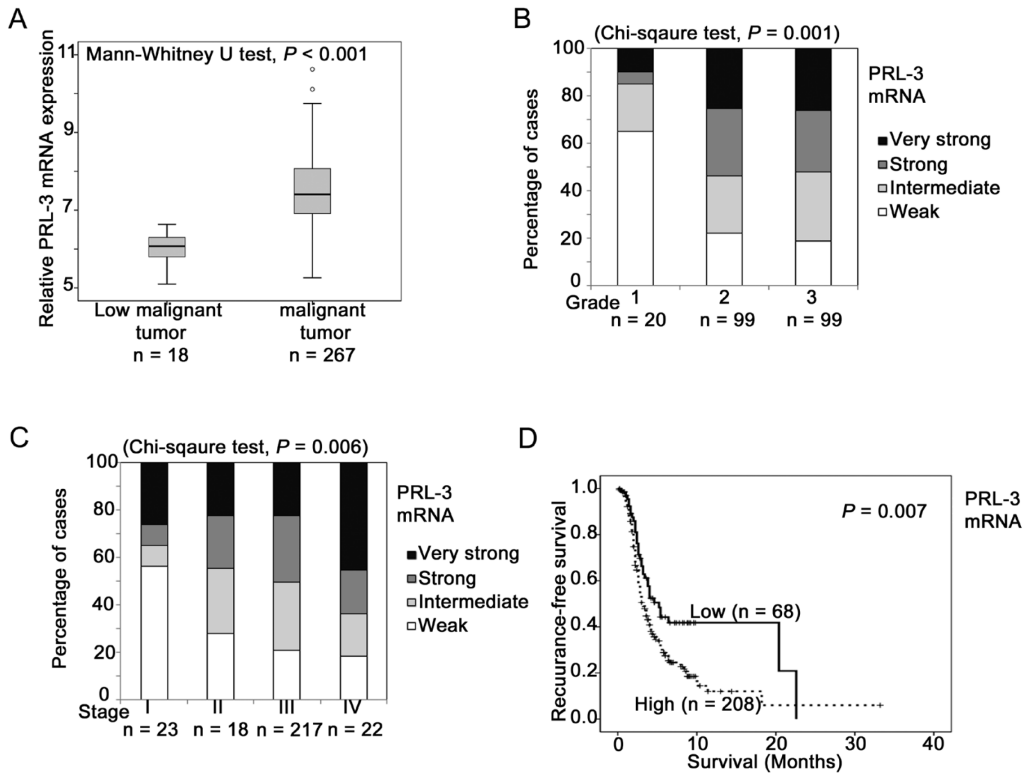

Figure S6. The prognostic value of PRL-3 in ovarian cancer cohort GSE9899. (**A**) PRL-3 mRNA level was significantly higher in patients with malignant ovarian tumors compared to those with low malignant potential tumors. (**B** and **C**) PRL-3 mRNA level was significantly higher in tumors with higher (**B**) grades or (**C**) stage. (**D**) Expression level of PRL-3 predicts recurrence-free survival

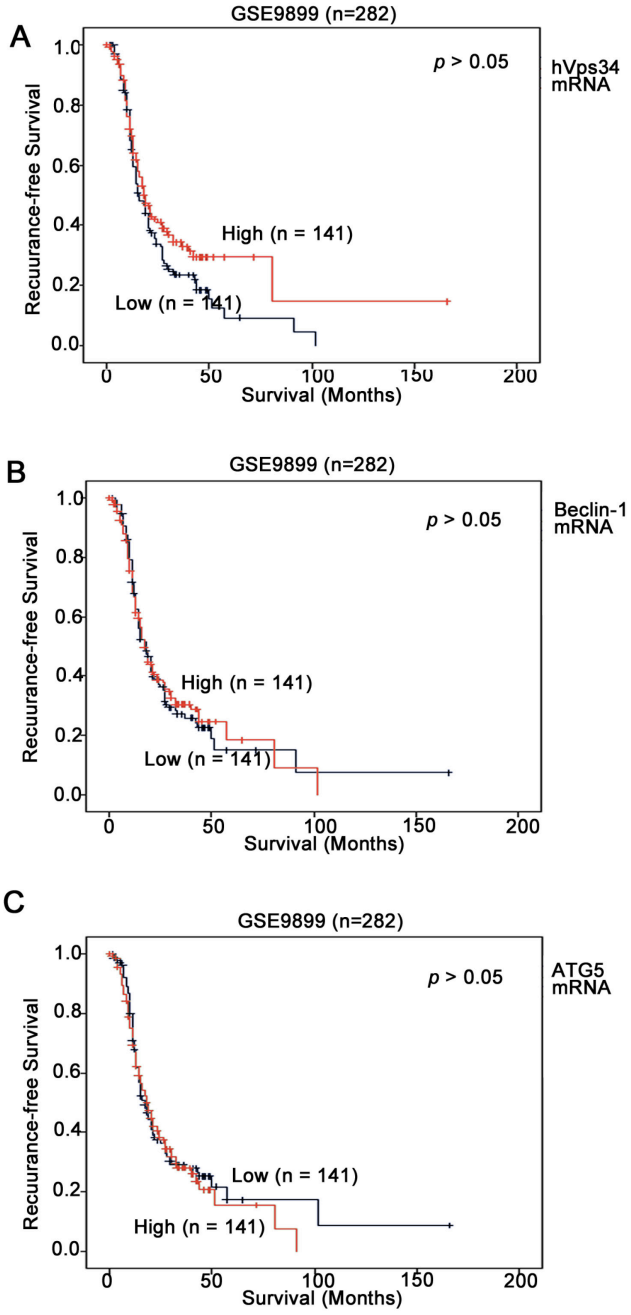

Figure S7. Autophagy genes alone have no prognostic value for recurrence-free survival in ovarian cancer cohort GSE9899. (A) The expression level of (A) hVps34, (**B**) Beclin-1, or (**C**) ATG5 does not correlate with recurrence free survival ($p > 0.05$)

PUBLICATIONS

Huang YH*, Al-Aidaroos AQ*, Yuen HF*, Zhang SD, Shen HM, Rozycka E, McCrudden CM, Tergaonkar V, Gupta A, Lin YB, Thiery JP, Murray JT, Zeng Q. A role of autophagy in PTP4A3-driven cancer progression. **Autophagy**. 2014 Aug 1;10(10).

Yuen HF*, McCrudden CM*, **Huang YH***, Tham JM, Zhang X, Zeng Q, Zhang SD, Hong W. TAZ expression as a prognostic indicator in colorectal cancer. **PLoS One**. 2013;8(1):e54211.

Yuen HF, Abramczyk O, Montgomery G, Chan KK, **Huang YH**, Sasazuki T, Shirasawa S, Gopesh S, Chan KW, Fennell D, Janne P, El-Tanani M, Murray JT. Impact of oncogenic driver mutations on feedback between the PI3K and MEK pathways in cancer cells. **Biosci Rep**. 2012 Aug;32(4):413-22.

Yuen HF, McCrudden CM, Grills C, Zhang SD, **Huang YH**, Chan KK, Chan YP, Wong ML, Law S, Srivastava G, Fennell DA, Dickson G, El-Tanani M, Chan KW. Combinatorial use of bone morphogenetic protein 6, noggin and SOST significantly predicts cancer progression. **Cancer Sci**. 2012 Jun;103(6):1145-54.

Yuen HF, Zhang SD, Wong AS, McCrudden CM, **Huang YH**, Chan KY, El-Tanani M, Khoo US. Regarding "Co-expression of SNAIL and TWIST determines prognosis in estrogen receptor-positive early breast cancer patients". **Breast Cancer Res Treat**. 2012 Jan;131(1):351-2.

REFERENCES

Adams, G.P., and Weiner, L.M. (2005). Monoclonal antibody therapy of cancer. Nature biotechnology *23*, 1147-1157.

Ahn, J.H., Kim, S.J., Park, W.S., Cho, S.Y., Ha, J.D., Kim, S.S., Kang, S.K., Jeong, D.G., Jung, S.K., Lee, S.H*., et al.* (2006). Synthesis and biological evaluation of rhodanine derivatives as PRL-3 inhibitors. Bioorganic & medicinal chemistry letters *16*, 2996-2999.

Aita, V.M., Liang, X.H., Murty, V.V., Pincus, D.L., Yu, W., Cayanis, E., Kalachikov, S., Gilliam, T.C., and Levine, B. (1999). Cloning and genomic organization of beclin 1, a candidate tumor suppressor gene on chromosome 17q21. Genomics *59*, 59-65.

Al-aidaroos, A.Q.O., Yuen, H.F., Guo, K., Zhang, S.D., Chung, T.-H., Chng, W.J., and Zeng, Q. (2013). Metastasis-associated PRL-3 induces EGFR activation and addiction in cancer cells. The Journal of clinical investigation *123*, 3459-3471.

Al-Aidaroos, A.Q.O., and Zeng, Q. (2010). PRL-3 phosphatase and cancer metastasis. Journal of Cellular Biochemistry *111*, 1087-1098.

Albertson, D.G. (2006). Gene amplification in cancer. Trends in genetics : TIG *22*, 447-455.

Alers, S., Loffler, A.S., Wesselborg, S., and Stork, B. (2012). Role of AMPK-mTOR-Ulk1/2 in the regulation of autophagy: cross talk, shortcuts, and feedbacks. Molecular and cellular biology *32*, 2-11.

Alonso, A., Sasin, J., Bottini, N., Friedberg, I., Friedberg, I., Osterman, A., Godzik, A., Hunter, T., Dixon, J., and Mustelin, T. (2004). Protein tyrosine phosphatases in the human genome. Cell *117*, 699-711.

Amado, R.G., Wolf, M., Peeters, M., Van Cutsem, E., Siena, S., Freeman, D.J., Juan, T., Sikorski, R., Suggs, S., Radinsky, R*., et al.* (2008). Wild-type KRAS is required for panitumumab efficacy in patients with metastatic colorectal cancer. Journal of clinical oncology : official journal of the American Society of Clinical Oncology *26*, 1626-1634.

Amaravadi, R.K., Lippincott-Schwartz, J., Yin, X.M., Weiss, W.A., Takebe, N., Timmer, W., DiPaola, R.S., Lotze, M.T., and White, E. (2011). Principles and current strategies for targeting autophagy for cancer treatment. Clinical cancer research : an official journal of the American Association for Cancer Research *17*, 654-666.

Ammer, A.G., and Weed, S.A. (2008). Cortactin branches out: roles in regulating protrusive actin dynamics. Cell motility and the cytoskeleton *65*, 687-707.

Andreyev, H.J., Norman, A.R., Cunningham, D., Oates, J.R., and Clarke, P.A. (1998). Kirsten ras mutations in patients with colorectal cancer: the multicenter "RASCAL" study. Journal of the National Cancer Institute *90*, 675-684.

Basak, S., Jacobs, S.B., Krieg, A.J., Pathak, N., Zeng, Q., Kaldis, P., Giaccia, A.J., and Attardi, L.D. (2008). The metastasis-associated gene Prl-3 is a p53 target involved in cell-cycle regulation. Molecular cell *30*, 303-314.

Berg, T.O., Fengsrud, M., Stromhaug, P.E., Berg, T., and Seglen, P.O. (1998). Isolation and characterization of rat liver amphisomes. Evidence for fusion of autophagosomes with both early and late endosomes. The Journal of biological chemistry *273*, 21883-21892.

Bilici, A., Ustaalioglu, B.B., Yavuzer, D., Seker, M., Mayadagli, A., and Gumus, M. (2012). Prognostic significance of high phosphatase of regenerating liver-3 expression in patients with gastric cancer who underwent curative gastrectomy. Digestive diseases and sciences *57*, 1568-1575.

Birbrair, A., Zhang, T., Wang, Z.M., Messi, M.L., Olson, J.D., Mintz, A., and Delbono, O. (2014). Type-2 pericytes participate in normal and tumoral angiogenesis. American journal of physiology Cell physiology *307*, C25-38.

Bjorkoy, G., Lamark, T., Brech, A., Outzen, H., Perander, M., Overvatn, A., Stenmark, H., and Johansen, T. (2005). p62/SQSTM1 forms protein aggregates degraded by autophagy and has a protective effect on huntingtin-induced cell death. The Journal of cell biology *171*, 603-614.

Bos, J.L. (1989). ras oncogenes in human cancer: a review. Cancer research *49*, 4682-4689.

Brink, M., de Goeij, A.F., Weijenberg, M.P., Roemen, G.M., Lentjes, M.H., Pachen, M.M., Smits, K.M., de Bruine, A.P., Goldbohm, R.A., and van den Brandt, P.A. (2003). K-ras oncogene mutations in sporadic colorectal cancer in The Netherlands Cohort Study. Carcinogenesis *24*, 703-710.

Brown, M.S., and Goldstein, J.L. (1993). Protein prenylation. Mad bet for Rab. Nature *366*, 14-15.

Brunet, A., Roux, D., Lenormand, P., Dowd, S., Keyse, S., and Pouyssegur, J. (1999). Nuclear translocation of p42/p44 mitogen-activated protein kinase is required for growth factor-induced gene expression and cell cycle entry. The EMBO journal *18*, 664-674.

Bryant, K.L., Mancias, J.D., Kimmelman, A.C., and Der, C.J. (2014). KRAS: feeding pancreatic cancer proliferation. Trends in biochemical sciences *39*, 91-100.

Buffart, T.E., Coffa, J., Hermsen, M.A., Carvalho, B., van der Sijp, J.R., Ylstra, B., Pals, G., Schouten, J.P., and Meijer, G.A. (2005). DNA copy number changes at 8q11-24 in metastasized colorectal cancer. Cellular oncology : the official journal of the International Society for Cellular Oncology *27*, 57-65.

Cai, Q., Lu, L., Tian, J.H., Zhu, Y.B., Qiao, H., and Sheng, Z.H. (2010). Snapin-regulated late endosomal transport is critical for efficient autophagy-lysosomal function in neurons. Neuron *68*, 73-86.

Castellano, E., and Downward, J. (2011). RAS Interaction with PI3K: More Than Just Another Effector Pathway. Genes & cancer *2*, 261-274.

Cespedes, M.V., Sancho, F.J., Guerrero, S., Parreno, M., Casanova, I., Pavon, M.A., Marcuello, E., Trias, M., Cascante, M., Capella, G.*, et al.* (2006). K-ras Asp12 mutant

neither interacts with Raf, nor signals through Erk and is less tumorigenic than K-ras Val12. Carcinogenesis *27*, 2190-2200.

Chambard, J.C., Lefloch, R., Pouyssegur, J., and Lenormand, P. (2007). ERK implication in cell cycle regulation. Biochimica et biophysica acta *1773*, 1299-1310.

Chen, N., and Debnath, J. (2010). Autophagy and tumorigenesis. FEBS letters *584*, 1427-1435.

Choi, M.-S., Min, S.-H., Jung, H., Lee, J.D., Lee, T.H., Lee, H.K., and Yoo, O.-J. (2011). The essential role of FKBP38 in regulating phosphatase of regenerating liver 3 (PRL-3) protein stability. Biochemical and biophysical research communications *406*, 305-309.

Cobb, M.H., and Goldsmith, E.J. (1995). How MAP kinases are regulated. The Journal of biological chemistry *270*, 14843-14846.

Codogno, P., Mehrpour, M., and Proikas-Cezanne, T. (2012). Canonical and non-canonical autophagy: variations on a common theme of self-eating? Nature reviews Molecular cell biology *13*, 7-12.

Coleman, M.L., Marshall, C.J., and Olson, M.F. (2003). Ras promotes p21(Waf1/Cip1) protein stability via a cyclin D1-imposed block in proteasome-mediated degradation. The EMBO journal *22*, 2036-2046.

Cramer, J.M., Zimmerman, M.W., Thompson, T., Homanics, G.E., Lazo, J.S., and Lagasse, E. (2014). Deletion of Ptp4a3 reduces clonogenicity and tumor-initiation ability of colitis-associated cancer cells in mice. Stem cell research *13*, 164-171.

D'Souza-Schorey, C., and Chavrier, P. (2006). ARF proteins: roles in membrane traffic and beyond. Nature reviews Molecular cell biology *7*, 347-358.

Degenhardt, K., Mathew, R., Beaudoin, B., Bray, K., Anderson, D., Chen, G., Mukherjee, C., Shi, Y., Gelinas, C., Fan, Y*., et al.* (2006). Autophagy promotes tumor cell survival and restricts necrosis, inflammation, and tumorigenesis. Cancer cell *10*, 51-64.

Deter, R.L., and De Duve, C. (1967). Influence of glucagon, an inducer of cellular autophagy, on some physical properties of rat liver lysosomes. The Journal of cell biology *33*, 437-449.

Dhillon, A.S., Hagan, S., Rath, O., and Kolch, W. (2007). MAP kinase signalling pathways in cancer. Oncogene *26*, 3279-3290.

Dunn, W.A., Jr. (1994). Autophagy and related mechanisms of lysosome-mediated protein degradation. Trends in cell biology *4*, 139-143.

Engelman, J.A., Chen, L., Tan, X., Crosby, K., Guimaraes, A.R., Upadhyay, R., Maira, M., McNamara, K., Perera, S.A., Song, Y*., et al.* (2008). Effective use of PI3K and MEK inhibitors to treat mutant Kras G12D and PIK3CA H1047R murine lung cancers. Nature medicine *14*, 1351-1356.

Eskelinen, E.L. (2011). The dual role of autophagy in cancer. Current opinion in pharmacology *11*, 294-300.

Fagerli, U.-M., Holt, R.U., Holien, T., Vaatsveen, T.K., Zhan, F., Egeberg, K.W., Barlogie, B., Waage, A., Aarset, H., and Dai, H.Y. (2008a). Overexpression and involvement in migration by the metastasis-associated phosphatase PRL-3 in human myeloma cells. Blood *111*, 806-815.

Fagerli, U.M., Holt, R.U., Holien, T., Vaatsveen, T.K., Zhan, F., Egeberg, K.W., Barlogie, B., Waage, A., Aarset, H., Dai, H.Y*., et al.* (2008b). Overexpression and involvement in migration by the metastasis-associated phosphatase PRL-3 in human myeloma cells. Blood *111*, 806-815.

Fiordalisi, J.J., Keller, P.J., and Cox, A.D. (2006). PRL tyrosine phosphatases regulate rho family GTPases to promote invasion and motility. Cancer research *66*, 3153-3161.

Fritz, G., Just, I., and Kaina, B. (1999). Rho GTPases are over-expressed in human tumors. International journal of cancer Journal international du cancer *81*, 682-687.

Glaumann, H., and Ahlberg, J. (1987). Comparison of different autophagic vacuoles with regard to ultrastructure, enzymatic composition, and degradation capacity--formation of crinosomes. Experimental and molecular pathology *47*, 346-362.

Guarino, M. (2010). Src signaling in cancer invasion. Journal of cellular physiology *223*, 14-26.

Guerrero, S., Casanova, I., Farre, L., Mazo, A., Capella, G., and Mangues, R. (2000). K-ras codon 12 mutation induces higher level of resistance to apoptosis and predisposition to anchorage-independent growth than codon 13 mutation or proto-oncogene overexpression. Cancer research *60*, 6750-6756.

Guo, J.Y., Chen, H.Y., Mathew, R., Fan, J., Strohecker, A.M., Karsli-Uzunbas, G., Kamphorst, J.J., Chen, G., Lemons, J.M., Karantza, V*., et al.* (2011a). Activated Ras requires autophagy to maintain oxidative metabolism and tumorigenesis. Genes & development *25*, 460-470.

Guo, K., Li, J., Tang, J.P., Koh, V., Gan, B.Q., and Zeng, Q. (2004a). Catalytic domain of PRL-3 plays an essential role in tumor metastasis: formation of PRL-3 tumors inside the blood vessels. Cancer biology & therapy *3*, 945-951.

Guo, K., Li, J., Tang, J.P., Koh, V., Gan, B.Q., and Zeng, Q. (2004b). Research Paper Catalytic Domain of PRL-3 Plays an Essential Role in Tumor Metastasis. Cancer biology & therapy *3*, 945-951.

Guo, K., Li, J., Tang, J.P., Tan, C.P., Hong, C.W., Al-Aidaroos, A.Q., Varghese, L., Huang, C., and Zeng, Q. (2011b). Targeting intracellular oncoproteins with antibody therapy or vaccination. Science translational medicine *3*, 99ra85.

Guo, K., Li, J., Wang, H., Osato, M., Tang, J.P., Quah, S.Y., Gan, B.Q., and Zeng, Q. (2006). PRL-3 initiates tumor angiogenesis by recruiting endothelial cells in vitro and in vivo. Cancer research *66*, 9625-9635.

Gupta, G.P., and Massague, J. (2006). Cancer metastasis: building a framework. Cell *127*, 679-695.

Guzinska-Ustymowicz, K., Kisluk, J., Terlikowski, S.J., Pryczynicz, A., Niewiarowska, K., Ustymowicz, M., Hawryluk, M., Poludniewski, M., and Kemona, A. (2013). Expression of phosphatase of regenerating liver-3 (PRL-3) in endometrioid cancer and lymph nodes metastases. Advances in medical sciences *58*, 221-226.

Hanada, T., Noda, N.N., Satomi, Y., Ichimura, Y., Fujioka, Y., Takao, T., Inagaki, F., and Ohsumi, Y. (2007). The Atg12-Atg5 conjugate has a novel E3-like activity for protein lipidation in autophagy. The Journal of biological chemistry *282*, 37298-37302.

Hanahan, D., and Folkman, J. (1996). Patterns and emerging mechanisms of the angiogenic switch during tumorigenesis. Cell *86*, 353-364.

Hanahan, D., and Weinberg, R.A. (2000). The hallmarks of cancer. Cell *100*, 57-70.

Hanahan, D., and Weinberg, R.A. (2011). Hallmarks of cancer: the next generation. Cell *144*, 646-674.

Hansen, T.E., and Johansen, T. (2011). Following autophagy step by step. BMC biology *9*, 39.

Hao, R.T., Zhang, X.H., Pan, Y.F., Liu, H.G., Xiang, Y.Q., Wan, L., and Wu, X.L. (2010). Prognostic and metastatic value of phosphatase of regenerating liver-3 in invasive breast cancer. Journal of cancer research and clinical oncology *136*, 1349-1357.

Hassan, N.M., Hamada, J., Kameyama, T., Tada, M., Nakagawa, K., Yoshida, S., Kashiwazaki, H., Yamazaki, Y., Suzuki, Y., Sasaki, A.*, et al.* (2011). Increased expression of the PRL-3 gene in human oral squamous cell carcinoma and dysplasia tissues. Asian Pacific journal of cancer prevention : APJCP *12*, 947-951.

Hatzivassiliou, G., Liu, B., O'Brien, C., Spoerke, J.M., Hoeflich, K.P., Haverty, P.M., Soriano, R., Forrest, W.F., Heldens, S., Chen, H.*, et al.* (2012). ERK inhibition overcomes acquired resistance to MEK inhibitors. Mol Cancer Ther *11*, 1143-1154.

He, C., and Klionsky, D.J. (2009). Regulation mechanisms and signaling pathways of autophagy. Annual review of genetics *43*, 67-93.

He, C., and Levine, B. (2010). The Beclin 1 interactome. Current opinion in cell biology *22*, 140-149.

Hilger, R.A., Scheulen, M.E., and Strumberg, D. (2002). The Ras-Raf-MEK-ERK pathway in the treatment of cancer. Onkologie *25*, 511-518.

Hu, L., Luo, H., Wang, W., Li, H., and He, T. (2013). Poor prognosis of phosphatase of regenerating liver 3 expression in gastric cancer: a meta-analysis. PloS one *8*, e76927.

Huang, Y.H., Al-Aidaroos, A.Q., Yuen, H.F., Zhang, S.D., Shen, H.M., Rozycka, E., McCrudden, C.M., Tergaonkar, V., Gupta, A., Lin, Y.B.*, et al.* (2014). A role of autophagy in PTP4A3-driven cancer progression. Autophagy *10*, 1787-1800.

Ihle, N.T., Byers, L.A., Kim, E.S., Saintigny, P., Lee, J.J., Blumenschein, G.R., Tsao, A., Liu, S., Larsen, J.E., Wang, J.*, et al.* (2012). Effect of KRAS oncogene substitutions on

protein behavior: implications for signaling and clinical outcome. Journal of the National Cancer Institute *104*, 228-239.

Itakura, E., and Mizushima, N. (2010). Characterization of autophagosome formation site by a hierarchical analysis of mammalian Atg proteins. Autophagy *6*, 764-776.

Itakura, E., and Mizushima, N. (2011). p62 Targeting to the autophagosome formation site requires self-oligomerization but not LC3 binding. The Journal of cell biology *192*, 17-27.

Ivanina, T.A., Sakina, N.L., Lebedeva, M.N., and Borovjagin, V.L. (1989). A study of the mechanisms of chloroquine retinopathy. II. Chloroquine effect on protein synthesis of retina. Ophthalmic research *21*, 272-277.

Jancik, S., Drabek, J., Radzioch, D., and Hajduch, M. (2010). Clinical relevance of KRAS in human cancers. Journal of biomedicine & biotechnology *2010*, 150960.

Janku, F., McConkey, D.J., Hong, D.S., and Kurzrock, R. (2011). Autophagy as a target for anticancer therapy. Nature reviews Clinical oncology *8*, 528-539.

Jiang, Y., Liu, X.Q., Rajput, A., Geng, L., Ongchin, M., Zeng, Q., Taylor, G.S., and Wang, J. (2011). Phosphatase PRL-3 is a direct regulatory target of TGFbeta in colon cancer metastasis. Cancer research *71*, 234-244.

Johnson, L.N. (2009). The regulation of protein phosphorylation. Biochemical Society transactions *37*, 627-641.

Jordan, C.T., Guzman, M.L., and Noble, M. (2006). Cancer stem cells. The New England journal of medicine *355*, 1253-1261.

Jung, C.H., Ro, S.H., Cao, J., Otto, N.M., and Kim, D.H. (2010). mTOR regulation of autophagy. FEBS letters *584*, 1287-1295.

Kabeya, Y., Mizushima, N., Ueno, T., Yamamoto, A., Kirisako, T., Noda, T., Kominami, E., Ohsumi, Y., and Yoshimori, T. (2000). LC3, a mammalian homologue of yeast Apg8p, is localized in autophagosome membranes after processing. The EMBO journal *19*, 5720-5728.

Kato, H., Semba, S., Miskad, U.A., Seo, Y., Kasuga, M., and Yokozaki, H. (2004). High expression of PRL-3 promotes cancer cell motility and liver metastasis in human colorectal cancer: a predictive molecular marker of metachronous liver and lung metastases. Clinical cancer research : an official journal of the American Association for Cancer Research *10*, 7318-7328.

Kaushik, S., and Cuervo, A.M. (2012). Chaperone-mediated autophagy: a unique way to enter the lysosome world. Trends in cell biology *22*, 407-417.

Khan, N., and Mukhtar, H. (2010). Cancer and metastasis: prevention and treatment by green tea. Cancer metastasis reviews *29*, 435-445.

Kim, E.K., and Choi, E.J. (2010). Pathological roles of MAPK signaling pathways in human diseases. Biochimica et biophysica acta *1802*, 396-405.

Kim, P.K., Hailey, D.W., Mullen, R.T., and Lippincott-Schwartz, J. (2008). Ubiquitin signals autophagic degradation of cytosolic proteins and peroxisomes. Proceedings of the National Academy of Sciences of the United States of America *105*, 20567-20574.

Kim, S.T., Lim do, H., Jang, K.T., Lim, T., Lee, J., Choi, Y.L., Jang, H.L., Yi, J.H., Baek, K.K., Park, S.H.*, et al.* (2011). Impact of KRAS mutations on clinical outcomes in pancreatic cancer patients treated with first-line gemcitabine-based chemotherapy. Mol Cancer Ther *10*, 1993-1999.

Kirisako, T., Ichimura, Y., Okada, H., Kabeya, Y., Mizushima, N., Yoshimori, T., Ohsumi, M., Takao, T., Noda, T., and Ohsumi, Y. (2000). The reversible modification regulates the membrane-binding state of Apg8/Aut7 essential for autophagy and the cytoplasm to vacuole targeting pathway. The Journal of cell biology *151*, 263-276.

Kirkin, V., Lamark, T., Sou, Y.S., Bjorkoy, G., Nunn, J.L., Bruun, J.A., Shvets, E., McEwan, D.G., Clausen, T.H., Wild, P.*, et al.* (2009). A role for NBR1 in autophagosomal degradation of ubiquitinated substrates. Molecular cell *33*, 505-516.

Komatsu, M., Waguri, S., Koike, M., Sou, Y.S., Ueno, T., Hara, T., Mizushima, N., Iwata, J., Ezaki, J., Murata, S.*, et al.* (2007). Homeostatic levels of p62 control cytoplasmic inclusion body formation in autophagy-deficient mice. Cell *131*, 1149-1163.

Kopito, R.R. (2000). Aggresomes, inclusion bodies and protein aggregation. Trends in cell biology *10*, 524-530.

Korolchuk, V.I., Menzies, F.M., and Rubinsztein, D.C. (2009). A novel link between autophagy and the ubiquitin-proteasome system. Autophagy *5*, 862-863.

Kraft, C., Kijanska, M., Kalie, E., Siergiejuk, E., Lee, S.S., Semplicio, G., Stoffel, I., Brezovich, A., Verma, M., Hansmann, I.*, et al.* (2012). Binding of the Atg1/ULK1 kinase to the ubiquitin-like protein Atg8 regulates autophagy. The EMBO journal *31*, 3691-3703.
Kranenburg, O. (2005). The KRAS oncogene: past, present, and future. Biochimica et biophysica acta *1756*, 81-82.

Krndija, D., Munzberg, C., Maass, U., Hafner, M., Adler, G., Kestler, H.A., Seufferlein, T., Oswald, F., and von Wichert, G. (2012). The phosphatase of regenerating liver 3 (PRL-3) promotes cell migration through Arf-activity-dependent stimulation of integrin alpha5 recycling. Journal of cell science *125*, 3883-3892.

Lai, W., Liu, L., Zeng, Y., Wu, H., Xu, H., Chen, S., and Chu, Z. (2013). KCNN4 channels participate in the EMT induced by PRL-3 in colorectal cancer. Medical oncology *30*, 566.

Lamark, T., Kirkin, V., Dikic, I., and Johansen, T. (2009). NBR1 and p62 as cargo receptors for selective autophagy of ubiquitinated targets. Cell cycle *8*, 1986-1990.

Laurent, C., Valet, F., Planque, N., Silveri, L., Maacha, S., Anezo, O., Hupe, P., Plancher, C., Reyes, C., Albaud, B.*, et al.* (2011). High PTP4A3 phosphatase expression correlates with metastatic risk in uveal melanoma patients. Cancer research *71*, 666-674.

Lawlor, M.A., and Alessi, D.R. (2001). PKB/Akt: a key mediator of cell proliferation, survival and insulin responses? Journal of cell science *114*, 2903-2910.

Li, J., Guo, K., Koh, V.W., Tang, J.P., Gan, B.Q., Shi, H., Li, H.X., and Zeng, Q. (2005). Generation of PRL-3- and PRL-1-specific monoclonal antibodies as potential diagnostic markers for cancer metastases. Clinical cancer research : an official journal of the American Association for Cancer Research *11*, 2195-2204.

Li, W.W., Li, J., and Bao, J.K. (2012). Microautophagy: lesser-known self-eating. Cellular and molecular life sciences : CMLS *69*, 1125-1136.

Li, Z.-R., Wang, Z., Zhu, B.-H., He, Y.-L., Peng, J.-S., Cai, S.-R., Ma, J.-P., and Zhan, W.-H. (2007). Association of tyrosine PRL-3 phosphatase protein expression with peritoneal metastasis of gastric carcinoma and prognosis. Surgery today *37*, 646-651.

Li, Z., Zhan, W., Wang, Z., Zhu, B., He, Y., Peng, J., Cai, S., and Ma, J. (2006). Inhibition of PRL-3 gene expression in gastric cancer cell line SGC7901 via microRNA suppressed reduces peritoneal metastasis. Biochemical and biophysical research communications *348*, 229-237.

Lian, Y.X., Chen, R., Xu, Y.H., Peng, C.L., and Hu, H.C. (2012). Effect of protein-tyrosine phosphatase 4A3 by small interfering RNA on the proliferation of lung cancer. Gene *511*, 169-176.

Liang, F., Liang, J., Wang, W.Q., Sun, J.P., Udho, E., and Zhang, Z.Y. (2007). PRL3 promotes cell invasion and proliferation by down-regulation of Csk leading to Src activation. The Journal of biological chemistry *282*, 5413-5419.

Lin, K.R., Lee, S.F., Hung, C.M., Li, C.L., Yang-Yen, H.F., and Yen, J.J. (2007). Survival factor withdrawal-induced apoptosis of TF-1 cells involves a TRB2-Mcl-1 axis-dependent pathway. The Journal of biological chemistry *282*, 21962-21972.

Liu, C., Qu, L., Dong, B., Xing, X., Ren, T., Zeng, Y., Jiang, B., Meng, L., Wu, J., and Shou, C. (2012). Combined phenotype of 4 markers improves prognostic value of patients with colon cancer. The American journal of the medical sciences *343*, 295-302.

Liu, X., Shi, Y., Han, E.K., Chen, Z., Rosenberg, S.H., Giranda, V.L., Luo, Y., and Ng, S.C. (2001). Downregulation of Akt1 inhibits anchorage-independent cell growth and induces apoptosis in cancer cells. Neoplasia *3*, 278-286.

Liu, Y., Zhou, J., Chen, J., Gao, W., Le, Y., Ding, Y., and Li, J. (2009). PRL-3 promotes epithelial mesenchymal transition by regulating cadherin directly. Cancer biology & therapy *8*, 1352-1359.

Liu, Y.Q., Li, H.X., Lou, X., and Lei, J.Y. (2008). Expression of phosphatase of regenerating liver 1 and 3 mRNA in esophageal squamous cell carcinoma. Archives of pathology & laboratory medicine *132*, 1307-1312.

Loeb, L.A., Loeb, K.R., and Anderson, J.P. (2003). Multiple mutations and cancer. Proceedings of the National Academy of Sciences of the United States of America *100*, 776-781.

Lowe, S.W., and Lin, A.W. (2000). Apoptosis in cancer. Carcinogenesis *21*, 485-495.

Maacha, S., Planque, N., Laurent, C., Pegoraro, C., Anezo, O., Maczkowiak, F., Monsoro-Burq, A.H., and Saule, S. (2013). Protein tyrosine phosphatase 4A3 (PTP4A3) is required for Xenopus laevis cranial neural crest migration in vivo. PloS one *8*, e84717.

Maekawa, M., Ishizaki, T., Boku, S., Watanabe, N., Fujita, A., Iwamatsu, A., Obinata, T., Ohashi, K., Mizuno, K., and Narumiya, S. (1999). Signaling from Rho to the actin cytoskeleton through protein kinases ROCK and LIM-kinase. Science *285*, 895-898.

Mancias, J.D., and Kimmelman, A.C. (2011). Targeting autophagy addiction in cancer. Oncotarget *2*, 1302-1306.

Mandic, A., Viktorsson, K., Heiden, T., Hansson, J., and Shoshan, M.C. (2001). The MEK1 inhibitor PD98059 sensitizes C8161 melanoma cells to cisplatin-induced apoptosis. Melanoma research *11*, 11-19.

Marais, R., Light, Y., Mason, C., Paterson, H., Olson, M.F., and Marshall, C.J. (1998). Requirement of Ras-GTP-Raf complexes for activation of Raf-1 by protein kinase C. Science *280*, 109-112.

Marc, P. (2012). Cytopathological diagnosis of non small cell lung cancer: recent advances including rapid on-site evaluation, novel endoscopic techniques and molecular tests. Journal of Pulmonary & Respiratory Medicine.

Mathew, R., Kongara, S., Beaudoin, B., Karp, C.M., Bray, K., Degenhardt, K., Chen, G., Jin, S., and White, E. (2007). Autophagy suppresses tumor progression by limiting chromosomal instability. Genes & development *21*, 1367-1381.

McGrath, J.P., Capon, D.J., Smith, D.H., Chen, E.Y., Seeburg, P.H., Goeddel, D.V., and Levinson, A.D. (1983). Structure and organization of the human Ki-ras proto-oncogene and a related processed pseudogene. Nature *304*, 501-506.

Meijer, A.J., and Codogno, P. (2004). Regulation and role of autophagy in mammalian cells. The international journal of biochemistry & cell biology *36*, 2445-2462.

Meijer, A.J., and Codogno, P. (2011). Autophagy: regulation by energy sensing. Current biology : CB *21*, R227-229.

Min, G., Lee, S.K., Kim, H.N., Han, Y.M., Lee, R.H., Jeong, D.G., Han, D.C., and Kwon, B.M. (2013). Rhodanine-based PRL-3 inhibitors blocked the migration and invasion of metastatic cancer cells. Bioorganic & medicinal chemistry letters *23*, 3769-3774.

Min, S.H., Kim, D.M., Heo, Y.S., Kim, H.M., Kim, I.C., and Yoo, O.J. (2010). Downregulation of p53 by phosphatase of regenerating liver 3 is mediated by MDM2 and PIRH2. Life sciences *86*, 66-72.

Ming, J., Liu, N., Gu, Y., Qiu, X., and Wang, E.H. (2009). PRL-3 facilitates angiogenesis and metastasis by increasing ERK phosphorylation and up-regulating the levels and activities of Rho-A/C in lung cancer. Pathology *41*, 118-126.

Miskad, U.A., Semba, S., Kato, H., Matsukawa, Y., Kodama, Y., Mizuuchi, E., Maeda, N., Yanagihara, K., and Yokozaki, H. (2007). High PRL-3 expression in human gastric cancer is a marker of metastasis and grades of malignancies: an in situ hybridization study. Virchows Archiv : an international journal of pathology *450*, 303-310.

Mizushima, N. (2007). Autophagy: process and function. Genes & development *21*, 2861-2873.

Mizushima, N. (2010). The role of the Atg1/ULK1 complex in autophagy regulation. Current opinion in cell biology *22*, 132-139.

Mizushima, N., Yamamoto, A., Hatano, M., Kobayashi, Y., Kabeya, Y., Suzuki, K., Tokuhisa, T., Ohsumi, Y., and Yoshimori, T. (2001). Dissection of autophagosome formation using Apg5-deficient mouse embryonic stem cells. The Journal of cell biology *152*, 657-668.

Mizushima, N., Yoshimori, T., and Levine, B. (2010). Methods in mammalian autophagy research. Cell *140*, 313-326.

Molleví, D.G., Aytes, A., Berdiel, M., Padullés, L., Martínez-Iniesta, M., Sanjuan, X., Salazar, R., and Villanueva, A. (2009). PRL-3 overexpression in epithelial cells is induced by surrounding stromal fibroblasts. Molecular cancer *8*, 46.

Mollevi, D.G., Aytes, A., Padulles, L., Martinez-Iniesta, M., Baixeras, N., Salazar, R., Ramos, E., Figueras, J., Capella, G., and Villanueva, A. (2008). PRL-3 is essentially overexpressed in primary colorectal tumours and associates with tumour aggressiveness. British journal of cancer *99*, 1718-1725.

Moores, S.L., Schaber, M.D., Mosser, S.D., Rands, E., O'Hara, M.B., Garsky, V.M., Marshall, M.S., Pompliano, D.L., and Gibbs, J.B. (1991). Sequence dependence of protein isoprenylation. The Journal of biological chemistry *266*, 14603-14610.

Morselli, E., Galluzzi, L., Kepp, O., Vicencio, J.M., Criollo, A., Maiuri, M.C., and Kroemer, G. (2009). Anti- and pro-tumor functions of autophagy. Biochimica et biophysica acta *1793*, 1524-1532.

Nakanishi, K., Sakamoto, M., Yasuda, J., Takamura, M., Fujita, N., Tsuruo, T., Todo, S., and Hirohashi, S. (2002). Critical involvement of the phosphatidylinositol 3-kinase/Akt pathway in anchorage-independent growth and hematogeneous intrahepatic metastasis of liver cancer. Cancer Res *62*, 2971-2975.

Nakatogawa, H., Suzuki, K., Kamada, Y., and Ohsumi, Y. (2009). Dynamics and diversity in autophagy mechanisms: lessons from yeast. Nature reviews Molecular cell biology *10*, 458-467.

Neufeld, G., Cohen, T., Gengrinovitch, S., and Poltorak, Z. (1999). Vascular endothelial growth factor (VEGF) and its receptors. FASEB journal : official publication of the Federation of American Societies for Experimental Biology *13*, 9-22.

Neumann, J., Zeindl-Eberhart, E., Kirchner, T., and Jung, A. (2009). Frequency and type of KRAS mutations in routine diagnostic analysis of metastatic colorectal cancer. Pathology, research and practice *205*, 858-862.

Nezis, I.P., Simonsen, A., Sagona, A.P., Finley, K., Gaumer, S., Contamine, D., Rusten, T.E., Stenmark, H., and Brech, A. (2008). Ref(2)P, the Drosophila melanogaster homologue of mammalian p62, is required for the formation of protein aggregates in adult brain. The Journal of cell biology *180*, 1065-1071.

Ooki, A., Yamashita, K., Kikuchi, S., Sakuramoto, S., Katada, N., and Watanabe, M. (2010). Phosphatase of regenerating liver-3 as a convergent therapeutic target for lymph node metastasis in esophageal squamous cell carcinoma. International journal of cancer Journal international du cancer *127*, 543-554.

Pankiv, S., Clausen, T.H., Lamark, T., Brech, A., Bruun, J.A., Outzen, H., Overvatn, A., Bjorkoy, G., and Johansen, T. (2007). p62/SQSTM1 binds directly to Atg8/LC3 to facilitate degradation of ubiquitinated protein aggregates by autophagy. The Journal of biological chemistry *282*, 24131-24145.

Park, J.E., Yuen, H.F., Zhou, J.B., Al-Aidaroos, A.Q., Guo, K., Valk, P.J., Zhang, S.D., Chng, W.J., Hong, C.W., Mills, K.*, et al.* (2013). Oncogenic roles of PRL-3 in FLT3-ITD induced acute myeloid leukaemia. EMBO molecular medicine *5*, 1351-1366.

Patterson, K.I., Brummer, T., O'Brien, P.M., and Daly, R.J. (2009). Dual-specificity phosphatases: critical regulators with diverse cellular targets. The Biochemical journal *418*, 475-489.

Peltier, J., O'Neill, A., and Schaffer, D.V. (2007). PI3K/Akt and CREB regulate adult neural hippocampal progenitor proliferation and differentiation. Developmental neurobiology *67*, 1348-1361.

Peng, L., Jin, G., Wang, L., Guo, J., Meng, L., and Shou, C. (2006). Identification of integrin α1 as an interacting protein of protein tyrosine phosphatase PRL-3. Biochemical and biophysical research communications *342*, 179-183.

Peng, L., Ning, J., Meng, L., and Shou, C. (2004). The association of the expression level of protein tyrosine phosphatase PRL-3 protein with liver metastasis and prognosis of patients with colorectal cancer. Journal of cancer research and clinical oncology *130*, 521-526.

Petiot, A., Ogier-Denis, E., Blommaart, E.F., Meijer, A.J., and Codogno, P. (2000). Distinct classes of phosphatidylinositol 3'-kinases are involved in signaling pathways that control macroautophagy in HT-29 cells. The Journal of biological chemistry *275*, 992-998.

Polato, F., Codegoni, A., Fruscio, R., Perego, P., Mangioni, C., Saha, S., Bardelli, A., and Broggini, M. (2005). PRL-3 phosphatase is implicated in ovarian cancer growth. Clinical cancer research : an official journal of the American Association for Cancer Research *11*, 6835-6839.

Poole, B., and Ohkuma, S. (1981). Effect of weak bases on the intralysosomal pH in mouse peritoneal macrophages. The Journal of cell biology *90*, 665-669.

Prior, I.A., Lewis, P.D., and Mattos, C. (2012). A comprehensive survey of Ras mutations in cancer. Cancer research *72*, 2457-2467.

Qian, F., Li, Y.-P., Sheng, X., Zhang, Z.-C., Song, R., Dong, W., Cao, S.-X., Hua, Z.-C., and Xu, Q. (2007a). PRL-3 siRNA inhibits the metastasis of B16-BL6 mouse melanoma cells in vitro and in vivo. Molecular medicine *13*, 151.

Qian, F., Li, Y.P., Sheng, X., Zhang, Z.C., Song, R., Dong, W., Cao, S.X., Hua, Z.C., and Xu, Q. (2007b). PRL-3 siRNA inhibits the metastasis of B16-BL6 mouse melanoma cells in vitro and in vivo. Molecular medicine *13*, 151-159.

Radke, I., Gotte, M., Kersting, C., Mattsson, B., Kiesel, L., and Wulfing, P. (2006). Expression and prognostic impact of the protein tyrosine phosphatases PRL-1, PRL-2, and PRL-3 in breast cancer. British journal of cancer *95*, 347-354.

Rafalski, V.A., and Brunet, A. (2011). Energy metabolism in adult neural stem cell fate. Progress in neurobiology *93*, 182-203.

Razi, M., Chan, E.Y., and Tooze, S.A. (2009). Early endosomes and endosomal coatomer are required for autophagy. The Journal of cell biology *185*, 305-321.

Ren, T., Jiang, B., Xing, X., Dong, B., Peng, L., Meng, L., Xu, H., and Shou, C. (2009). Prognostic significance of phosphatase of regenerating liver-3 expression in ovarian cancer. Pathology oncology research : POR *15*, 555-560.

Rouleau, C., Roy, A., Martin, T.S., Dufault, M.R., Boutin, P., Liu, D., Zhang, M., Puorro-Radzwill, K., Rulli, L., and Reczek, D. (2006). Protein tyrosine phosphatase PRL-3 in malignant cells and endothelial cells: expression and function. Molecular cancer therapeutics *5*, 219-229.

Russell, R.C., Tian, Y., Yuan, H., Park, H.W., Chang, Y.Y., Kim, J., Kim, H., Neufeld, T.P., Dillin, A., and Guan, K.L. (2013). ULK1 induces autophagy by phosphorylating Beclin-1 and activating VPS34 lipid kinase. Nature cell biology *15*, 741-750.

Saha, S., Bardelli, A., Buckhaults, P., Velculescu, V.E., Rago, C., St Croix, B., Romans, K.E., Choti, M.A., Lengauer, C., Kinzler, K.W*., et al.* (2001). A phosphatase associated with metastasis of colorectal cancer. Science *294*, 1343-1346.

Schubbert, S., Shannon, K., and Bollag, G. (2007). Hyperactive Ras in developmental disorders and cancer. Nature reviews Cancer *7*, 295-308.

Shaw, R.J., Kosmatka, M., Bardeesy, N., Hurley, R.L., Witters, L.A., DePinho, R.A., and Cantley, L.C. (2004). The tumor suppressor LKB1 kinase directly activates AMP-activated kinase and regulates apoptosis in response to energy stress. Proceedings of the National Academy of Sciences of the United States of America *101*, 3329-3335.

Shin, I., Yakes, F.M., Rojo, F., Shin, N.Y., Bakin, A.V., Baselga, J., and Arteaga, C.L. (2002). PKB/Akt mediates cell-cycle progression by phosphorylation of p27(Kip1) at threonine 157 and modulation of its cellular localization. Nature medicine *8*, 1145-1152.

Shirasawa, S., Furuse, M., Yokoyama, N., and Sasazuki, T. (1993). Altered growth of human colon cancer cell lines disrupted at activated Ki-ras. Science *260*, 85-88.

Sun, Z.H., and Bu, P. (2012). Downregulation of phosphatase of regenerating liver-3 is involved in the inhibition of proliferation and apoptosis induced by emodin in the SGC-7901 human gastric carcinoma cell line. Experimental and therapeutic medicine *3*, 1077-1081.

Sundar, J., and Gnanasekar, M. (2013). Can dehydroepiandrostenedione (DHEA) target PRL-3 to prevent colon cancer metastasis? Medical hypotheses *80*, 595-597.

Takegawa, K., DeWald, D.B., and Emr, S.D. (1995). Schizosaccharomyces pombe Vps34p, a phosphatidylinositol-specific PI 3-kinase essential for normal cell growth and vacuole morphology. Journal of cell science *108 (Pt 12)*, 3745-3756.

Tamagawa, H., Oshima, T., Yoshihara, K., Watanabe, T., Numata, M., Yamamoto, N., Tuschida, K., Shiozawa, M., Morinaga, S., Akaike, M.*, et al.* (2012). The expression of the phosphatase regenerating liver 3 gene is associated with outcome in patients with colorectal cancer. Hepato-gastroenterology *59*, 2122-2126.

Tanida, I., Minematsu-Ikeguchi, N., Ueno, T., and Kominami, E. (2005). Lysosomal turnover, but not a cellular level, of endogenous LC3 is a marker for autophagy. Autophagy *1*, 84-91.

Tanida, I., Ueno, T., and Kominami, E. (2008). LC3 and Autophagy. Methods in molecular biology *445*, 77-88.

Tanoue, T., Adachi, M., Moriguchi, T., and Nishida, E. (2000). A conserved docking motif in MAP kinases common to substrates, activators and regulators. Nature cell biology *2*, 110-116.

Tanti, J.F., and Jager, J. (2009). Cellular mechanisms of insulin resistance: role of stress-regulated serine kinases and insulin receptor substrates (IRS) serine phosphorylation. Current opinion in pharmacology *9*, 753-762.

Thiery, J.P. (2002). Epithelial-mesenchymal transitions in tumour progression. Nature reviews Cancer *2*, 442-454.

Thiery, J.P. (2003). Epithelial-mesenchymal transitions in development and pathologies. Current opinion in cell biology *15*, 740-746.

Tidyman, W.E., and Rauen, K.A. (2009). The RASopathies: developmental syndromes of Ras/MAPK pathway dysregulation. Current opinion in genetics & development *19*, 230-236.

Ustaalioglu, B.B., Bilici, A., Barisik, N.O., Aliustaoglu, M., Vardar, F.A., Yilmaz, B.E., Seker, M., and Gumus, M. (2012). Clinical importance of phosphatase of regenerating liver-3 expression in breast cancer. Clinical & translational oncology : official publication of the Federation of Spanish Oncology Societies and of the National Cancer Institute of Mexico *14*, 911-922.

Vigil, D., Cherfils, J., Rossman, K.L., and Der, C.J. (2010). Ras superfamily GEFs and GAPs: validated and tractable targets for cancer therapy? Nature reviews Cancer *10*, 842-857.

Villanueva, J., Yung, Y., Walker, J.L., and Assoian, R.K. (2007). ERK activity and G1 phase progression: identifying dispensable versus essential activities and primary versus secondary targets. Molecular biology of the cell *18*, 1457-1463.

Vivanco, I., and Sawyers, C.L. (2002). The phosphatidylinositol 3-Kinase AKT pathway in human cancer. Nature reviews Cancer *2*, 489-501.

Vogelstein, B., Lane, D., and Levine, A.J. (2000). Surfing the p53 network. Nature *408*, 307-310.

Vousden, K.H., and Lu, X. (2002). Live or let die: the cell's response to p53. Nature reviews Cancer *2*, 594-604.

Walsh, C.T., Garneau-Tsodikova, S., and Gatto, G.J., Jr. (2005). Protein posttranslational modifications: the chemistry of proteome diversifications. Angewandte Chemie *44*, 7342-7372.

Wang, H., Quah, S.Y., Dong, J.M., Manser, E., Tang, J.P., and Zeng, Q. (2007). PRL-3 down-regulates PTEN expression and signals through PI3K to promote epithelial-mesenchymal transition. Cancer research *67*, 2922-2926.

Wang, H., Vardy, L.A., Tan, C.P., Loo, J.M., Guo, K., Li, J., Lim, S.G., Zhou, J., Chng, W.J., Ng, S.B.*, et al.* (2010). PCBP1 suppresses the translation of metastasis-associated PRL-3 phosphatase. Cancer cell *18*, 52-62.

Wang, J., Han, W., Zborowska, E., Liang, J., Wang, X., Willson, J.K., Sun, L., and Brattain, M.G. (1996). Reduced expression of transforming growth factor beta type I receptor contributes to the malignancy of human colon carcinoma cells. The Journal of biological chemistry *271*, 17366-17371.

Wang, J., Sun, L., Myeroff, L., Wang, X., Gentry, L.E., Yang, J., Liang, J., Zborowska, E., Markowitz, S., Willson, J.K.*, et al.* (1995). Demonstration that mutation of the type II transforming growth factor beta receptor inactivates its tumor suppressor activity in replication error-positive colon carcinoma cells. The Journal of biological chemistry *270*, 22044-22049.

Wang, L., Peng, L., Dong, B., Kong, L., Meng, L., Yan, L., Xie, Y., and Shou, C. (2006). Overexpression of phosphatase of regenerating liver-3 in breast cancer: association with a poor clinical outcome. Annals of oncology : official journal of the European Society for Medical Oncology / ESMO *17*, 1517-1522.
Wang, L., Shen, Y., Song, R., Sun, Y., Xu, J., and Xu, Q. (2009). An anticancer effect of curcumin mediated by down-regulating phosphatase of regenerating liver-3 expression on highly metastatic melanoma cells. Molecular pharmacology *76*, 1238-1245.

Weidberg, H., Shpilka, T., Shvets, E., Abada, A., Shimron, F., and Elazar, Z. (2011). LC3 and GATE-16 N termini mediate membrane fusion processes required for autophagosome biogenesis. Developmental cell *20*, 444-454.

Weiss, G., Maaetoft-Udsen, K., Stifter, S.A., Hertzog, P., Goriely, S., Thomsen, A.R., Paludan, S.R., and Frokiaer, H. (2012). MyD88 drives the IFN-beta response to Lactobacillus acidophilus in dendritic cells through a mechanism involving IRF1, IRF3, and IRF7. Journal of immunology *189*, 2860-2868.

Wennerberg, K., Rossman, K.L., and Der, C.J. (2005). The Ras superfamily at a glance. Journal of cell science *118*, 843-846.

Wilhelm, S.M., Carter, C., Tang, L., Wilkie, D., McNabola, A., Rong, H., Chen, C., Zhang, X., Vincent, P., McHugh, M.*, et al.* (2004). BAY 43-9006 exhibits broad spectrum oral antitumor activity and targets the RAF/MEK/ERK pathway and receptor tyrosine kinases involved in tumor progression and angiogenesis. Cancer research *64*, 7099-7109.

Wortzel, I., and Seger, R. (2011). The ERK Cascade: Distinct Functions within Various Subcellular Organelles. Genes & cancer *2*, 195-209.

Wu, Y., and Wu, P.Y. (2009). CD133 as a marker for cancer stem cells: progresses and concerns. Stem cells and development *18*, 1127-1134.

Xing, X., Lian, S., Hu, Y., Li, Z., Zhang, L., Wen, X., Du, H., Jia, Y., Zheng, Z., Meng, L.*, et al.* (2013). Phosphatase of regenerating liver-3 (PRL-3) is associated with metastasis and poor prognosis in gastric carcinoma. Journal of translational medicine *11*, 309.

Xing, X., Peng, L., Qu, L., Ren, T., Dong, B., Su, X., and Shou, C. (2009). Prognostic value of PRL-3 overexpression in early stages of colonic cancer. Histopathology *54*, 309-318.

Xu, J., Cao, S., Wang, L., Xu, R., Chen, G., and Xu, Q. (2011). VEGF promotes the transcription of the human PRL-3 gene in HUVEC through transcription factor MEF2C. PloS one *6*, e27165.

Xu, Y., Zhu, M., Zhang, S., Liu, H., Li, T., and Qin, C. (2010). Expression and prognostic value of PRL-3 in human intrahepatic cholangiocarcinoma. Pathology oncology research : POR *16*, 169-175.

Yamamoto, A., Tagawa, Y., Yoshimori, T., Moriyama, Y., Masaki, R., and Tashiro, Y. (1998). Bafilomycin A1 prevents maturation of autophagic vacuoles by inhibiting fusion between autophagosomes and lysosomes in rat hepatoma cell line, H-4-II-E cells. Cell structure and function *23*, 33-42.

Yang, J., Liang, X., Niu, T., Meng, W., Zhao, Z., and Zhou, G.W. (1998). Crystal structure of the catalytic domain of protein-tyrosine phosphatase SHP-1. The Journal of biological chemistry *273*, 28199-28207.

Yang, Z.J., Chee, C.E., Huang, S., and Sinicrope, F.A. (2011). The role of autophagy in cancer: therapeutic implications. Mol Cancer Ther *10*, 1533-1541.

Ye, S.C., Foster, J.M., Li, W., Liang, J., Zborowska, E., Venkateswarlu, S., Gong, J., Brattain, M.G., and Willson, J.K. (1999). Contextual effects of transforming growth factor beta on the tumorigenicity of human colon carcinoma cells. Cancer research *59*, 4725-4731.

Young, A.R., Chan, E.Y., Hu, X.W., Kochl, R., Crawshaw, S.G., High, S., Hailey, D.W., Lippincott-Schwartz, J., and Tooze, S.A. (2006). Starvation and ULK1-dependent cycling

of mammalian Atg9 between the TGN and endosomes. Journal of cell science *119*, 3888-3900.

Yue, Z., Jin, S., Yang, C., Levine, A.J., and Heintz, N. (2003). Beclin 1, an autophagy gene essential for early embryonic development, is a haploinsufficient tumor suppressor. Proceedings of the National Academy of Sciences of the United States of America *100*, 15077-15082.

Zeng, Q., Dong, J.M., Guo, K., Li, J., Tan, H.X., Koh, V., Pallen, C.J., Manser, E., and Hong, W. (2003). PRL-3 and PRL-1 promote cell migration, invasion, and metastasis. Cancer research *63*, 2716-2722.

Zeng, Q., Hong, W., and Tan, Y.H. (1998a). Mouse PRL-2 and PRL-3, two potentially prenylated protein tyrosine phosphatases homologous to PRL-1. Biochemical and biophysical research communications *244*, 421-427.

Zeng, Q., Si, X., Horstmann, H., Xu, Y., Hong, W., and Pallen, C.J. (2000). Prenylation-dependent association of protein-tyrosine phosphatases PRL-1, -2, and -3 with the plasma membrane and the early endosome. The Journal of biological chemistry *275*, 21444-21452.

Zeng, Q., Tan, Y.H., and Hong, W. (1998b). A single plasmid vector (pSTAR) mediating efficient tetracycline-induced gene expression. Analytical biochemistry *259*, 187-194.

Zhang, F.L., and Casey, P.J. (1996). Protein prenylation: molecular mechanisms and functional consequences. Annual review of biochemistry *65*, 241-269.

Zhang, J., Xiao, Z., Lai, D., Sun, J., He, C., Chu, Z., Ye, H., Chen, S., and Wang, J. (2012a). miR-21, miR-17 and miR-19a induced by phosphatase of regenerating liver-3 promote the proliferation and metastasis of colon cancer. British journal of cancer *107*, 352-359.

Zhang, W., and Liu, H.T. (2002). MAPK signal pathways in the regulation of cell proliferation in mammalian cells. Cell research *12*, 9-18.

Zhang, Y., Cheng, Y., Ren, X., Zhang, L., Yap, K.L., Wu, H., Patel, R., Liu, D., Qin, Z.H., Shih, I.M.*, et al.* (2012b). NAC1 modulates sensitivity of ovarian cancer cells to cisplatin by altering the HMGB1-mediated autophagic response. Oncogene *31*, 1055-1064.

Zheng, P., Meng, H.-M., Gao, W.-Z., Chen, L., Liu, X.-H., Xiao, Z.-Q., Liu, Y.-X., Sui, H.-M., Zhou, J., and Liu, Y.-H. (2011). Snail as a key regulator of PRL-3 gene in colorectal cancer. Cancer biology & therapy *12*, 742-749.

Zhou, J., Bi, C., Chng, W.J., Cheong, L.L., Liu, S.C., Mahara, S., Tay, K.G., Zeng, Q., Li, J., Guo, K.*, et al.* (2011). PRL-3, a metastasis associated tyrosine phosphatase, is involved in FLT3-ITD signaling and implicated in anti-AML therapy. PloS one *6*, e19798.

Zhou, J., Wang, S., Lu, J., Li, J., and Ding, Y. (2009). Over-expression of phosphatase of regenerating liver-3 correlates with tumor progression and poor prognosis in nasopharyngeal carcinoma. International journal of cancer Journal international du cancer *124*, 1879-1886.

Zimmerman, M.W. (2013). Targeted deletion of PTP4A3 inhibits colon carcinogenesis and angiogenesis (Doctoral dissertation). University of Pittsburgh School of Medicine.

Zimmerman, M.W., McQueeney, K.E., Isenberg, J.S., Pitt, B.R., Wasserloos, K.A., Homanics, G.E., and Lazo, J.S. (2014). Protein-tyrosine phosphatase 4A3 (PTP4A3) promotes vascular endothelial growth factor signaling and enables endothelial cell motility. The Journal of biological chemistry *289*, 5904-5913.

Zuber, J., Tchernitsa, O.I., Hinzmann, B., Schmitz, A.C., Grips, M., Hellriegel, M., Sers, C., Rosenthal, A., and Schafer, R. (2000). A genome-wide survey of RAS transformation targets. Nature genetics *24*, 144-152.